Analysis and evaluation in shoreline detection in the South Holland province, using images in quad polarization mode from TerraSAR-X

DIEGO GURREONERO ROBINSON
March, 2011

SUPERVISORS:
Ms. Dr. Ir. W. Bijker
Dr. V.A Tolpekin

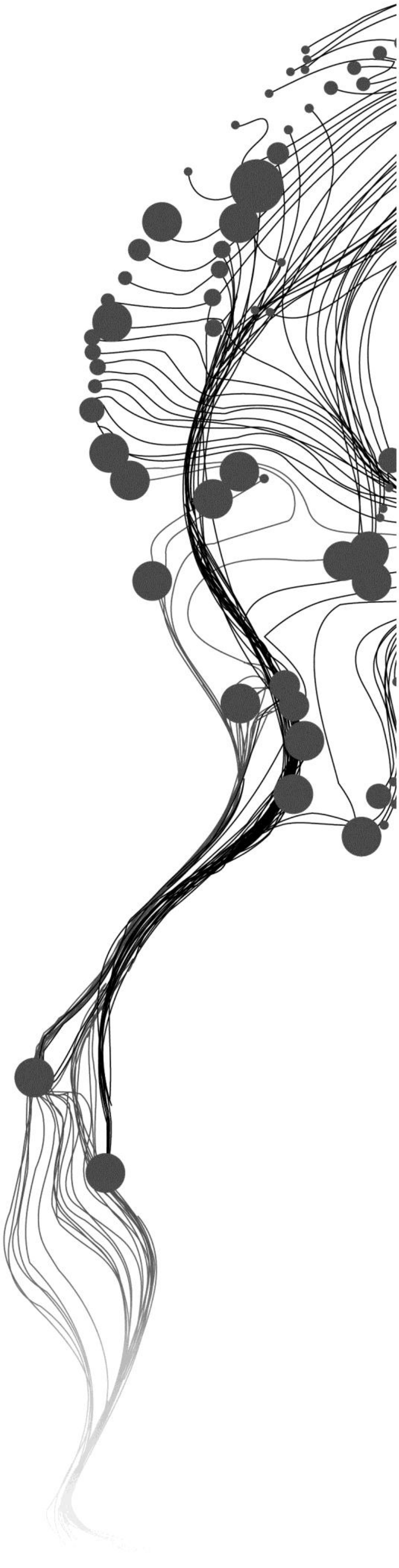

Analysis and evaluation in coastline detection in the South Holland province, using images in quad polarization mode from TerraSAR-X

DIEGO GURREONERO ROBINSON
Enschede, the Netherlands, March, 2011

Thesis submitted to the Faculty of Geo-Information Science and Earth Observation of the University of Twente in partial fulfilment of the requirements for the degree of Master of Science in Geo-information Science and Earth Observation.
Specialization: Geoinformatics

SUPERVISORS:
Ms. Dr. Ir. W. Bijker
Dr. V.A Tolpekin

THESIS ASSESSMENT BOARD:
Prof.Dr.Ir. A. Stein (Chair)
Dr. T. Woldai, Twente University, ITC Faculty (External)

If you perceive that there are four possible ways in which something can go wrong, and circumvent these, then a fifth way, unprepared for, will promptly develop. (Murphy's Law)

ABSTRACT

In the Netherlands, the coastal zone is a dynamic area because of the geographic position, natural and human changes. Global warming conditions, their natural environment conservation and the economic activities, are demanding nowadays continuous accurate and detailed coastline detection.

The launch of new satellites between 2007 and 2008 such as Advanced Land Observing Satellite (ALOS) in L-band, Radarsat-2 in C-band and TerraSAR-X in X-band which are able to operate in polarimetric SAR mode, quad-polarization (HH, HV, VH and VV), with a high spatial resolution, in some cases, as fine as 3 m, represents a new alternative for shoreline detection. For this study, TerraSAR-X quad polarization was obtained at 3 m azimuth resolution during the Dual Receive Antenna (DRA) campaign.

The purpose of this work is to detect the shoreline by the polarimetric decomposition in three different scattering mechanisms, which are; volume scatter from a cloud of randomly oriented dipoles, double bounce scatter from a pair of orthogonal surfaces with different dielectric constants, and Bragg scatter or surface scatter from a moderately rough surface. This composite scattering model provides a useful way to classify the image from the different mechanisms described before. After the decomposition, region growing segmentation was applied to group neighboring pixels with similar values and therefore identifies the shoreline.

Den Haag beach has been chosen for analysis in this study. The primary applied methodology is the Freeman and Durden decomposition and two subsequent classifications; Wishart supervised with Maximum Likelihood and without supervised classification before the region growing segmentation. The output segmentation vector is validated by comparing with nautical charts and Google Earth image to analyze the differences in the coastline. Buffer method is used to evaluate the accuracy and precision of the final outputs.

Quad polarization radar data for shoreline mapping detection is still in its nascent stages. Our results show potential for shoreline mapping. Further exploration of the possibilities, including better validation is needed, as the distance to Baseline at a given tide level depends on the local topography of the coast and it is not equal in all places. After final analysis, Method 1 applying supervised Wishart classification produces better results than Method 2 using buffer method. For visual interpretation both methods reach an acceptable output.

Keywords: *Polarimetric SAR, polarimetric decomposition, supervised classification, shoreline extraction.*

RESUMEN

En los Países Bajos, la zona de costa es un área dinámica debido a su posición geográfica, a los cambios producidos por el hombre y cambios de la naturaleza. Las condiciones de calentamiento global, la conservación de su medio ambiente y sus actividades económicas, demandan en estos días, una continua, precisa y detallada detección de costas.

El lanzamiento de nuevos satélites entre el 2007 y 2008, tales como Advanced Land Observing Satellite (ALOS) en banda L, Radarsat-2 en banda C y TerraSAR-X en banda X, son capaces de operar en modo polimétrico, quad-polarization (cuatro polarizaciones) (HH, HV, VH and VV), con alta resolución espacial, en algunos casos, hasta los 3 m, representa una nueva alternativa para la detección de costas. Para este estudio, imágenes de TerraSAR-X con quad polarization fueron obtenidas con una resolución en azimut de 3 m, durante la campaña denominada, Dual Receive Antenna (DRA).

El propósito de esta investigación es la detección de la línea de costa, descomponiendo los componentes polimétricos en tres diferentes mecanismos de dispersión (scattering), los cuales son; volumen, doble y de superficie. Este tipo de descomposición muestra una gran ayuda a la hora de clasificar la imagen en diferente tipo de clases, proveniente desde los diferentes tipos de mecanismos descritos anteriormente. Después de la descomposición, segmentación con región de agrandamiento (region growing) fue aplicado para agrupar los pixeles adyacentes con valores similares y posteriormente identificar la línea de costa.

La playa de la Haya fue elegida para el análisis en este estudio. La principal metodología es la descomposición por Freeman and Durden y luego dos clasificaciones; la Wishart clasificación supervisada con Maximum Likelihood y sin ninguna clasificación supervisada o pre clasificación. Los resultados en vectores, provenientes de la segmentación fueron validados comparándolos con cartas náuticas e imágenes de Google Earth, con la finalidad de analizar las diferencias en la línea de costa. La detección por medio de Buffers fue creado para la evaluación de la exactitud y precisión de los resultados finales.

La data de radar en quad polarization para el mapeo y detección de la línea de costa aún permanece en una etapa inicial, aunque nuestros resultados muestren un potencial para el mapeo de la línea de costa. Posterior investigación de las posibilidades, incluyendo una mejor validación es necesaria, debido a que la línea de base a un nivel de marea no va a ser igual en todos los lugares, dependiendo de la topografía en lugares específicos de la costa.

Luego de los análisis finales empleando la detección por medio de Buffers, el Método 1, empleando la Wishart clasificación supervisada obtuvo mejores resultados con respecto a la Método 2. Empleando interpretación visual, ambos métodos alcanzaron un resultado aceptable.

Palabras claves: *Polarimetría SAR, descomposición polarimétrica, supervisión clasificada, extracción de la línea de costa.*

ACKNOWLEDGEMENTS

I owe my deepest gratitude to the Faculty of Geo-Information Science and Earth Observation of the University of Twente in the Netherlands with the support of their staff for making this thesis possible. This thesis would not have been possible without the support of the Peruvian Navy in especial the Peruvian Hydrographic Service, which I am grateful for their support and confidence.

It is a pleasure to thank those who made this thesis possible, specially my two supervisors. Ms. Dr. Ir. W. Bijker and Dr. V.A Tolpekin, for their continuous support, patience, motivation and immense knowledge, thank you also for your time, advices and recommendations.

I also extend my most sincere thanks to all the lecturers from GFM course and to Dr. T. Woldai for the advanced module in SAR, with whom I had the possibility to work with radar data in detail for first time.

I would like to show my gratitude to the German Aerospace Centre (DLR) to give me the opportunity to work with the experimental data with the proposal number COA 0956. To the Netherlands Hydrographic Service (NLHS), Rijkswaterstaat and to the PolSARpro team for their guidance, recommendations and time, making this thesis a friendly and scientific environment.

To my dear friends, I do not have a specific word to show my thankfulness to them. They made me feel like one more member of their family, with different culture, religion, food, music and enthusiasm. (Bolivia, Cambodia, China, Indonesia, Guatemala, South Korea, Albania, Iran, Georgia, Cuba, Peru, Ecuador, Colombia and España) my deeply gratitude for each one of you guys, Thank you! Gracias!

Last but not least, I would like to thank my family. They did a special work behind this thesis, giving me a silence support and at the same time making me feel their entire love.

Finally, I dedicate this thesis to my wife Katty. We just know that this time is making us better as couple and stronger to build our lovely family in the future. Te Amo.

TABLE OF CONTENTS

LIST OF FIGURES

LIST OF TABLES

1. INTRODUCTION

1.1. Motivation and problem statement

In the Netherlands, the coastal zone is a dynamic area because of the geographic position, natural and human changes. Global warming conditions, their natural environment conservation and the economic activities, are demanding nowadays a continuously, accurate and detailed coastline detection. Dutch authorities have a requirement for coastline estimation. Furthermore, the current sea defences are sufficient for now but expert's recommendations and some new calculations showed many weak spots. In addition, sea level rise and continuing rains increase the river current (made more extreme by global warming) over the years. In consequence, coastline is changing rapidly, because, water from the river can't flow normally to the ocean and the land subsidence is increasing. So frequent mapping is required.

For that reason, the Second Delta Committee [1], gave its advice in 2008. It expects a sea level rise of 65 to 130 cm by the year 2100 and of 2 to 4 m by the year 2200.

In that sense, I am focusing my evaluation and analysis in coastline detection in the South Holland province, using quad polarization mode. In addition, I am following the recommendations 9th and 10th [1]. These recommendations are demanding continuous monitoring of that area, task that are usually difficult and expensive by means of field surveys, local environment and human preparation.

Cost-effectiveness is an important point and for that purpose, remote sensing can be an economic solution. This research will explore some possibilities for extracting relevant coastal zone information from polarimetric SAR data, in specific the new quad polarization mode from TerraSAR-X.

Various methods for coastline extraction from optical imagery have been developed. Coastline can even be extracted from a single band image but these methods are not suitable for certain areas in the world which have a cloudy, foggy and rainy environment.

The development of Synthetic Aperture Radar is ideal to deal with this kind of environment, because SAR is an active imaging method, it is independent of sun illumination, it uses microwaves that permit to penetrate clouds and partially canopy, soil, rain and snow.

Second generation imaging SAR sensors were designed to provide data with a spatial resolution of around 25m (12.5 m pixels) and dual-polarization mode. For that mode Greidanus [2], concludes that beach is characterized using cross polarization mode and suggested to use this property as an indicator of land-water boundary detection.

Polarimetric radar can measure the scattering properties of a target. There are four typical combinations (HH, VV, HV and VV), where the first letter indicates the transmitted polarization and the second indicates the received polarization [3].

The launch of the new satellites between 2007 and 2008 such as Advanced Land Observing Satellite (ALOS) in L-band, TerraSAR-X in X-band and Radarsat-2 in C-band are able to operate in polarimetric mode (4 polarizations simultaneously / quad-polarization), that means that four images are acquired simultaneously and a high spatial resolution as fine as 1m, which represents a new alternative for shoreline detection. According to van der Sanden [4] the new mode permits more accurate and more complete retrieval of information.

While dual polarized data only have two different polarization states (e.g. VV and HH), quad polarized data contain the complete scattering information with regard to polarization (VV, VH, HV, HH). By measuring the full polarization properties of the backscattered wave, we can learn more about the target than by using a single polarization. Different polarization mode can detect different surface roughness.

E.g. HH polarization can be used to determine urban settlement and HV polarization can be used in the same area, to determine the surface relief. In more detail Table 1 shows some anticipated effects of new radar sensors for different applications by using different polarization modes from RADARSAT-2 [4].
The use of quad polarization mode provided detailed information about the structure and shape of the scattering surfaces. Complementary information content has been improving the ability to characterize physical properties of objects (e.g. length, location, etc.), more detailed information and the retrieval of bio- or geophysical properties of the Earth's surface [5]. At more information coming from different polarization modes, like the dielectric and geometric characteristic of the surface, the images are also having more speckle. For that reason, it was one of my objectives, to explore and analyse the characteristics of the quad polarization speckle reduction filters.
In the case of coastline mapping, the problem is that it requires an integration of several scientific disciplines including tidal models and variations, SAR image geo-referencing and SAR image classification. Detection of coastlines under different tide levels can be also a problem during the analysis.
Work with new products and services or innovate applications is interesting from a scientific point of view. However, quad polarization radar data for shoreline mapping detection and other applications remains in its nascent stages, as a result of limited availability and evaluation. For that reason, it was also my purpose to explore the new modes for further research and applications.
TerraSAR-X did a special campaign for quad-pol data collection and the data is available just for that period, so, it is limited [6]. I explored the data and we found six images with quad polarization mode in my area of research. The images have the particularity that, 2 images are in low tide, two other images are between high and low tide and two more in high tide. It was interesting to analyse and maximize the new functionality of quad polarization to detect the difference between wet and dry coast and to estimate if the tide prediction are according with the real tide.
Only with the continuous research of this relatively new operational space borne quad polarization data, we can maximize the benefits of these technological innovations.

Table 1-1: Anticipated effect of new RADARSAT-2 features on applications potential in terms of data information content [4]

	RADARSAT-2 feature					
Application	Selective single-polarization	Selective dual-polarization	Quad-polarization	Ultra-fine spatial resolution	Selective look direction	Improved orbit control
Agriculture						
Crop type	–	–/+	+	–	–	–
Crop condition	–	–/+	+	–/+	–/+	–
Crop yield	–	–	–/+	–/+	–	–
Cartography						
DEM interferometry	–	–	–	+	–	+
DEM stereoscopy	–	–	–	+	–	–/+
DEM polarimetry	NA	NA	+	NA	–	–/+
Cartographic feature extraction	–	–	–/+	+	–	–/+
Disaster management						
Floods	–	–	–	–	+	–
Geological hazards	–	–/+	–/+	–/+	+	– (+)[a]
Hurricanes	–/+	–	–/+	–	+	–
Oil spills	–/+	–	–	–/+	+	–
Search and rescue	–	–	+	–/+	+	–/+ (+)[a]
Forestry						
Forest type	–	–	–/+	–/+	–	–
Clearcuts	–/+	–	–	–/+	–	–
Fire scars	–/+	–	–	–/+	–	–
Biomass	–	–	–	–	–	–
Geology						
Terrain mapping	–	–/+	–/+	–/+	–	– (+)[a]
Structure	–	–/+	–/+	–/+	–	–
Lithology	–	–	–	–	–	–
Hydrology						
Soil moisture	–	–	–/+	–	–/+	–
Snow	–	–	–/+	–	–/+	–
Wetlands	–	–/+	–/+	–/+	–	–
Oceans						
Winds	–/+	–	–	–	–	–
Ships	–/+	–/+	–/+	+	–/+	–/+
Waves	–	–	–/+	–	–	–
Currents	–/+	–	–	–	–	–
Coastal zones	–/+	–/+	–/+	–/+	–	–
Sea and land ice						
Sea ice edge and ice concentration	–/+	–	–/+	–	–/+	–
Sea ice type	–	–	–/+	–	–	–
Sea ice topography and structure	–/+	–	–/+	–	–/+	–
Icebergs	–/+	–	–/+	+	–/+	–/+
Polar glaciology	–/+	–	–/+	–	+	– (+)[a]

Note: –, minor; –/+, moderate; +, major; NA, not applicable.
[a]Using interferometric SAR (InSAR) techniques.

1.2. Research identification

The aim of this research is to evaluate how the high spatial resolution from TerraSAR-X satellite by using the experimental quad polarization data, from the Dual Receive Antenna, as fine as 3 m, in Stripmap mode is suitable to map the shoreline of the South Holland province. This area is ideal and it has some special requirements and recommendations as we mention in Section 1.1. The availability of the data in that area is product of a special campaign did it by DLR, during March and April 2010 and provided only for scientific purposes.

1.2.1. Research objectives

The main objective of this research is to evaluate the use of the complete backscattering information coming from the polarimetric data, by using the experimental quad polarization mode from TerraSAR-X, with high spatial resolution as fine as 3 m, to map the shoreline of the South Holland province as study area.

There are three sub objectives for this research proposal:

1. To improve the quality of SAR images in shoreline detection using the complete polarimetric backscattering information from quad polarization mode in the South Holland province.
2. To improve the accuracy of the shoreline detection, using the new high spatial resolution from TerraSAR-X, in different water sea level (tidal) scenarios.
3. To explore the new modes for further research and applications.

1.2.2. Research questions

1. To improve the quality of SAR images in shoreline detection using more detailed backscattering information from quad polarization mode in the South Holland province.
   a. Which physical characteristics from quad polarization mode are suitable to improve shoreline detection?
   b. How can we deal with the increasing speckle to create high quality shoreline information?
2. To evaluate the shoreline detection, using the new high spatial resolution in different sea level (tidal) scenarios
   a. How good can the shoreline be improved by using TerraSAR-X sensor, using the new high spatial resolution?
   b. How well can the shorelines in the South Holland area be detected, using different sea levels?
3. To explore the new modes for further research and applications
   a. What is the new contribution of TerraSAR- X in quad polarization mode for shoreline detection?

1.3. Innovation aimed

The successful launch of TerraSAR-X in June 2007 was the start of a campaign to map the Earth at an unprecedented level of accuracy. The aim of TerraSAR-X is to create new high –quality radar images of the Earth's surface over the next five years [7]. TerraSAR-X is able to produce image data with a resolution as fine as 1 meter in spotlight mode and 3 meter in stripmap mode. It can operate in several polarization modes, such as single, dual and quad polarization.

According to van der Sanden [4], new spaceborne satellites can be able to improve the utility of many data products for 32 applications in the fields of agriculture, cartography, disaster management, forestry, geology, hydrology, oceans, and sea and land ice (see Table 1.1).

Few investigations have concentrated on the detection of shoreline using SAR images. Most of them applying single and dual polarization with a spatial resolution of around 25 meters (12.5 m pixels) and they defined that with cross polarization the visual detection of the shoreline is good. But, according to Moon [8], results obtained from NASA AIRSAR L-band and RADARSAT-2 C-band, do not fully agree with ground measurement.

This research provides a new approach to evaluate the complete backscattering information coming from the polarimetric data by using the experimental quad polarization mode to detect and map increase the high quality the shoreline of the South Holland province, using high spatial resolution, increasing from 10-20 meters to as fine as 3 meter, using Stripmap mode. That allows extracting more information out of the measurement data for shoreline detection in the South Holland province.

Finally, quad polarization mode for shoreline mapping and other applications remains in its nascent stages. For that reason, it is also my purpose to explore the new quad polarization mode to evaluate the contribution of TerraSAR-X for shoreline detection.

2. ACTIVE MICROWAVE SYSTEMS AND RELATED WORK

The main characteristic of the active systems is that they provide their own illumination, while, in the opposite site, the passive systems depend on external sources of illumination or thermal radiation. That main characteristic offers more options and more applications than are possible with passive systems.
Active microwave systems are almost independent of weather conditions and time of day. Although heavy precipitation can cause difficulties, these are less significant than for passive systems with the same wavelength [9].
The Microwave portion of the spectrum includes wavelengths within the approximate range of 1 mm to 1 m.

2.1. Radar Active microwave

Radar is an acronym for radio detection and ranging. Radar was developed to be able to detect the presence of objects by using radio waves and to determine their distance and sometimes their angular position [3]. The fundamental equation showing the amount of signal received by a radar system from a particular target is called the radar equation [9].

$$W_r = \left(\frac{W_t G_t}{4\pi R^2}\right)(\sigma)\left(\frac{1}{4\pi R^2}\right) A_r \tag{2-1}$$

Here, W_r is the received power, W_t the transmitted power, G_t the gain of the transmitting antenna, R the slant range to the target (distance from radar to target), A_r the effective aperture of the receiving antenna; and σ, the effective backscattering cross section.
In the above radar equation, the parameters which influence surface radar backscatter are related to several additional system parameters and target parameters. See Table 2.1.

Table 2-1: Fundamental system and target parameters that influence Radar power return [10]

Fundamental system and target parameters that influence Radar power return	
System Parameters	Target Parameters
Wavelength or Frequency	Surface Roughness
Polarization	Complex Dielectric Constant
Look Angle	Slope Angle & Orientation
Look Direction	
Resolution	
Direct interplay of system and target parameters	
Surface roughness: Defined in terms of system wavelength	
Look angle ($\emptyset$) and slope angle (α): Combine to determine Incidence angle (θ)	
Look direction and slope (or target) orientation: Influence the area and geometry of the target presented to the radar	

Imaging radar was developed as reconnaissance military sensor in the late 1940s. It became a very useful tool, not only because it can penetrate almost all kind of weather situation, but also because it is an active sensor, day or night imaging system. However, and after the military declassification, the radar technology is having very good acceptance in the scientific environment, because it can be able to detect some natural resources, because it can detect their dielectric property that optical images cannot detect.
Imaging radar system works using an antenna fixed below the spacecraft. That antenna is pointing to the side, and it is well known as side-looking radar (SLR). Microwave energy is transmitted from an antenna in very short bursts or pulses.
In Figure 2.1, the radar system transmits a radar pulse to the area of interest that pulse is going radially way and in 10 different times (1 to 10). The solid line shows the transmitted pulse and the dashed line represents the reflected pulse from the target or area of interest.

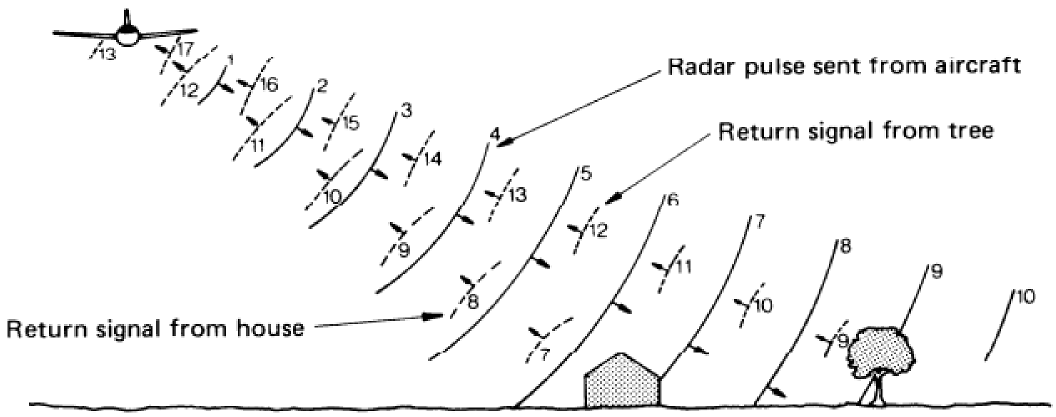

Figure 2-1: Propagation of one radar pulses, indicating the wave front location at time intervals 1-17 [3]

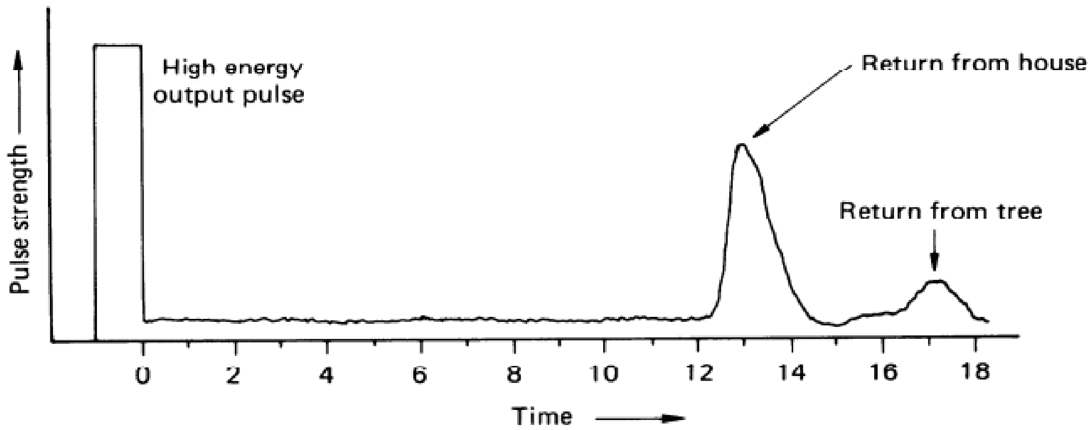

Figure 2-2: Resulting antenna return [3]

During the time interval 6 (Figure 2.1), the pulse reached the object (house) and immediately the pulse starts the reflection in time interval 7 (dashed line) and then that echo reaches the sensor at time 12. While the transmitted pulse still detecting the area of interest and in time interval 9 (solid line), the pulse reached the tree and this reflected echo (dashed line) reaches the antenna at time 17 [3]. In Figure 2.2, because tree reflectance has volume backscattering, some information is reflected to many angles and just some pulses are going back to the sensor, also the dielectric component of tree leaf decrease the reflectivity of radar waves. For that reason, as tree is less reflective of radar waves than house, a weaker response is recorded.

2.2. Synthetic Aperture Radar (SAR)

As higher resolution, longer antenna the sensor needs, but in the reality is not possible. In that sense, SAR systems employ a short physical antenna by using Doppler effect and the azimuth resolution can be described as $A_r = \frac{l}{2}$, where l is the antenna length. SAR systems permit much finer resolution than real aperture system [9]. By employing short antenna, they modified data recording and processing techniques, reducing or synthesizing the effect of a very long antenna. The result of this operation mode is a very narrow and effective antenna beamwidth, even at far ranges. The use of long antenna or a short operating wavelength was not required anymore [3]. SAR imaging systems have more technology and for that reason, are more sophisticated and complex than RAR systems [10].
Radar equation for the synthetic aperture system is obtained by approximating the following equation [9]:

$$W_r = \frac{W_t G^2 \lambda^2 \sigma^0 r_a r_r}{(4\pi)^3 \, R^4} = kTBFS_i \tag{2-2}$$

The received power has been shown both in terms of radar equation and in terms of the signal-to-noise ratio and noise level in the receiver. The central term in this equation is like equation (2-2) with everything assumed constant across the illuminated area. The area itself is given by $r_a r_r$, the product of azimuth and range resolution.
The receiver noise is $kTBFS_i$, where k = Boltzmann's constant, T = temperature (°K), B = band width (Hz), F = receiver noise figure. The quantity S_i is the signal to noise ratio required for a single pulse return.

2.3. Incidence angle

Incidence angle (θ), is the angle between the radar line-of-sight and the local vertical from the surface (Figure 2.3-A and 2.3-B) with respect to the geoid. This angle has a big influence on the radar backscatter and for the appearance of objects on the imagery. The next section presents more detail about the influence of incidence angle on the geometric characteristics.
In general, reflectivity from distributed scatters decreases with increasing incidence angle. Figure 2.3-A illustrates incidence angle incorporating look angle (α) and the curvature of the earth. In contrast, Figure 3-B illustrates the "local incidence angle" and takes into account the local slope angle (α). For example, surface roughness changes as a function of the local incidence angle [10].

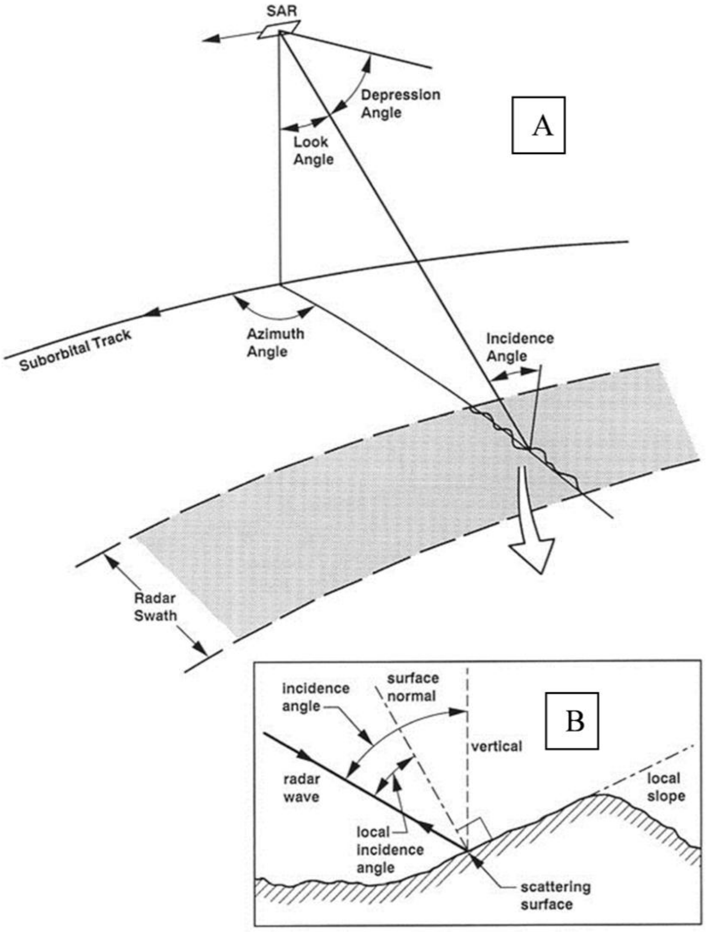

Figure 2-3: Schematic Diagrams of System (2.3-A) and local (2.3-B) Incidence Angle (θ) [10]

2.4. Scattering mechanism and geometric characteristics of radar imagery

The geometric characteristics of radar imagery in comparison from both photography and scanner imagery are different, because radar is a distance rather than an angle measuring system. The effects on image geometry are many and varied, such as scale distortion, relief displacement [3].

2.4.1. Slant-range scale distortion

Radar records objects in respect to the distance from aircraft or spacecraft to the object, thus forming a slant range image [10]. In Figure 2.4, the spacing between pixels in the range direction and the time interval between received pulses are directly proportional to each other, but not proportional to the true horizontal distance along the ground. That effect compresses the image scale at near range, while expanding it at far range.

In that sense, in ground-range format, the image pixels are spaced in direct proportion to their distance along a theoretical flat ground surface [3]. For that reason, most users of radar imagery prefer the data to be displayed in a ground range projection.

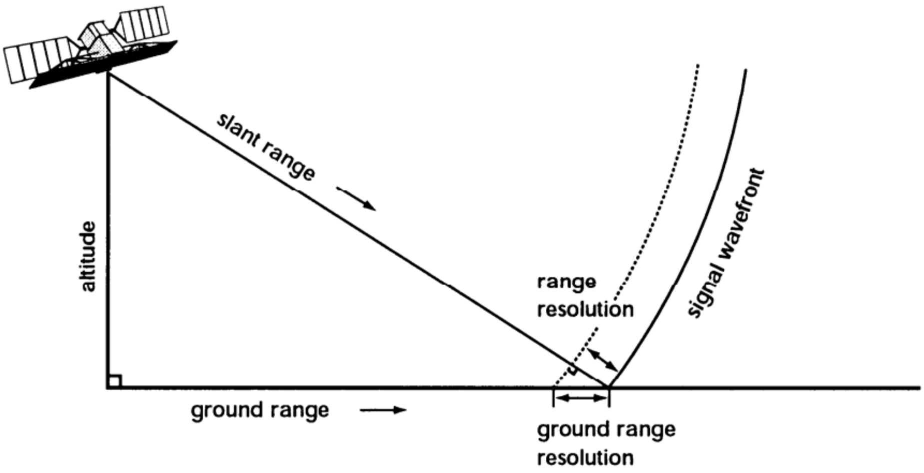

Figure 2-4: Slant and ground range resolution [11]

Using trigonometry, ground range distance can be calculated from slant range distance and platform altitude to convert to the proper ground range format.

2.4.2. Roughness and geometric characteristics

Roughness characteristic of the target, influence the appearance of a feature on radar imagery. Henderson [10], describe three scales of roughness; microscale, mesoscale and macroscale.

For microscale roughness, is when the surface is smooth and the energy is reflected away from the surface, resulting the angle of reflection the same as the angle of incidence and the energy is reflected and not backscattered (Figure 2.5–a). Microscale roughness of the target strongly determines image tone; in this case the surface appears as darker toned area on an image. It is also called specular reflection.

Mesoscale roughness occurs in forest covered landscape, canopy variation, it is also related to surface elevation changes and slope variability in relation to the spatial resolution of the system. Mesoscale roughness is related to image texture.

Macroscale roughness has a directly relation with the terrain slope and it is strongly accentuated by radar shadowing. Macroscale roughness is the most important image interpretation key, because we can delimit geomorphic or geologic regions as well as landuse regions [10].

This arises through variations in the relative sensor/terrain geometry for differing terrain orientations. Variations in local incidence angle result in relatively high returns from slopes facing the sensor and relatively low returns, or no returns, from slopes facing away from the sensor [3].

Surface is considered "rough" when it has a diffuse reflection, because of the geometric characteristic of the area reflected which scatters the energy equally in all directions (Figure 2.5-b). A significant portion of the energy will be backscattered to the radar, such that a rough surface will appear lighter in tone on an image.

Corner reflection occurs when the target object reflect most of the energy directly back to the antenna (Figure 2.5–c). The result is a very bright appearance of the object reflected. That effect occurs when there are buildings, metallic structures for urban environments and folded rocks for natural environments.

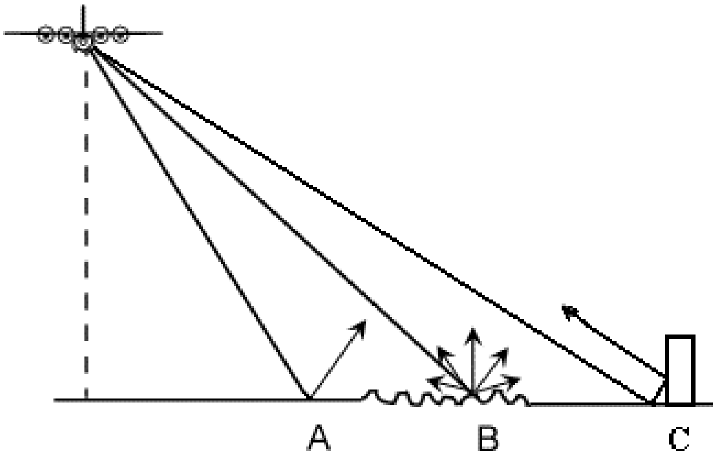

Figure 2-5: Roughness and geometric characteristics

2.4.3. Electrical / Dielectric characteristics

The intensity of radar returns can be determined by using the electrical and the geometric characteristics of the terrain features. One measure of an object's electrical character is the complex dielectric constant. Last parameter is an indication of the reflectivity and conductivity of various materials [3].

The most natural materials have a dielectric constant from 3 to 8 when dry; water has a dielectric constant of about 80. The presence of some moisture in soil and vegetation can significantly increase radar reflectivity [10]. The changes in radar signal are more often linked to changes in moisture content than they are to change in the material themselves.

2.5. Radar image speckle

Radar signals reach the terrain surface in many angles, depending on the incidence angle of transmitted signal and local incidence angle. The backscatter signal is subject to random fluctuations, resulting from the interaction of the radar wave or pulse and the rough terrain surface. That effect is known as fading [10] and this is responsible for speckle. In Figure 2.6, we can analyse the interface pattern between the signals adding in phase and out of phase.

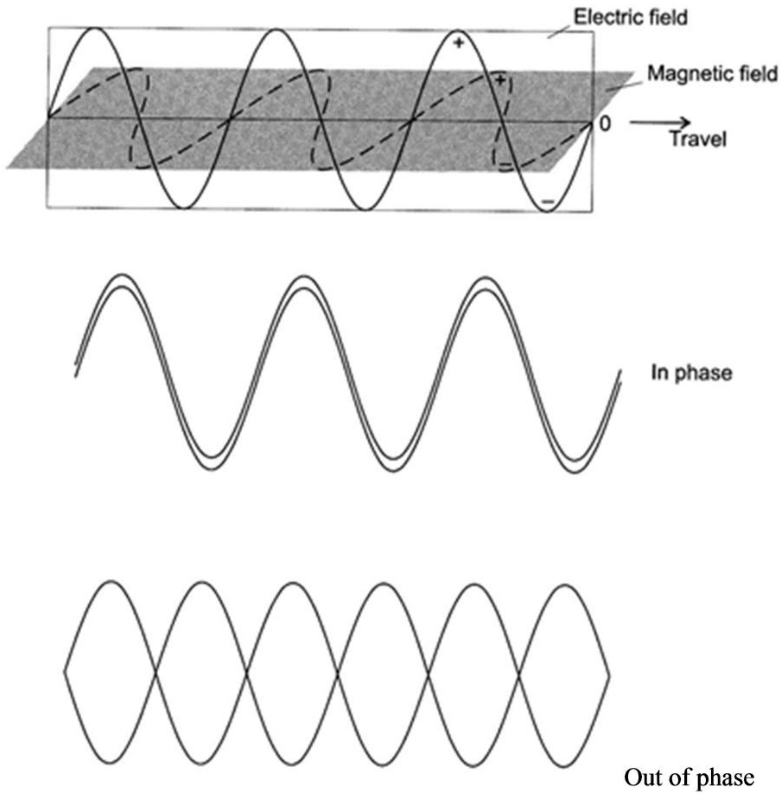

Figure 2-6: Electromagnetic wave, in phase and out of phase, modified from [3]

In the previous figure, the effect causes a pixel-to-pixel variation in intensities, and the variation manifests itself as a granular speckle pattern in SAR images. As we illustrate in the following Figure 2.7.

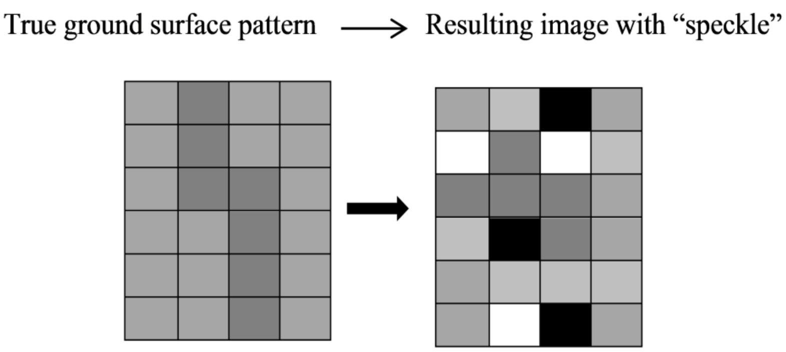

Figure 2-7: Pixel to pixel variations in speckle effects, modified from [3]

Speckle in SAR images complicates the image interpretation and image analysis, and reduces the effectiveness of image segmentation and feature classification [12].
All radar images contain some degree of speckle, a seemingly random pattern of brighter and darker pixels in the image [3].

There are two principles components which influence the transmission characteristics of the signals from all radar systems, those are; wavelength / frequency and polarization of the energy pulse used. Radar wavelength and frequency are inter-related as we can show in the following equations:

Where c is the speed of light $(3 \times 10^{8}\,\mathrm{ms}^{-1})$, f is frequency and λ is wavelength.

$$c = f\lambda \qquad \text{or} \qquad \lambda = \frac{c}{f} \tag{2-3}$$

There is various letters code (see Table 3) for the various wavelength bands (e.g., K, X, C, L). Radar signals are relatively unaffected by clouds. However, echoes from heavy precipitation can be considerable [3].

Table 2-2: Radar Band designations

Band Designation	Wavelength λ (cm)	Frequency $v = c\lambda^{-1}$ [MHz (10^{6}cycles $\sec^{-1}$)]
K	1.1 – 1.67	26,500 – 18,000
X	2.4 – 3.75	12,500 – 8,000
C	3.75 – 7.5	8,000 – 4,000
L	15 – 30	2,000 – 1000

Radar signals can be transmitted and/or received in different modes of polarization. In Figure 2.8, the polarization of an electromagnetic wave describes the direction of the electric field, oscillating along the geometric plane. Typically, radar signals are transmitted in a plane of polarization that is either parallel to the antenna axis (horizontal polarization, H) or perpendicular to that axis (vertical polarization, V).

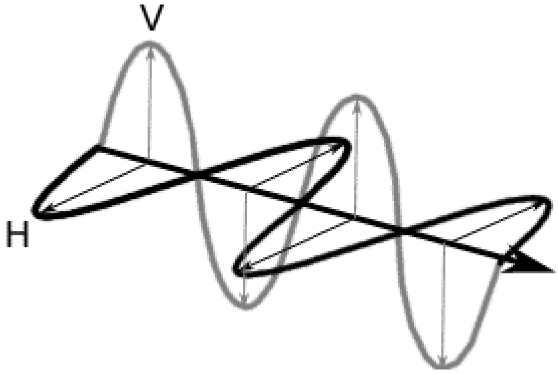

Figure 2-8: Horizontally polarized (H) and vertically polarized (V)

2.6. Polarization, polarimetric and scattering matrix

2.6.1. Polarization

In polarization, the electromagnetic wave has three vectors field. As we show in Figure 2.9, the direction of propagation (Z) is one vector; the electric (E) and the magnetic (H) fields are the other two vectors fields.
Linear polarized radar systems can operate in horizontal or vertical polarization microwave radiation (Figure 2.9). In one hand, if the electric vector field is parallel to the X-axis (vertical) the wave would be vertically polarized. On the other hand, if the electric vector field is parallel to the Y-axis (horizontal), the wave would be horizontally polarized [10].

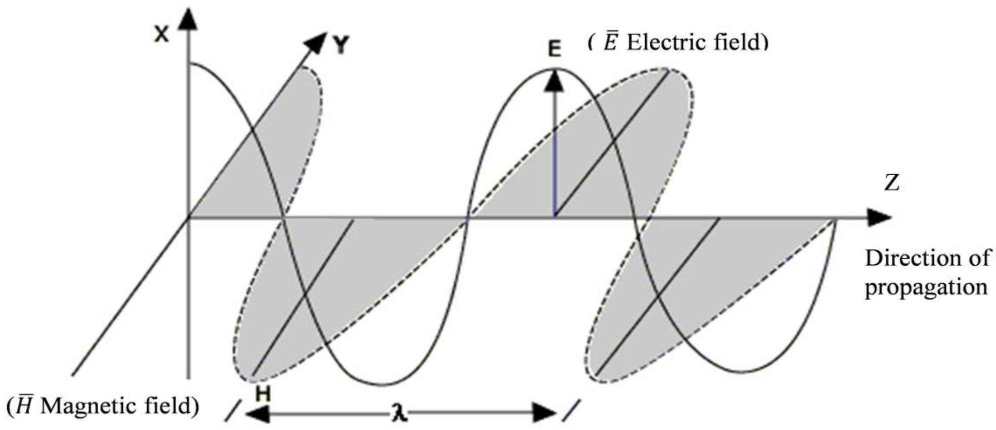

Figure 2-9: Components of an electromagnetic wave, modified from [10]

There are four typical polarization combinations (HH, HV, VV, and VH), where the first letter indicates the transmitted polarization and the second indicates the received polarization [3]. The HH and VV cases are referred to as like-polarized or co-polarized signals, while HV and VH are referred to as being cross-polarized.
To be able to understand the interaction of the target and the polarized signal it was necessary to do some research and then several statements can been made. If the surface plane of linear features is parallel to the polarized signal of the transmitted microwave radiation, the like-polarized or co-polarized radar returns stronger signal than transmitted and received signal in orthogonal plane.
As an example, we can evaluate the wheat field. The natural geometric characteristic of this field is in vertical shape, in that sense; we can expect that VV will have a stronger returned signal than HH. In this case, the like polarized image (HH-VV) will have a stronger returned signal than the cross polarized image (HV or VH) [10].
A system that measures all four of these orthogonal polarization states (HH, HV, VH and VV) is referred to as being "fully polarimetric" or quadrature-polarized.

2.6.2. Polarimetric

Polarimetric radar systems are sensitive to the polarization states of both the transmitted and received radar signals as difference as single-polarization radar systems. Single-channel polarization measured only one component of the scattered wave, a vector quantity. The additional polarization properties coming

from the reflected signal of the surface is lost. To retain all the information from the scattered wave, a vector measurements process is needed [13].
The multidimensional information provided by SAR systems via multiple polarizations increase the possibility to investigate Earth terrain. The multiple frequencies or polarizations permits the analysis of different scattering mechanism and therefore, different components of the scattering layers [14].
Imaging radar polarimeter permits measurement of the full polarization response of every resolution element. It also permits the measurement of the amplitude and relative phase of all transmitted and receiving polarizations [13].
One of the main advantages of polarimetry in the application context is that choosing the correct transmit and receive polarization; the contrast between targets and backgrounds can be maximized [15].

2.6.2.1. Polarimetric measurements

The complex (amplitude and phase) scattering matrix for each resolution of the radar image in polarimetric systems is called the basic quantity measured [13].
Normally in single-channel data, one of the copolarized measure S_{hh} or S_{vv} , is available and for distributed targets, the phase does not have useful information[14]. If a radar system is configured to measure all possible combinations available from the horizontal and vertical polarizations, then the complete scattering matrix for a resolution element may be determined.
By comparing the theoretical and observed polarization signatures permits the analysis and identification of the dominant scattering mechanism[16].

2.6.3. Scattering matrix

As has been mentioned before, when the transmitted horizontally or vertically polarization reach to the target, the backscattered wave can return in both horizontal and vertical polarizations. In that sense, the two orthogonal radar polarizations, linear horizontal (H) and linear vertical (V), are used to measure the scattering matrix in SHH, SHV, SVH and SVV. Those components are necessary to describe the electromagnetic wave.

$$\begin{bmatrix} E_h^s \\ E_v^s \end{bmatrix} = \begin{bmatrix} S_{hh} & S_{hv} \\ S_{vh} & S_{vv} \end{bmatrix} \begin{bmatrix} E_h^i \\ E_v^i \end{bmatrix} \tag{2-4}$$

The scattering matrix S, describes the transformation of the electric field of the incident wave to the electric field of the scattered wave (1-5). When the superscript i refers to the incident wave and s refers to the scattered wave.
Polarization synthesis is the process which any combination of the transmitting and receiving antenna is calculated by having a previous knowledge of the scattering matrix S [16]. By having the scattering matrix, the strength and polarization of the scattered wave of the incident wave can be obtained [17].
Copolar, are the diagonal elements in the scattering matrix, since they have the same polarization attributes. Cross polar are the off diagonal elements and they relate the orthogonal polarization states.
Polarimetric SAR can be affected by different distortions and by the uncorrected spatial or temporal variations in power or gain, like;

- Crosstalk, due to coupling of orthogonal polarizations on transmits and/or receives;
- Channel imbalance caused by different transmitted powers in the H and V channels, differing gains on receive and/or system-induced phase shifts between channels.

The most important distortion is Crosstalk, because it scrambles the information in the different channels. Many methods are well developed [18]. Channel imbalance can be separated into correction of phase and amplitude distortions. Calibration targets or internal calibration tones are needed to remove these effects [14].

2.7. The TerraSAR-X system

The successful launch of TerraSAR-X on 15 June 2007 from the Russian Baikonur Cosmodrome in Kazakhstan marked the start of a campaign to map the Earth at an unprecedented level of accuracy, in more detail (Table 2.3). The aim is to create new, high-quality radar images of the Earth's surface over the next five years [7].

TerraSAR-X is a German Earth-observation satellite and the objective of the mission is to provide value-added SAR (Synthetic Aperture Radar) data in the X-band, for research and development purposes as well as scientific and commercial applications.

Table 2-3: Technical Data [7]

TerraSAR-X (Stripmap and quad polarization mode)	
Launch date	15 June 2007
Launch site	Baikonur, Kazakhstan
Orbit altitude	514 km
Satellite mass	about 1230 kg
Satellite size	5 m height x 2.4 m diameter
Radar frequency	9.65 Ghz
Lifetime	at least 5 years
Wavelength	3.1 cm
Azimuth resolution	6.6 m
Revisit Time	11 days
Incidence angle range (Stripmap/Scan-SAR)	20 – 45 degrees

2.7.1. Capabilities

TerraSAR-X is an X-band radar sensor with a range of different modes of operation, different swath widths, resolutions and polarizations. TerraSAR-X thus offers space-based observation capabilities that were previously unavailable, like different polarization modes;

- Single polarization,
- Dual polarization and,
- Quad polarization (still under experiment)

For TerraSAR-X, quad polarization mode is still under experimental mode, because of the new operation system to collect data. The antenna is electrically split into front (fore) and behind (aft), segment during receive [19]

Different polarizations can be selected in both segments. Figure 2.10 illustrate the complete antenna transmits alternating H and V polarized pulses. The backscattered signal is received at the same time, in H polarization and the other one in V polarization by the both partitions of the antenna [20].

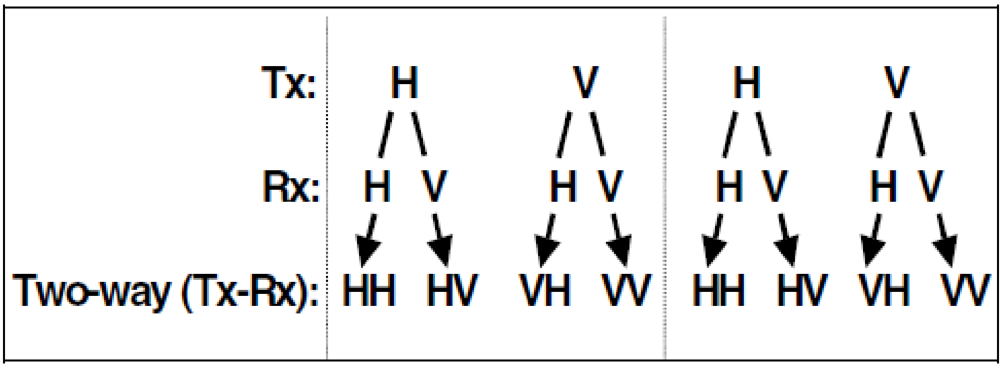

Figure 2-10: Polarization scheme for full polarimetric mode exploiting the DRA [20]

This can be done, because of the number of polarization are doubled by doubling the pulse repetition frequency (PRF) and the horizontal and vertical transmitting polarization in a pulse to pulse alternating mode like in dual polarization mode [19].
The sensor operates in three different modes (Figure 2.11):

- Spotlight mode, an area 10 kilometres long and 10 kilometres wide is recorded at a resolution of 1 to 2 meters,
- ***Stripmap mode covers a 30-kilometre-wide strip at a resolution between 3 and 6 meters and,***
- ScanSAR mode, a 100-kilometre-wide strip is captured at a resolution of 16 meters.

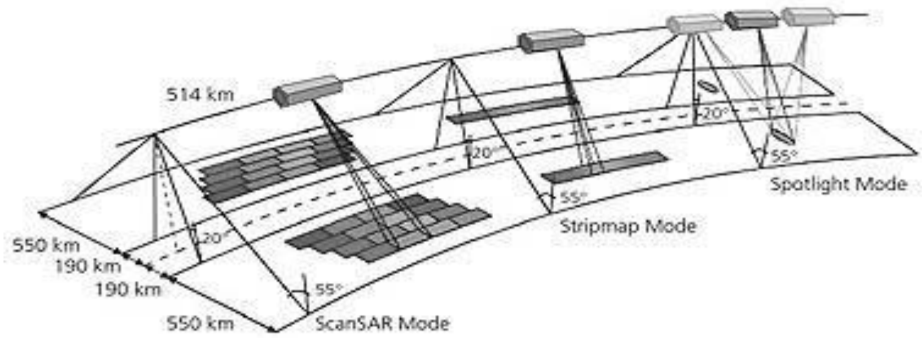

Figure 2-11: TerraSAR-X modes [21]

For Stripmap mode, the image strip has a constant image quality in azimuth, because the ground swath is illuminated continuously in a sequence of pulses while the antenna beam is pointed to a fixed angle in elevation and azimuth [21].
This mode permits to distinguish target points in different distances, perpendicular to the flight direction of the sensor by transit time measurements (Figure 2.12). The conversion of the measured transit time into a position on the ground is done by the inclined imaging geometry. Typically, stripmap mode works with angle of incidence between 20 and 60 degrees [7].

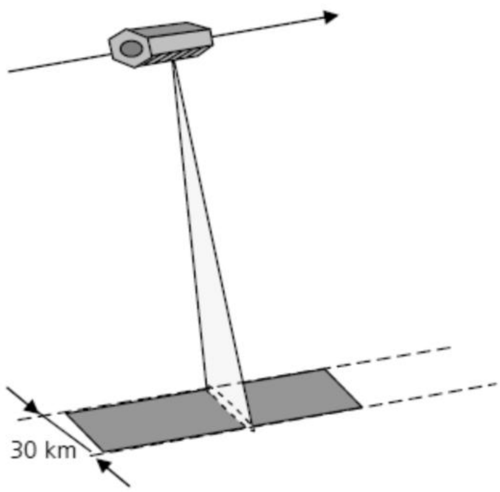

Figure 2-12: TerraSAR-X, Stripmap mode [21]

2.7.2. Dual Receive Antenna (DRA)

It was demonstrated during the last few years, that a secondary antenna and receiving channel can upgrade the existing SAR sensors for several reasons.

Dual Receive Antenna in TerraSAR-X sensor works without any mast or secondary antenna. DRA applies the group antenna concept and the antenna is electrically divided into two sections in azimuth direction in along track. In Figure 2.13 illustrates the principles of DRA. For transmission, the complete antenna is used, but receiving, the antenna is split it into two separate partitions. Finally, the signals of both receiving antennas are detected and recorded separately [20].

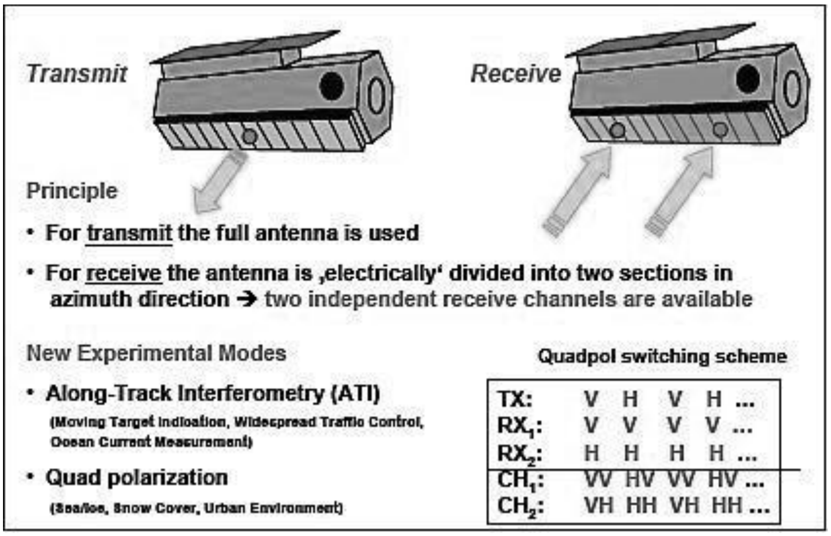

Figure 2-13: Dual receive antenna from TerraSAR-X [20]

2.8. Related work

Review of previous studies and related topics. In this section I identified two components:

- The first part deals with studies in coastline detection using single, dual polarization and airborne data.
- The second part deals with quad polarization in other applications.

The extraction of the coastline is always an important but difficult and expensive task by means of field surveys, local environment and human preparation.

Nowadays, the coastline extraction is a visual photo-interpretation of high resolution aerial images. This task is performed by cartographers, using several techniques, such as acquisition and evaluation of data from aerial platforms, geometric correction and ground checking of some points in the aerial images. Those techniques require experience, time and they are affected by human errors, like, manual interpretation and extraction of the coastline from the images acquired.

In the past, many researchers were trying to extract the coastline in an accurate, not expensive and simple way. For that purpose, SAR sensor is suitable for that work. Maureen [22] investigated some polarimetric methods for extracting the shoreline slope and to enhance the shoreline's land-water boundary from airborne SAR imagery. Greidanus [2] focused on the use of different polarization modes and analysis of different incidence angle for sea wave measurement, coast line determination, and estimation of surf zone parameters, concluding that the beach is well characterized by an increased co-cross correlation and they suggest to use that previous analysis as an indicator of land-water boundary. Automated delineation, using filters and speckle reduction was applied by Yu [23], the results were acceptable when comparing the automated delineation with the manual delineation. Baghdadi [24] describes the usefulness of airborne SAR imagery for coastline detection, using single and dual polarization with different incidence angle. They concluded for applying visual interpretation, cross polarization is good enough for coastline detection as well as co-polarization using high incidence angle.

For the second part, as I mention before, there are not many studies until now using this new sensor, and even quad polarization mode is still on experiment. Moon [8] describe that tidal flat compositions can be obtained from fully polarimetric SAR data. That paper shows how coastline can be detected with hydrodynamic modelling and global positioning system (GPS) measurements, using AIRSAR data.

A new research using quad polarization in combination with Landsat images for land cover classification is having good results [25], they conclude that the combination of radar with optical increase the overall classification accuracy.

The German Aerospace Centre (DLR) did a special campaign for quad-polarization data collection during April and May 2010. This information is being provided only for scientific purposes. There are more than 200 proposals already submitted and it is my intention, to work in this special campaign, using this quad polarization data for scientific purpose.

3. COASTAL GEOMORPHOLGY, STUDY AREA AND MATERIALS

3.1. Coastal definition and classification

The Coastal zone is of variable width and may change in time. Coastal zone has several descriptions and definitions from many authors and international organizations. Carter [26] describes coast as "the space in which terrestrial environments influence marine (lacustrine) environments and vice versa". Bird [27] describes coast as "a zone of varying width, including the shore and extending to the landward limit penetration of marine influence". Nelson [28] "A coastal zone is the interface between the land and water".

The coast is divided by the following terms [26]; the shore (Figure 3.1) is the zone between the water's edge at low tide and the coastline; it contains the foreshore, exposed at mean low water level (MLWL) or low tide and hided or submerged at mean high water level (MHWL) or high tide, and the backshore, extending from the high tide or MHWL and inundated in not normal conditions, like storms or anomaly high tides.

The coastline is defined most of the time as the land margin in the backshore zone. Coastline can be referred as the sea which adjoins the coast, comprising the nearshore and offshore zones, as coastal waters [27].

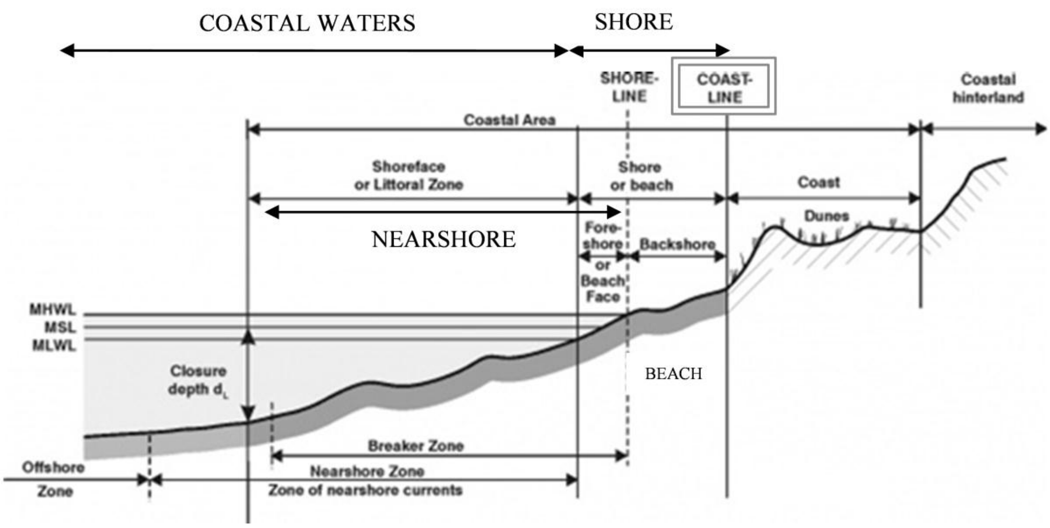

Figure 3-1: Coastal terminology (adapted from ([27]))

In this research, the objectives described in Section 1.2.1, are related to the detection of the coastline in the South Holland province but, as it is described in this Section, the definition and position of this line is ambiguous and difficult to determine. For that reason, the possibility to work with the National Entity in charge of Coastal Management was a good option.

The Netherlands Hydrographic Service determine the coast Baseline by using some techniques, described in the following sections and it is related by international conventions [29] with the Lowest Astronomical Tide (LAT) more information Section 3.2 and it is included in the Nautical Charts (Section 3.3.4). In that sense, the analysis and validation of the shoreline output from the radar images are going to be by using the coast Baseline and the nautical charts defined and determined by the Hydrographic Service.

According the literature, the definition of "shoreline" is closer with the definition of Baseline and for terms of analysis and description; the word "coastline" will be change to "shoreline".

3.2. Tides

Tides are directly related to the gravitational effects of the sun and the moon in relation to the earth. Tides are movements of the ocean and consequently; it regulates the sea levels along the coast [27].

In comparison from the Sun, the Moon is much closer to the Earth. In that sense, the Moon has a larger effect on the Earth, producing a bulge toward the moon (Figure 3.2). That effect also occurs at the same time in the opposite side of the Earth, due to inertial forces. This effect remains stationary while the Earth rotates [28].

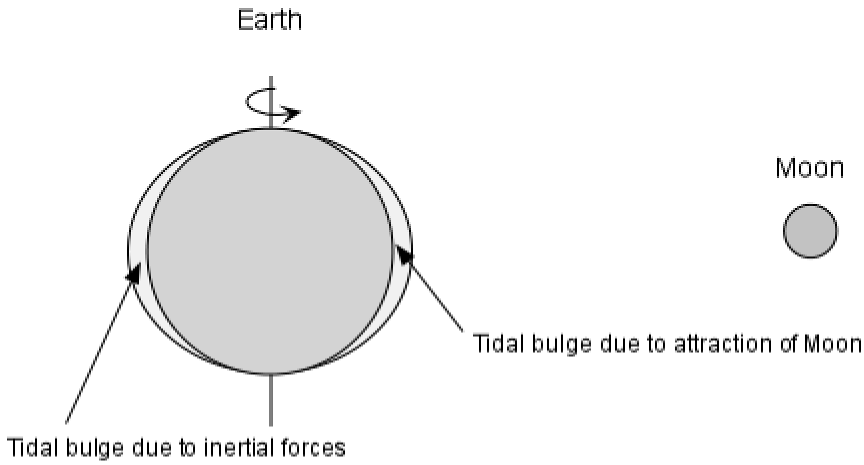

Figure 3-2: Earth tidal bulge produced by the Moon gravitational effect [28]

Even the Sun, that is far away from the Earth exerts a gravitational attraction on the Earth, consequently there are monthly tidal cycles produced from the relative position of the Moon and Sun [28].

The combination between the Sun and Moon when they are in the same side of the Earth, produce the highest high tide and it is called New Moon or on opposite side of the Earth, Full Moon (Figure 3.3). Therefore, when the Sun and Moon are not in the opposite side of the Earth, produced the lowest high tides and it is called Quarter Moons.

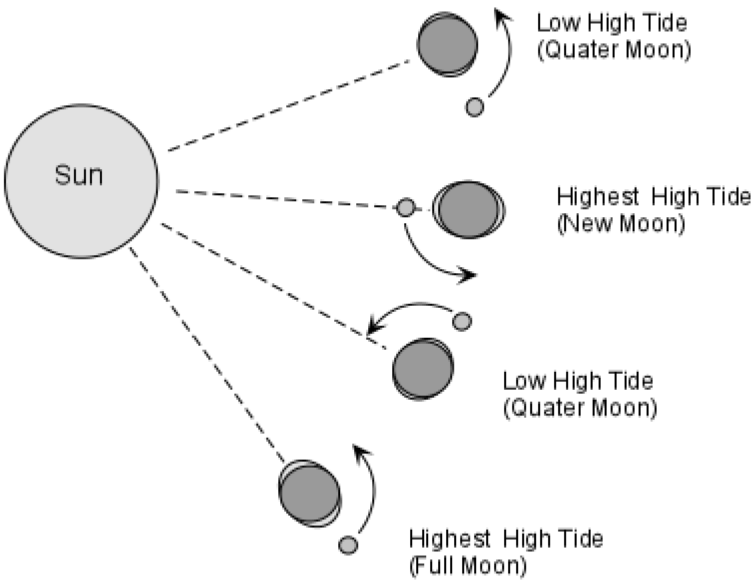

Figure 3-3: Sun gravitational attraction between the Earth and Moon [28]

3.3. Coastline by the Netherlands Hydrographic Service

The Netherlands Hydrographic Service, in the area of Geodesy and Tides deals with four main applications [30], but for our purpose, the second application that is the establishment of the correct coordinate systems and the conversion between those systems are going to be part of this section.
To determine the exact lines and areas, the choice of the system is directly influenced by the calculations of the positions [30]. Some examples are the determinations of boundaries according to the United Nations Convention on the Law of the Sea, maritime navigation, hydrographic measurements, and nautical cartography.
Horizontal and vertical coordinate systems are the reference for geographic data. Those systems can be deduced by mathematical and physical models for the surface of the earth. The correct choice of the system influences directly the calculation of position, lines and areas.

3.3.1. Vertical coordinate system

The vertical coordinate system in a Nautical chart is the chart datum and it is the surface to which the depth values in the nautical chart and corresponding tidal prediction refer. By convention, that datum should be calculated in the way that the true depth is always larger than the charted depth during normal conditions. By international standardization, the Lowest Astronomical Tide (LAT) (see Figure 3.4) is taking as chart datum. The difference between Mean Sea Level (MSL) and the chart datum differs per tide gauge.
In the Netherlands, the height reference on land is the Normaal Amsterdams Peil (NAP). The NAP surface approximately equals Mean Sea Level along the shore. For all locations in the tide tables, differences between NAP and LAT are given [30].

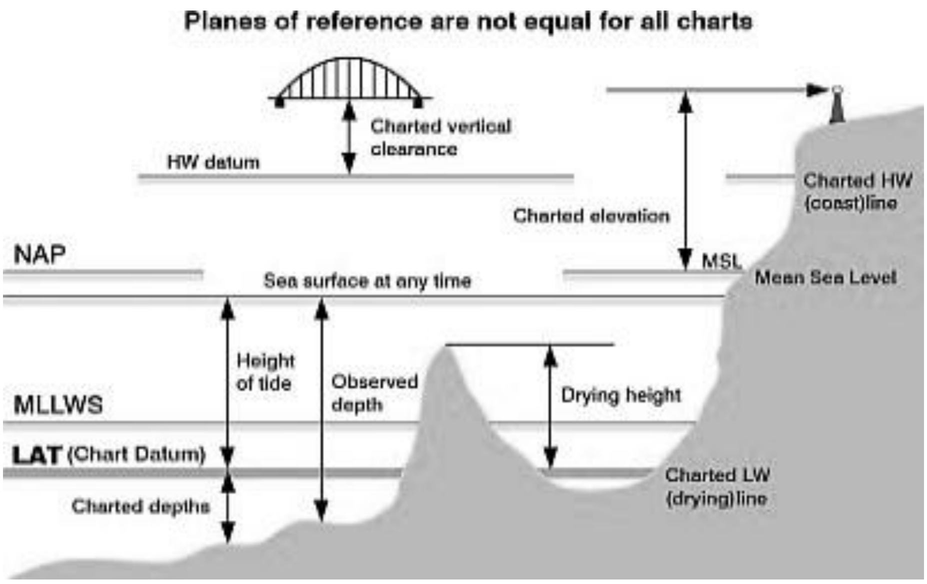

Figure 3-4: Tidal levels and charted data [30]

3.3.2. Horizontal coordinate system

Geographic coordinates, latitude and longitude are determined related to the equator and the Greenwich meridian. The projection coordinates of the Geographical coordinates are in meters and they are expressed in degrees. Therefore, any person in the world can find their own position on a chart or map, destinations can be planned and visualization of lines and areas can be show.
For that, mathematical models of the Earth are measured. Such a model is called a geodetic datum. At sea, the global standard datum is WGS-84 [30]

3.3.3. Netherlands Baselines

Baseline can be defined as a boundary line that determines the beginnings and ends of the sovereignty and jurisdiction of a maritime state.

According to UNCLOS [31] Baseline can be defined in two aspects; Article 5, Normal Baseline is drawn at the low-water line of a coastal state as marked on large-scale charts officially recognized by the coastal state.

In some situations when the normal Baseline cannot be measured because of the morphology of the coast, in Article 7, Straight Baseline is determined by different aspects.

Because of their morphology, Netherlands Baselines are normal and straight Baselines (Figure 3.5). Straight Baselines are established by law and they cannot change in time. The straight Baselines near estuaries and ports; work as boundary between the territorial sea and the internal waters. The normal Baselines are the zero metre depth contours [30]. For the Netherlands normal Baselines, scales larger than 1:150,000, are following the International regulations, according with the fourth edition of IHO publication S4 "REGULATIONS OF THE IHO FOR INTERNATIONAL (INT) CHARTS AND CHART SPECIFICATIONS OF THE IHO" (Article B-126) [29].

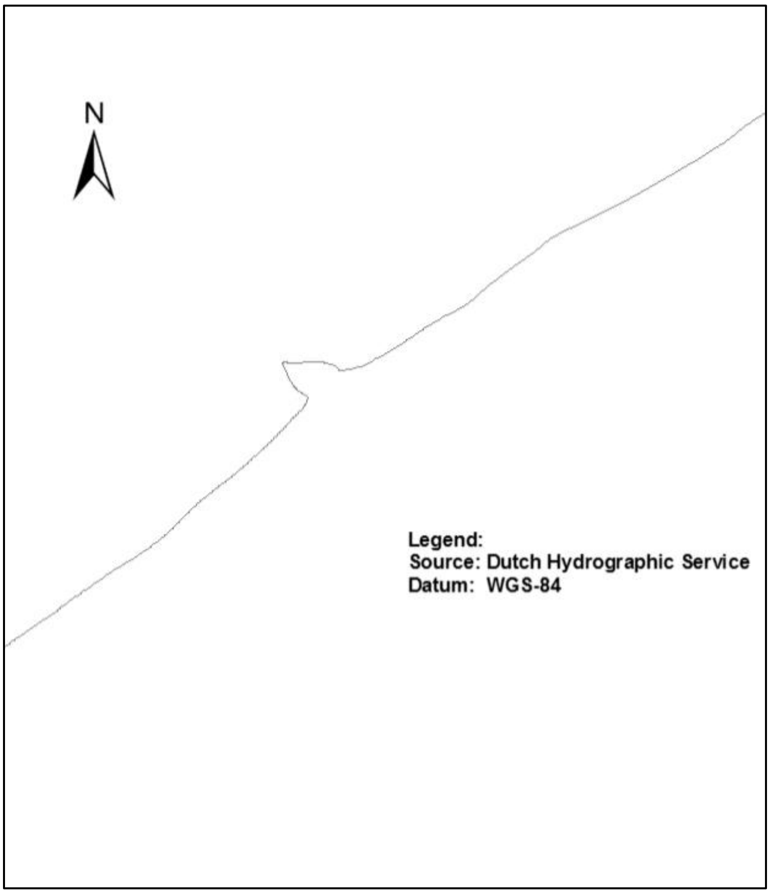

Figure 3-5: Netherlands Baseline acquire from [30]

3.3.4. Nautical charts

Nautical charts are created to permit a safe navigation to the sailor and to provide seabed information to any national or foreign user. In such way, chart catalogues are divided in two functions; for marine navigation and for information sources. The second one, is more suitable for this research, because it provides the shape of the seabed, required for example for; construction engineers for offshore developments, dredging contractors, oceanographers, defence departments and coastal zone managers [29].

For that reason, the Royal Netherlands Navy by the Hydrographic Service is providing hydrographic data, especially for education or research purposes. The hydrographic information in Figure 3.6 was done by using many techniques like, hydrography, geodesy, topography, oceanography, etc.
The purpose to include nautical charts in this research is to compare, evaluate and validate the output after the classification and segmentation of the polarimetric data. As it is mentioned in Section 3.1, the determination of shoreline is not well defined and the position of the line edge between land and sea is not clear at all. Therefore, every Hydrographic service has the objective to determine that line for the reasons already explained.

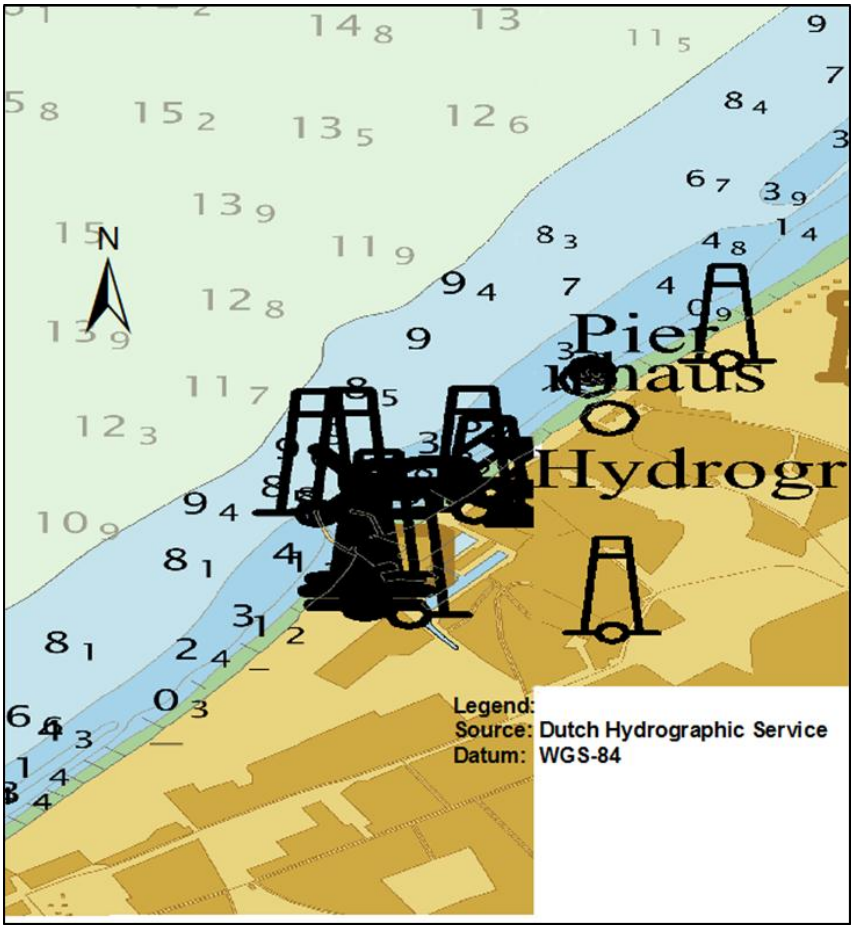

Figure 3-6: Nautical charts of the study area for validation purposes acquire from [30]

3.4. Study area

The study is located in the South Holland province of The Netherlands. The area extends approximately from 52° 12' N, 4° 13' E to 51° 41' N, 4° 17' E. The area is located above the sea level and presents many water bodies. It is mainly flat and the beach in the north part of the study area is long and almost straight. South Holland province is the most densely populated of the twelve Dutch provinces.
South Holland is the most important province in terms of economy, agriculture and the provision of services. The largest city in the South Holland Province is Rotterdam. This city has the most important and largest port in Europe. Rotterdam is on the banks of the river Nieuwe Maas ('New Meuse'), one of the channels in the delta formed by the Rhine and Meuse rivers.

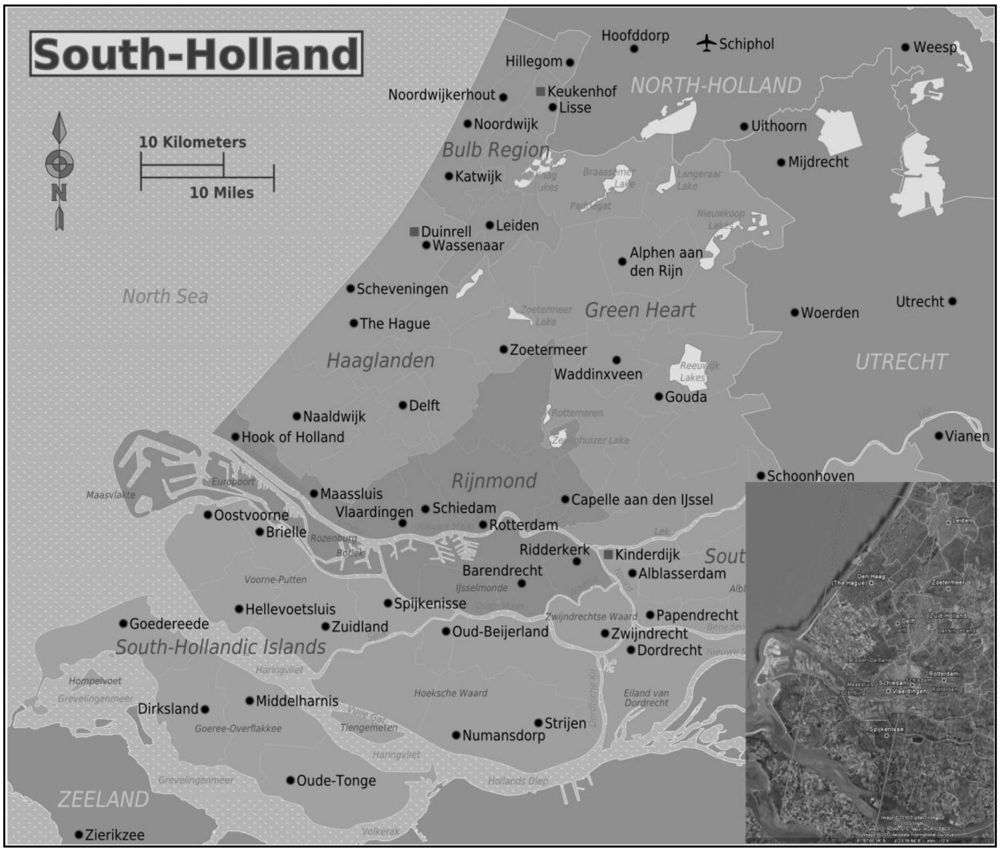

Figure 3-7: Map of South Holland province

In Figure 3.6; Rijnmond is a region around the mouth of the Rhine River and its hinterland. This region in specific, can suffer floods from the river and also from the sea, it is also suffering the adverse effects of salination and finally, the subsidence is making the situation worse. Furthermore, the current sea defences, such as the Maeslantkering storm surge barrier, have been designed to cope with a 50 cm sea level rise, are sufficient for now but expert's recommendations and some new calculations showed many weak spots. In addition, sea level rise and continuing rains increase the river volume (made more extreme by global warming) over the years. In consequence, the shoreline is changing rapidly, because, water from the river cannot flow normally to the sea.

For that reason, the Second Delta Committee [1] recommends some options to avoid future floods. One option is to reinforce the dikes, but it is very difficult and expensive because it is a highly urbanised area. Another option is to close the Nieuwe Waterweg permanently. This option would be good, because it can provide fresh water and is beneficial for urban development but not for natural systems. The safe discharge capacity of the Dutch Rhine is about, 16,000 m3/s. Future design for discharges of 18,000 m3/s through the Rhine will demand more measures in the river bed and floodplain of the IJssel and the Waal [1]. The shore line will be affected for all the issues mentioned before. In that sense, the Committee wants as soon as possible the measures for the River programme to be implemented without any delay.

Cost-effectiveness is an important point and for that purpose, remote sensing can be an accurate, economic and easy solution.

3.5. Materials: Radar images

The German Aerospace Center (DLR) did a special campaign for data collection during March and April 2010. The data was collected in a specific mode, quad polarization, using as sensor TerraSAR-X with high spatial resolution.

The data was available for all the research community and provided free of charge, after submission and approval of a research proposal.

To make this thesis possible, the research proposal was sent and approved within one month after the submission. DLR provided the data via FTP, and it includes 6 packages of images, each package contains an image in quad polarization mode, with 4 layers corresponding to 4 polarizations. The study area was selected before and included in the proposal.

Table 3-1: TerraSAR-X images from DRA campaign: six (6) images

Id Image	Date UTC	Hour UTC	Characteristics
dt_304_delft	April 28, 2010	6:08:16	Stripmap' mode covers a 30-kilometre-wide strip at a resolution between 3 and 6 meters, Quad polarization mode
dt_275_delft	April 26, 2010	17:26:35	
dt_481_delft	May 9, 2010	6:08:16	
dt_116_delft	April 17, 2010	6:08:16	
dt_450_delft	May 7, 2010	17:26:35	
dt_086_delft	April 15, 2010	17:26:35	

Acquisition mode	"SM" /"HH/HV/VH/VV"
Product type	"SSC"
Orb cycle/ no/ dir	97/16080/48/"D"

Acquisition mode	"SM" /"HH/HV/VH/VV"
Product type	"SSC"
Orb cycle/ no/ dir	96/15890/25/"A"

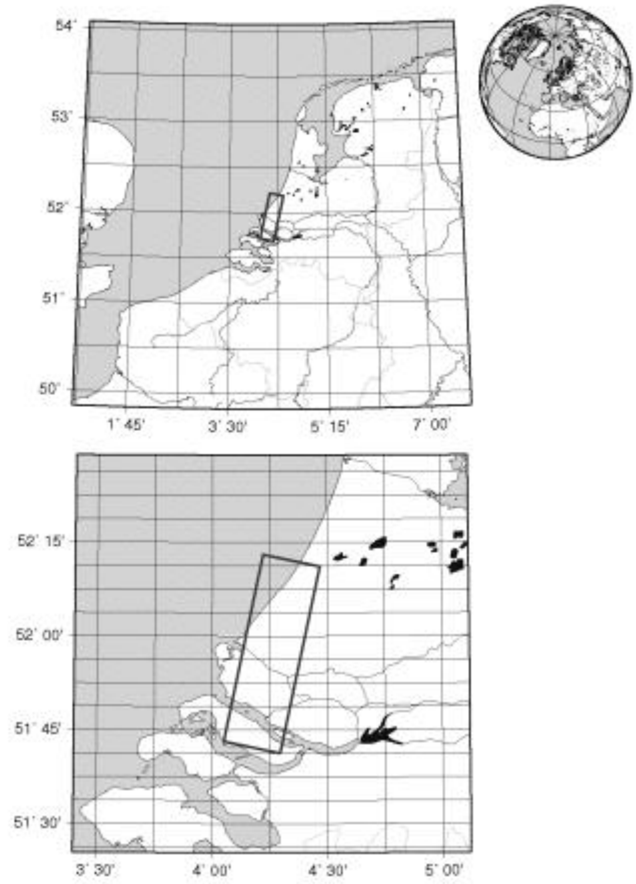

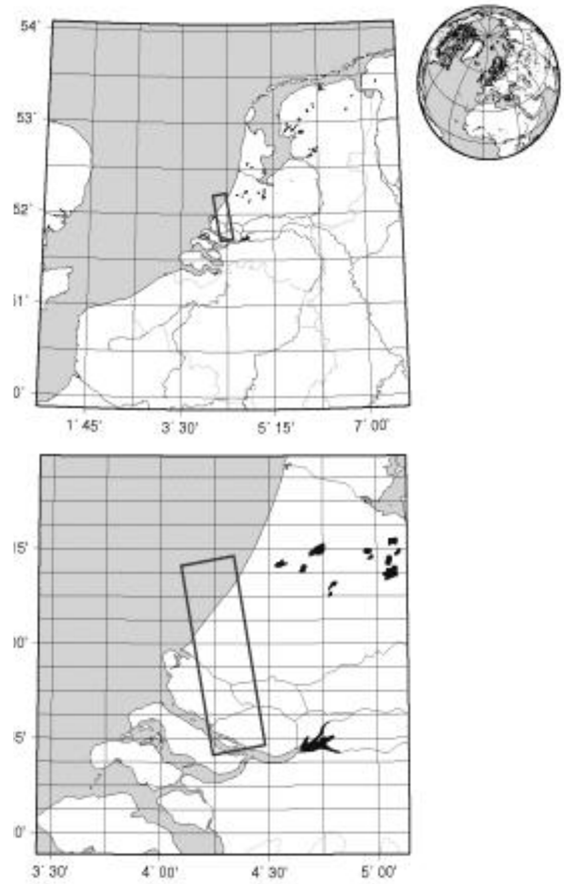

3.5.1. Tide information

The tide information was acquired from the Ministerie van Verkeer en Waterstaat [32]. Rijkswaterstaat monitors water to guarantee the safety of water in all The Netherlands. Rijkswaterstaat has four monitoring programs; physical, biological, chemical and morphological.

The last one, morphological monitoring, determines a large number of offshore areas along the coast, it also determines the depth and position of the sea bottom and how the shoreline changes over the time. Table 3.2 shows the different tide levels for the different days from the radar images.

Table 3-2: Tidal information [32]

Tidal information	
Image 1	Date: 2010 / 04 / 17 Time: 06hr 08 min 36 sec
Station	Tide level (cm)
Terneuzen Hoek van Holland Rotterdam	200 107 138
Image 2	Date: 2010 / 04 / 28 Time: 06hr 08 min 29 sec
Station	Tide level (cm)
Terneuzen Hoek van Holland Rotterdam	8 14 81
Image 3	Date: 2010 / 05 / 09 Time: 06hr 08 min 30 sec
Station	Tide level (cm)
Terneuzen Hoek van Holland Rotterdam	-174 -77 -39
Image 4	Date: 2010 / 04 / 26 Time: 17hr 26 min 51 sec
Station	Tide level (cm)
Terneuzen Hoek van Holland Rotterdam	-20 16 75
Image 5	Date: 2010 / 04 / 15 Time: 17hr 26 min 50 sec
Station	Tide level (cm)
Terneuzen Hoek van Holland Rotterdam	203 106 145
Image 6	Date: 2010 / 05 / 07 Time: 17hr 26 min 51 sec
Station	Tide level (cm)
Terneuzen Hoek van Holland Rotterdam	-108 -50 -28

4. METHODOLOGY

This chapter describes the methodology that has been used to achieve the objectives of this research and to address the research questions mentioned in the outline of this thesis in Chapter 1.

Quad polarization images from TerraSAR-X are still under experiment. In that sense, we dealt with many difficulties to achieve the objectives. There were not many software packages capable to handle the data, just one program PolSARpro was able to make this research possible, but it was not fully validated, as shown on their website [33].

The main objective of this research is to evaluate the use of the complete backscattering information coming from the polarimetric data, by using the experimental quad polarization mode from TerraSAR-X, with high spatial resolution as fine as 3 m, to map the shoreline of the South Holland province as study area.

The detection of shoreline from SAR imagery is possible due to the large contrast between backscatter from water and land; as an example, if the sea is relatively calm, it acts as a specular reflector; very low backscatter is coming back from the surface and this contrast well with land that typically has higher backscatter. The shoreline detection can be more difficult due to wind induced surface roughness on the water which reduces the contrast between land and water [34]. Waves and tides also complicate the shoreline extraction due to the change of dry land to wetland and vice versa.

For the analysis and decomposition of the polarimetric data, Freeman and Durden decomposition was selected, because it is capable to identify the difference between single or specular, double and volume bounce.

Taking advantage of that decomposition and the low backscattering from water, the line between land and sea is going to be extracted by doing some classification and segmentation analysis of the complete polarimetric data.

Previous research as shown in Chapter 2 was done by using co- or cross-polarization, without analysing the complete information coming from the surface, and therefore, the analysis did not include the complete information from the different scattering mechanisms. In this research, the complete scatter information was analysed and processed to detect the shoreline in an unprecedented high spatial resolution coming from spaceborne radar sensor. Figure 4.1, is the general workflow followed to achieve the objectives of this thesis.

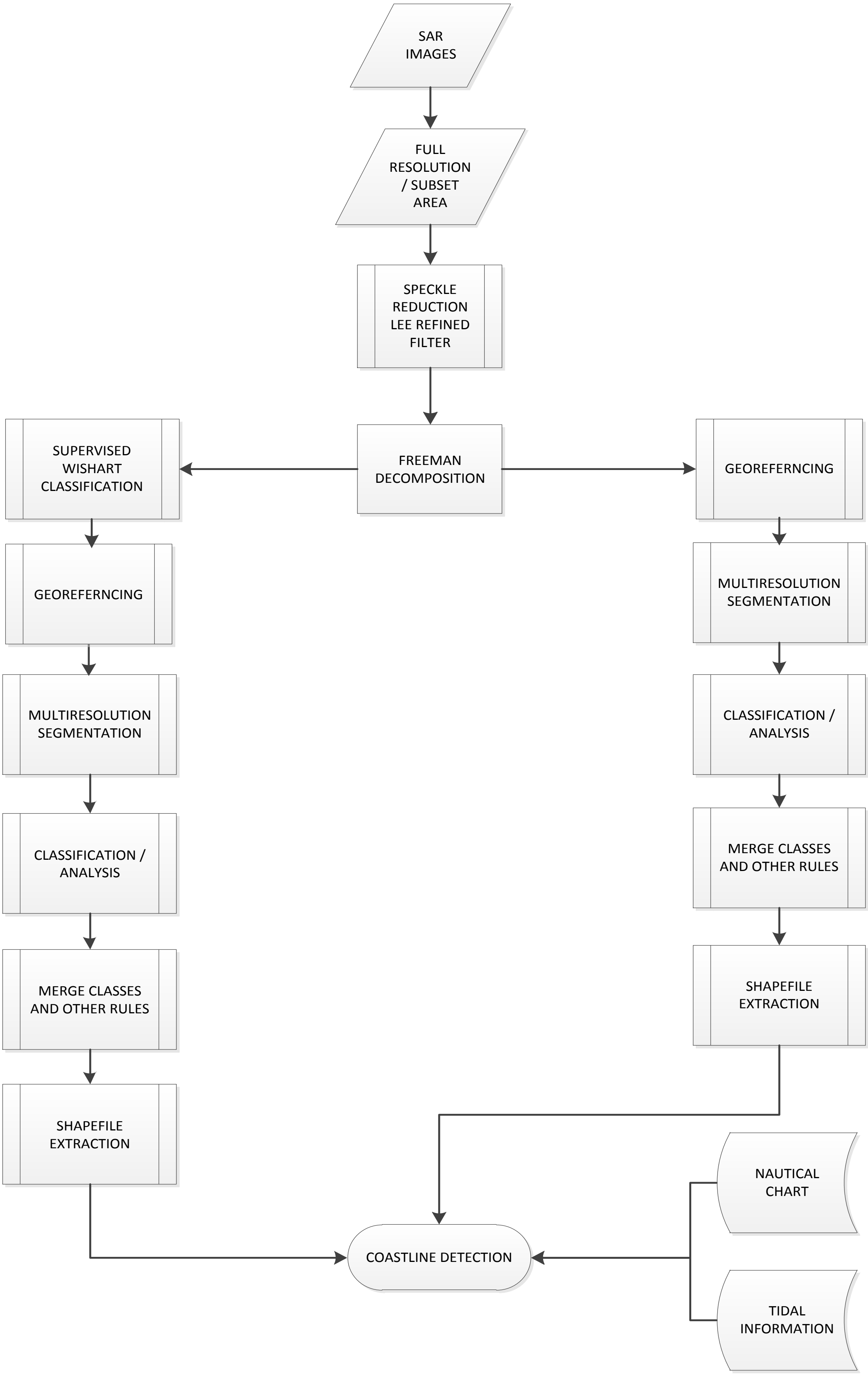

Figure 4-1: General workflow applied

4.1. Data processing

Imaging radar can be considered relatively new remote sensing in comparison to aerial photography [10]. For geoscientists, the application of radar images to solve problems and to achieve better understanding of the environment is having good results.
Figure 4.2 represents the first step of the methodology and describes the processing of the SAR images.

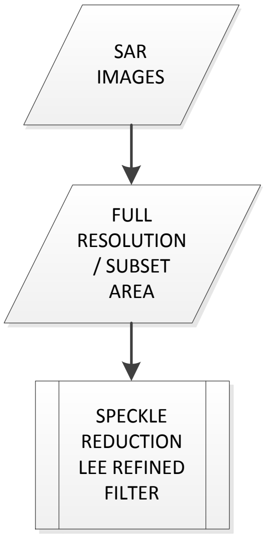

Figure 4-2: Data process workflow

The data was analyzed by using different software, one of them, NEST DATA 4A, was able to analyze the data but it does not have decomposition analysis applications.
ENVI program in SARscape module was used to analyze the pixel size of the images and for editing the header information.
At the beginning, during the implementation, multilooking processing was applied to average amplitudes (or intensities) of several (L) pixels to get a larger pixel, to reduce speckle, and to make the pixels square.
However, the georeferencing after the decomposition was not possible to do with the few programs able to work with the data, and for that reason, ENVI program was used to change the header information, since this required to be in their original resolution, without any distortion, the idea to apply multilooking process was discarded and the images were processed with their full resolution, without any distortion.
Nevertheless, the images were having a strong speckle, product of the four polarizations information and because of the high spatial resolution. In that way and because multilook was not applied, speckle reduction for polarimetric data was a mandatory step.
The next sections will explain the methodology applied in this thesis. In Chapter 5 and 6 are going to show the results and analysis of the other images by following the same methodology.

4.1.1. Speckle reduction

Due to the big amount of information coming from the polarimetric data, speckle also increases and it complicates the image interpretation by reducing the accuracy of image segmentation and classification. The speckle reduction for single polarization is much easier than for multi-polarization, because the filter should preserve the polarimetric properties and it should deal with the cross-product terms [35]. In that sense, the selection of the appropriate speckle filter for polarimetric data was important.
While choosing processing steps, the aim is to try to preserve the high resolution of the images without distortions of the images. As it is mentioned in Section 2.7.3, polarimetric data is affected by different distortions; one of them is cross talk. The selected speckle filter must have the particularity to preserve the

spatial resolution, avoid different distortions like cross talk, and to preserve the polarimetric properties and scattering characteristics.

Novak [36] proposed a polarimetric whitening filter (PWF) by combining the three complex elements (HH,HV,VV) of the polarimetric scattering matrix to reduce speckle. Lee [37] developed an algorithm to take advantage of the polarization diversity to suppress the speckle effect, but the off-diagonal terns of the covariance matrix were not filtered. Goze [38] improved Lee's approach by including all elements of the covariance matrix for one look imagery.

The main problem of these filters is that they introduce cross talk between channels. Therefore, the polarimetric properties are not correctly preserved. After testing different kind of speckle filters for polarimetric data mentioned before, Lee [35] proposed an algorithm able to deal with those deficiencies, by preserving the polarimetric properties and statistical correlation between channels, not introducing cross talk, and not degrading the image quality.

Some principles of this polarimetric filter are listed below:

- Each element of the covariance matrix is filtered independently in the spatial domain, to avoid cross talk.
- To preserve polarimetric properties, the elements should be filtered in a similar way to multilook processing.

These principles make Lee speckle filter the most appropriate filter for this research. Nevertheless, the filter was tested before, and analyzed by comparing different windows size. See Chapter 5, section 5.1.1.

4.2. Polarimetric Decomposition and georeferencing

In this section, the polarimetric data was decomposed to be able to separate pixels into three dominant scattering categories: volume, double and surface bounce, to improve understanding of the polarimetric signatures coming from the scattering mechanism and to extract more information from targets.

To determine the correct decomposition, several theorems were reviewed. Huynen [39] based on the dichotomy, that is the procedure in which a whole is divided into two parts or in a half, proposed the use of the Kennaugh matrix K. Van Zyl [40] classified the dominant scattering mechanism for each pixel. Those using an Eigen vector or Eigen values by decomposing the target scattering matrix into three orthogonal components, proposed by Holm and Barnes [41], Krogager [42]. Cloude and Pottier [43] did a review of these decomposition theorems.

These theorems are based on mathematical models and the combinations of three scattering matrices cannot be easily related to the physical scattering models. More theorems like "model based" decomposition by Freeman and Durden [44] and Yamaguchi [45] are more suitable for this research. The Freeman and Durden decomposition technique uses the physically based, three component scattering mechanism model to the polarimetric SAR data without using any ground control point measurements.

This decomposition was used by Lee [46] and it gave good results by not changing the scattering signatures after applying the speckle reduction filter that was proposed before.

Freeman and Durden [44] model includes three scattering mechanism components; canopy scatter from randomly oriented dipoles, first order Bragg surface and double-bounce scattering mechanism. The composite scattering model is used to describe the naturally occurring scatters from the polarimetric backscattering information.

The advantage of the Freeman and Durden decomposition theorem is, that it is not based on a purely mathematical algorithm; it is also based on the physics of radar scattering. The three-component scattering mechanism model is useful to distinguish between different surface cover types and to detect and determine the current state of the surface cover [12].

Another advantage is that the decomposition can always be applied but it has two important applicability limitations. The first is that assumed three-component scattering model is not always applicable if we consider the surface scattering with entropy different from zero. The second limitation is the assumption that the correlation coefficients $\langle S_{HH}S^{*}{}_{VH}\rangle = \langle S_{HV}S^{*}{}_{VV}\rangle = 0$, that is, reflection symmetry.
For more information about the algorithms see [44].

4.2.1. Georeferencing

The georeferencing of TerraSAR-X data in the experimental mode was not possible using PolSARpro program. On the other hand, NEST DATA 4A program was able to georeference the data but it was not possible to export the data to PolSARpro format (.bin) after the georeferencing. Even, NEST DATA 4A does not have the polarimetric decomposition applications.
Therefore, the Classified Wishart image described in Section 4.3 and the Freeman and Durden RGB image were exported to ENVI software. The header information from our study area a sample TerraSAR-X quad polarization image already georeferenced by the DLR team, was extracted with the purpose to edit the header of the Classified Wishart image and the Freeman and Durden RGB image with the correct header information.
Once the image is georeferenced and after applying the different methods implemented in this research, the raster image in .tif format is exported to ArcMap 10 to do the final georeferencing process.
Affine transformation was selected because it is a linear (or first order) transformation and transform one 2D Cartesian coordinate system to another 2D Cartesian coordinate system. It relates the two 2D Cartesian coordinate systems through a rotation, a scale change in x – and y – direction, followed by a translation [47].
Some properties of this transformation are:

- Carry parallel lines into parallel lines
- While an affine transformation preserves proportions on lines, it does not necessarily preserve angles or lengths.

During the affine transformation, well detected structures such as harbour, port and the Den Haag pier were taken as reference places to take the tie points. In this research, above 10 tie points were acquired to make the affine transformation more accurate. The minimum number of tie points for this transformation method is 3.
The Nautical charts provided by the Netherlands Hydrographic Service were used as reference data. These data explained in Section 3.3.4 are suitable for this georeference process.

4.3. Data analysis

After the decomposition of the polarimetric data in three different backscattering scenarios mentioned in Section 4.2, it was necessary to analyze the data by classifying the image and then applying segmentation based on region growing or vice versa, to obtain the polygons according the same neighboring pixel values.
Land-use classification is one of the most important applications to analyze and explore the polarimetric data. There are two kinds of classification; supervised and unsupervised. Some good algorithms have been developed to assess different kind of data and in different kind of scenarios.
For supervised classification, training sets for each class should be selected based on ground control point maps or scattering contrast difference in polarimetric SAR images. The supervised classification can be more difficult to perform if ground control point is not available. Therefore, the selection of training sets should be precise.

Two classifications were applied; the first method shown in Figure 4.3 describes the methodology by first applying supervised classification of polarimetric data using Supervised Wishart Maximum Likelihood statistics.
The supervised Wishart polarimetric classification works with the Maximum Likelihood (ML) statistical classification based on the multivariate complex Wishart probability density function of second order matrix representations [48].

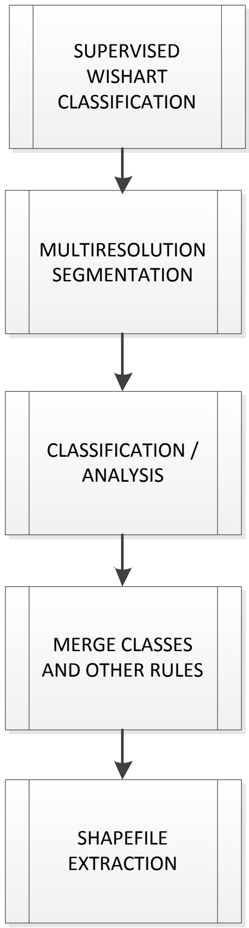

Figure 4-3: Workflow of the first analysis process

The classifier starts by "learning" the Wishart statistics of the user defined training areas, after that, the whole data sets are classified by assigning to each pixel the closest class following the Maximum Likelihood decision rule.
In this study, the training areas were defined by using the graphic interface application from PolSARpro program. The graphic interface permits the selection of areas of interest on a visual interpretation of the data to be classified.
After that, the areas of interest were selected using Freeman and Durden decomposition image Figure 4-4, by classifying it from the different backscattering information.
Sixteen sub classes were selected and divided in four main classes, see Figure 4-5. As this research is more interested in classify water (sea) and land, five sub classes were selected to determine specular bounce (sea) in blue color, four classes to surface bounce (land fields) in green, four classes to volume bounce (forest, irregular building shapes) in red and three classes to double bounce (normal building shape) in yellow.

After this important and time consuming step, the training process starts by collecting the coordinates of each training area and computing each class.

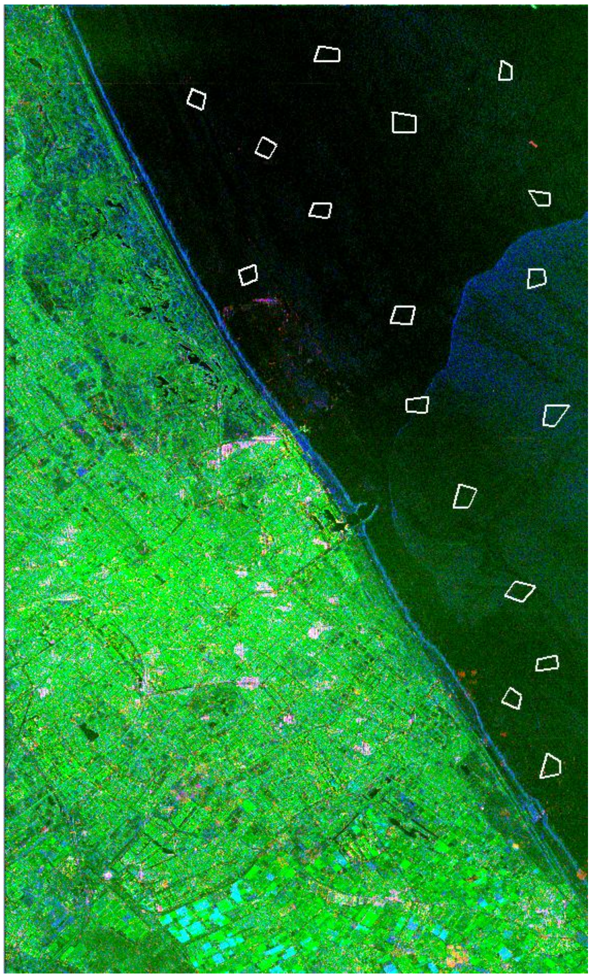

Figure 4-4: Example of classification by different backscattering information from Freeman and Durden decomposition image

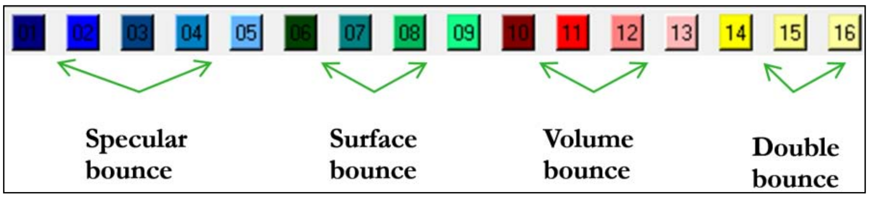

Figure 4-5: Selection and identification by colours of different sub classes

After the classification, the program creates two different outputs; the image classified in .bmp format and a confusion matrix in .txt file. By visual interpretation, the image shows a correct classification following the backscattering information.

4.3.1. Segmentation analysis with eCognition – Developer 8 for Method 1

Following the workflow in Figure 4-3, the segmentation using multiresolution based on region growing was applied with eCognition – Developer 8. But before the selection of this program, some other programs were evaluated, such as InfoPack 1.0, Spring 4.3 and SegSAR, to determine the most suitable segmentation method for the analysis.

After testing each one, the programs could not process polarimetric data and because the purpose of this research is to use all the scattering information, eCognition – Developer 8 was selected as the most appropriate because it can work with the complete polarimetric SAR data.

For the segmentation, a multiresolution segmentation algorithm was selected because it locally minimizes the average heterogeneity of the image object and maximizes their respective homogeneity [49].
The Multiresolution segmentation consecutively merges pixels or existing image objects. This segmentation works with the bottom-up segmentation algorithm based on region growing technique.
Before generating the segmented image, some segmentation settings were included to get better results. One of them, Image layer weight was used to modify the layer weights, depending on their importance or suitability for segmentation.
In this research, three layers were analysed; double bounce (layer1), volume scattering (layer2) and specular bounce (layer3). The scale parameter was included to determine the maximum allowed heterogeneity for the resulting image object. In this case, it took some time to determine the most suitable scale parameter for the specific image, varying from 180 to 220.
The shape value for the composition of homogeneity criterion was used to modify the relationship between shape and colour criteria. It can be modified depending on the different characteristics of the image and finally, for compactness value, the higher the value, the more compact the image object may be.
However, this kind of segmentation requires a large memory and the performance is significantly slower than other segmentation techniques and in some cases it is not the best option.

4.3.2. Classification analysis with eCognition – Developer 8 for Method 1

The classification analysis was performed on the classified Wishart segmented image to be able to classify the image by defining different kinds of threshold and rules conditions in the different layers.
First of all, the class "water" was created with a threshold condition including all the polygons in mean layer3 with a certain number of ratios to classify the polygons as water. The ratios are according with the characteristics of the objects. The idea is to classify the same polygons with the same number of ratios.
After that basic classification, some darkness polygons were remaining and a long line parallel the coast. Therefore, three other classes were created; "water_v_dark" to identify the darkness polygons inside the sea, "wave_border" to determine the long parallel polygons between the land and sea and the "water_strong" to determine very strong values inside the sea.
For "wave_border" class, two threshold conditions were included; the first, in geometry objects features, a length / width threshold condition with values with similar ratios and the second, in relation to neighbouring objects, a relation border to "water" threshold condition with 50% relative borders to detect the surrounded by half of its border was included.
After "wave_border" classification, the already created class "water_v_dark" with the threshold condition including all the polygons less than 10 ratios in the mean layer1 was executed to classify the remaining polygons on the sea, continuously, merge region technique was applied to merge each image object into the neighbour image object with the largest common border. The merge consists of including as class filter, "water", "wave_border" and "water_v_dark". Then, the unclassified class is merged with the purpose to group the land area in one class. Inside the classified land class, there were some polygons classified as "water". For those, classification with threshold condition including all the polygons with area less than 100,000 pxl in "water" class was reclassified. As result, the previous polygons in "water" class change to unclassified class and consequently merged as unclassified class. Next, the class "water_strong" with threshold condition including all the polygons in mean layer1 with a certain number of ratios were classified as "water_strong". Finally, the four classes, "water", "water_border", "water_v_dark" and "water_strong" were merged to classify the complete sea surface.

4.3.3. Reporting results

The output extraction is possible by exporting the results in shape file / raster file with all the image objects and in .tif format not to lose the georeference information achieved before and explained in Section 4.2.1.

After the Shape file or Raster file is extracted, the result is exported to ArcMap10 with the purpose to further process the data before the validation process. These processes are described below:

- The georeference Raster file is exported to ArcMap10 with the purpose to reorient the position of the mirror image. As it was not possible to georeference the image using the appropriate program, the image needs to be shifted to the correct position. In that sense, by using the "mirror" tool from "Projections and Transformations", the raster image was reoriented by flipping it, from left to right, along the vertical axis through the centre of the raster.
- The next step should reduce the irregular shape and make it smoother. For that, the raster image should be converted to polygon before using any filter. The polygon in shape file is simplified by removing extraneous bends while the real shape is well preserve according to the simplification tolerance.

The simplification algorithm used in this step was Bend simplify. This kind of method is slower but the results that it produces are more realistic to the original shape. The algorithm works by eliminating insignificant bends along the polygon. The simplification tolerance used in this case was 200 meters.

The final output is ready to be validated by using the data described in Section 3.3.3 and 3.3.4.

4.3.4. Segmentation analysis eCognition – Developer 8 for Method 2

The second classification method shown in Figure 4-6 describes the methodology by applying first the multiresolution segmentation described in Section 4.3.1 and then the classification using the Freeman and Durden decomposition image without any Wishart or other pre-classification.

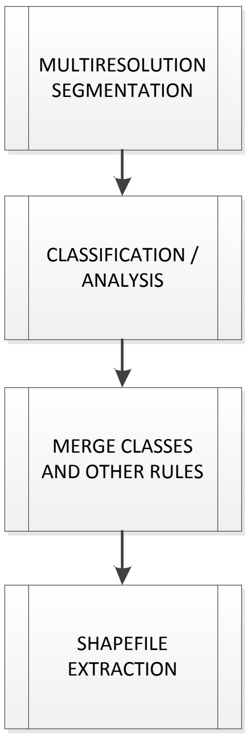

Figure 4-6: Workflow of the second analysis process

The same as before, image layer weight was used to modify the layers weights. For this method, only layer2 (volume) received more weight than the others to have more detailed information, information that helps during the segmentation.
The scale parameter was included to determine the maximum allowed heterogeneity for the resulting image object. In this case, it took some time to determine the most suitable scale parameter for the specific image.
The shape value for the composition of the homogeneity criterion was used as before and in this specific case, it was around 0.3 ratios. It can be modified depending on the different characteristic of the image and finally, for compactness value, it was around 0.6 ratios.
However, this kind of segmentation requires a large memory and the performance is significantly slower than other segmentation techniques and in some cases is not the best option.

4.3.5. Classification analysis eCognition – Developer 8 for Method 2

The classification analysis was performed on the classified Freeman and Durden segmented image to be able to classify the image by defining different kinds of threshold and rules conditions in the mean brightness layer. That layer is the mean brightness combination of the three layers described in Section 4.3.1. First of all, the class "water" was created with a threshold condition including all the polygons with brightness values less than 31 ratios to be classified as water.
After that basic classification, some darkness polygons remained as well as a long line parallel to the coast. In that sense, two other classes were created; "water_v_dark" to identify the darkness polygons inside the sea, and "wave-border" to determine the long parallel polygons between the land and sea.
For the "wave_border" class, two threshold conditions were included; the first, in geometry objects features, a length / width threshold condition with values with certain number of ratios and the second, in relation to neighbour objects, a relation border to "water" threshold condition with 50% relative borders to detect the surrounded by half of its border was included.
After "wave_border" classification, region merge technique was applied to merge each image object with the neighbour image object with the largest common border. The merge consists of including as class filter, "water" and "wave_border". Then, the unclassified class is merged with the purpose to group the land area in one class.
Continuously, the already created class "water_v_dark" with the threshold condition including all the polygons less than 110 ratios in the layer2 was executed to classify the remaining polygons in the sea.
Next step, the three classes, "water", "water_border" and "water_v_dark" are merged to classify the complete sea surface.
As final step, inside the classified land class, there were some polygons classified as "water". For those, classifications with threshold condition including all the polygons with area less than 100,000 pixels in "water" class were reclassified. As a result, the previous polygons in "water" class changed to unclassified class and consequently merged as unclassified class.

4.3.6. Output extraction

The output extraction is possible by exporting the results in shape file / raster file with all the image objects and in .tif format not to lose the georeference information achieved before and explained in Section 4.2.1.
After the Shape file or Raster file is extracted, the result is exported to ArcMap10 the same as the final processes described in Section 4.3.3.
The simplification algorithm used in this step was again Bend simplify. The simplification tolerance used in this case was 200 meters.
The final output is ready to be validated by using the data described in Section 3.3.3 and 3.3.4.

5. ANALYSIS, RESULTS AND VALIDATION

The following Chapter describes and shows the preliminary results, final results and the validation process between the outputs achieved from the six quad polarization images and the data obtained from the Netherlands Hydrographic Service.
Every preliminary result has a short legend about the rules conditions and the reference (sections) of the method applied in that output. After the preliminary results, the final results are shown matching with the validation data. The last section is a description of the validation methods and the final results.
The validation section has an important role to appreciate, first of all, which method per each image has better result and which image fit better with the reality. For that, two validation methods are implemented in this research. The first one, by comparing with buffer method using as reference data the Baseline information from the Netherlands Hydrographic Service. The second, by preforming image interpretation technique, using the Nautical Charts. Both methods will be explained in Section 5.1.6

5.1. Speckle reduction results

As it is described in Section 4.1.1, speckle reduction was a mandatory step to reduce the abundant speckle inside the images, but before running the Refined Lee filter, it was tested and the results Figure 5.1 were analysed by comparing different window size. Figure 5-1 compares the Freeman and Durden decomposition (a) Filtered image with 11×11 window size and (b) Filtered image with 5×5 window size.

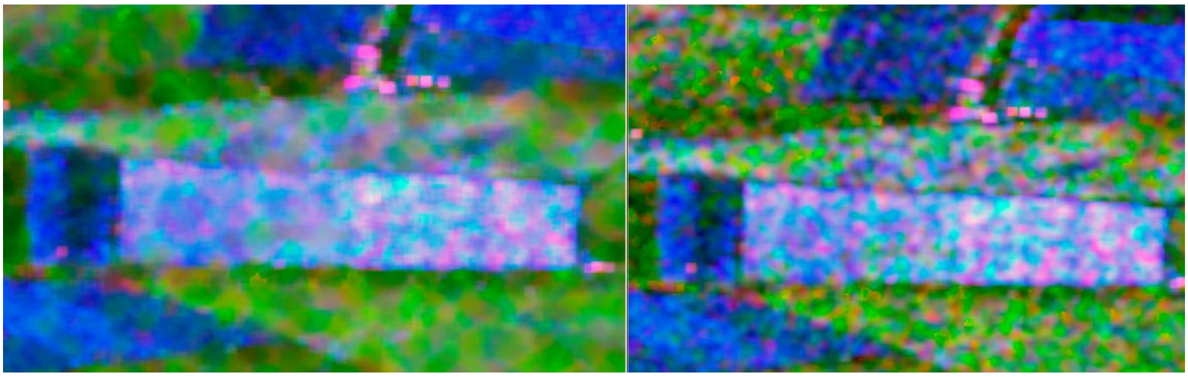

(a) (b)

Figure 5-1: Sample area from the Freeman and Durden decomposition output in RGB colours, where Red represents Double bounce, Green represents volume bounce and Blue represents surface bounce. (a) Filtered image with 11×11 window size, (b) Filtered image with 5×5 window size

According to the results, a larger 11×11 window size provides more speckle smoothing; a smaller 5×5 window filter was selected for better texture preservation. As the purpose of this research is to analyse the shoreline, windows size 5 x 5 better preserves the edge between land and water.
The following is an example of the data after the application of the filter with window size 5×5. Figure 5-2 shows the tested area and below in Figure 5-3 and 5-4, the different signatures.

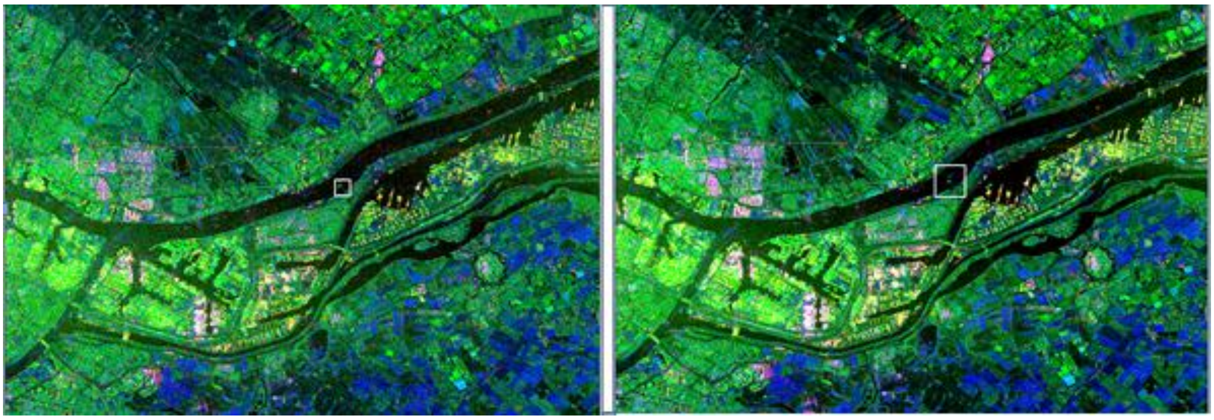

(a) (b)

Figure 5-2: Area of interest (AOI) selection from the Freeman and Durden decomposition output in RGB colours, where Red represents Double bounce, Green represents volume bounce and Blue represents surface bounce. Comparison of Freeman and Durden decomposition images from the original data (a) and from filtered data (b).

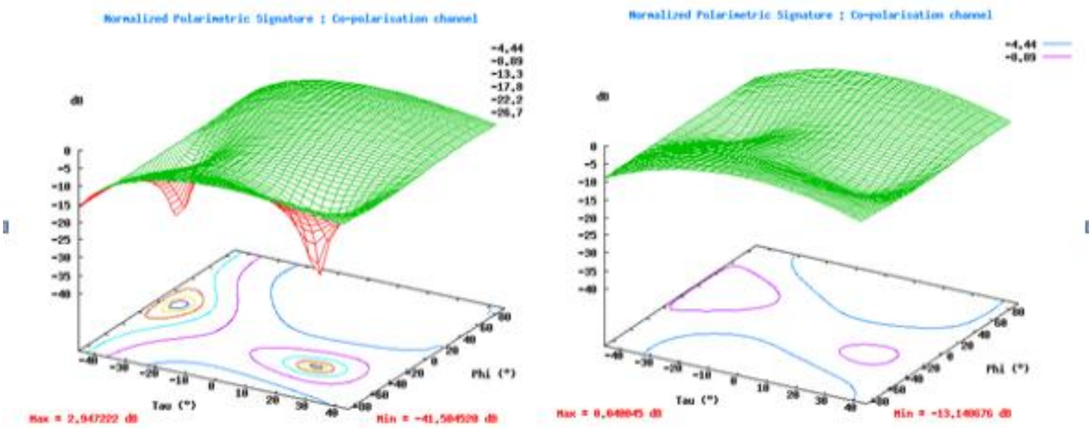

(a) (b)

Figure 5-3: (a) Original co-polarization signature. (b) Filtered co-polarization signature. Preservation of polarimetric properties is illustrated using co-polarization signatures. The contour plots are similar, indicating the preservation of polarimetric properties, but loosing information at the moment to reduce speckle in the image. The sample point was collected in the land near the shoreline

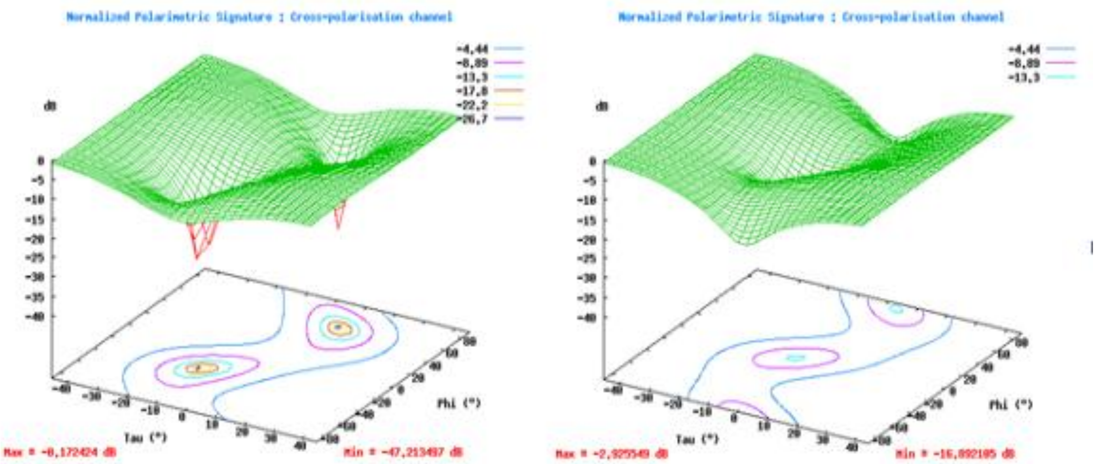

(a) (b)

Figure 5-4: Comparison of cross-polarization signatures. The original cross-polarization signature (a) and cross polarization (b) agrees well, but loosing again some information after the filter.

In both Figures, 5-3 and 5-4, the images are preserving the signature and the texture still similar to each other. At the moment that the filter is reducing the speckle, there is a loss of information, information that can be important for the analysis, but on the other hand, the image is much better for segmentation and classification processes.

5.2. Decomposition results

This Section shows the results from the decomposition described in Section 4.2, where the polarimetric data was decomposed to be able to separate pixels into three dominant scattering categories: volume, double and surface bounce. The Freeman and Durden decomposition technique uses the physically based, three component scattering mechanism model to the polarimetric SAR data without using any ground control point measurements.

Figure 5-5 shows the three Freeman and Durden decomposition layers in specular (a), double (b) and volume (c) bounce. The decomposition looks according the reality, the surface bounce (a) identifies properly the agriculture area and smooth land; shown in high values. Double bounce (b) has good performance to identify the building areas, in more detail, the areas near the harbor, also shown in high values and finally, volume bounce (c) where the high values appear almost in all the north area of the image. This is because X band has short wavelength and the backscattering information coming from the double and volume backscattering is confused and detected as volume. The X band has the characteristic that it has low surface penetration and it is good for terrain surveys and reconnaissance.

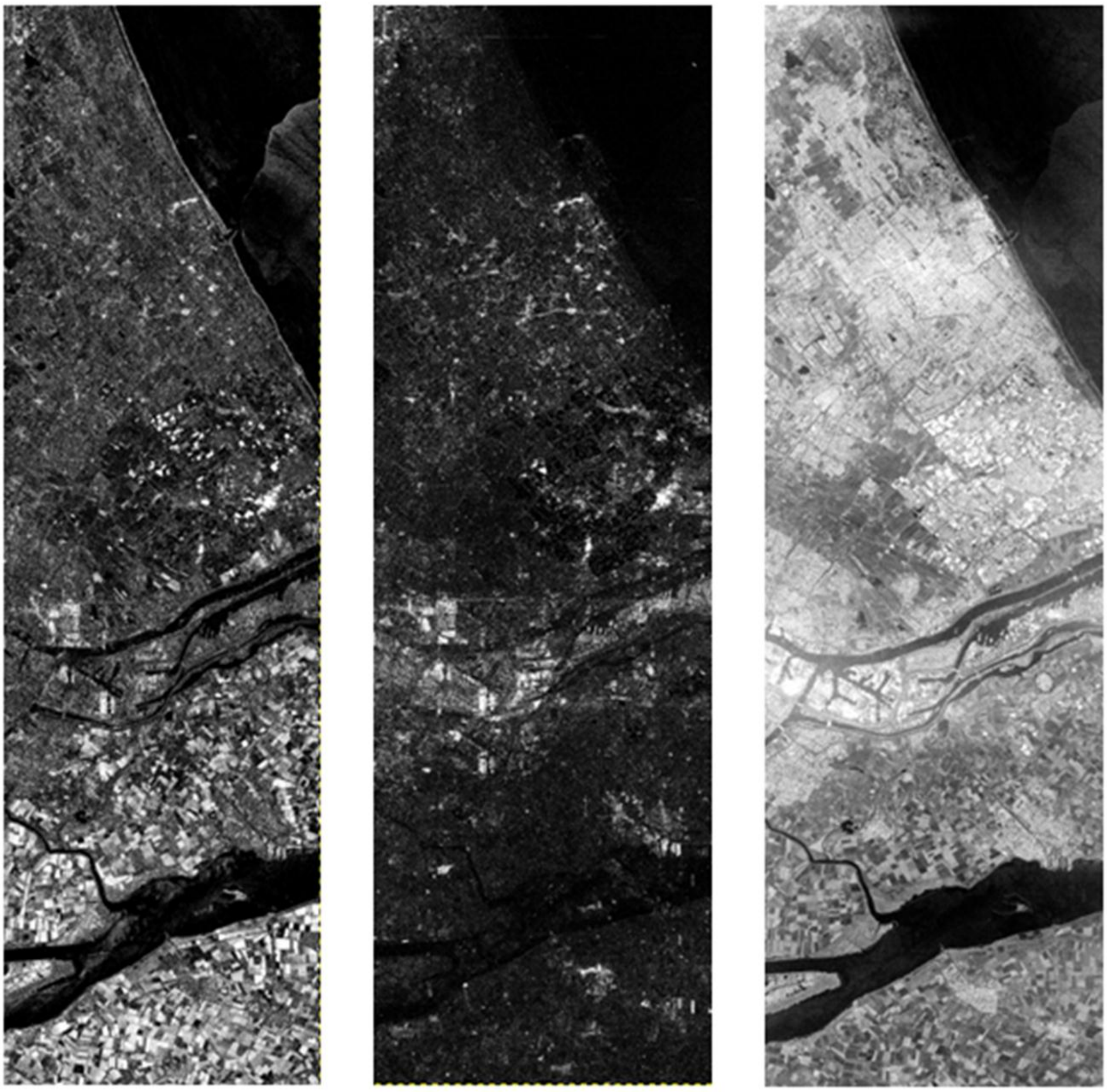

(a) (b) (c)

Figure 5-5: (a) Shows Specular bounce backscattering from Freeman and Durden distribution; the light areas represent the specular bounce (farming land), (b) Double bounce backscattering from Freeman and Durden distribution; the light areas represent the double bounce (building areas) and (c) Volume bounce backscattering from Freeman and Durden distribution; the light areas represent the volume bounce (vegetation area, not regular building shape)

After the Freeman and Durden decomposition, the three different layers are combined in one RGB image to better analyse the decomposition layers for application in the supervised Wishart classification described in Section 4.3.

Figure 5-6 shows the Freeman and Durden decomposition output in RGB colours, where Red represents double bounce, Green represents volume bounce and Blue represents surface bounce.

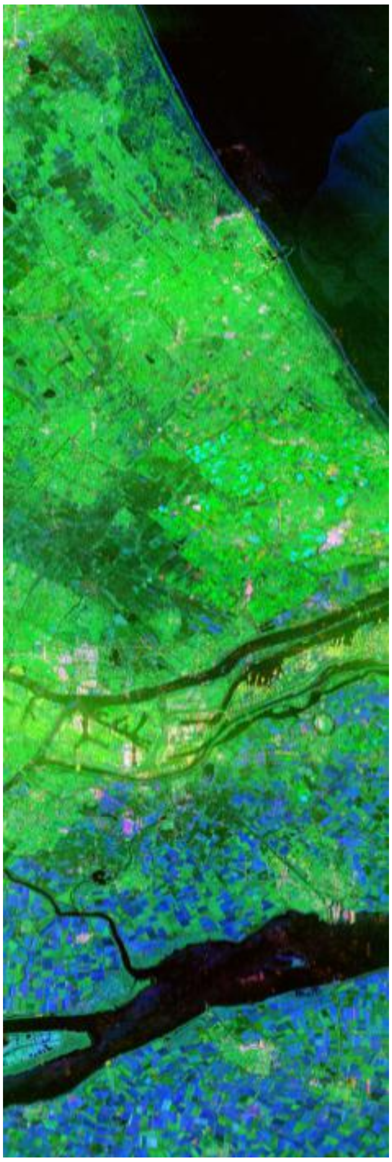

Figure 5-6: Freeman and Durden decomposition output in RGB colours, where Red represents Double bounce, Green represents volume bounce and Blue represents surface bounce.

5.3. Results of Method 1

The first method first applied supervised classification of polarimetric data using Supervised Wishart Maximum Likelihood statistics. After the classification in a subset area (North area) shown in Figure 5.7 the program records classified image in .bmp format, see Figure 5-7.

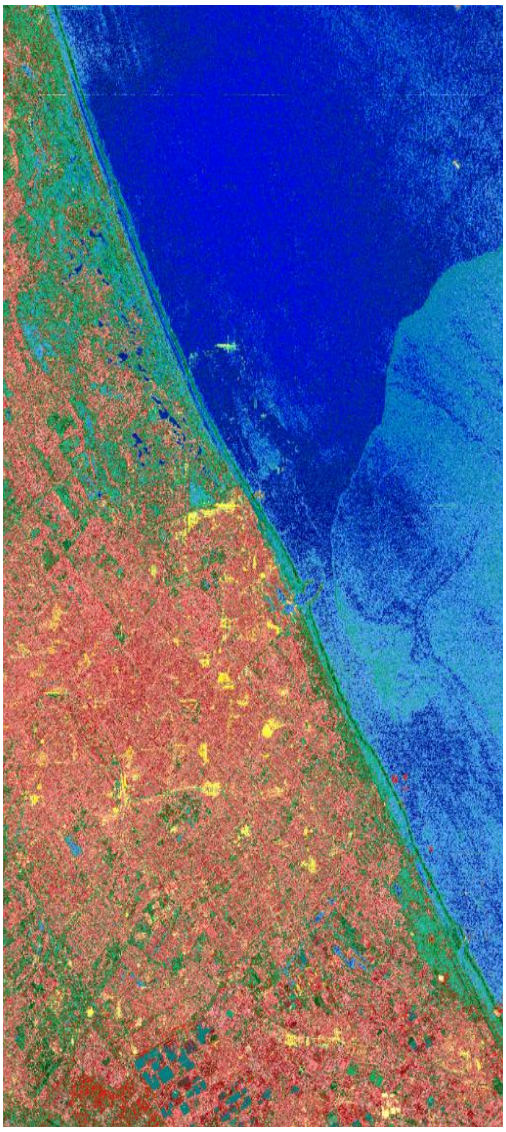

Figure 5-7: Classified image after Wishart supervised classification

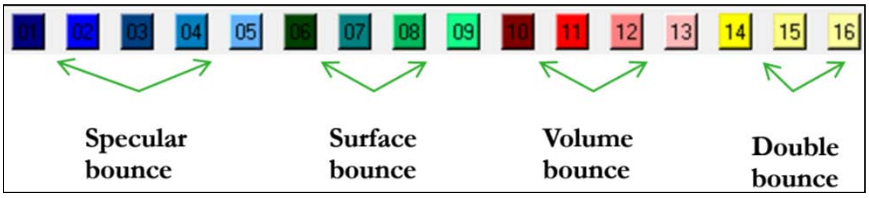

For the segmentation, a multiresolution segmentation algorithm was selected because it locally minimizes the average heterogeneity of the image object and maximizes their respective homogeneity [49]. The process described in Section 4.3.1 produced a segmented image shown in Figure 5-8 (a).

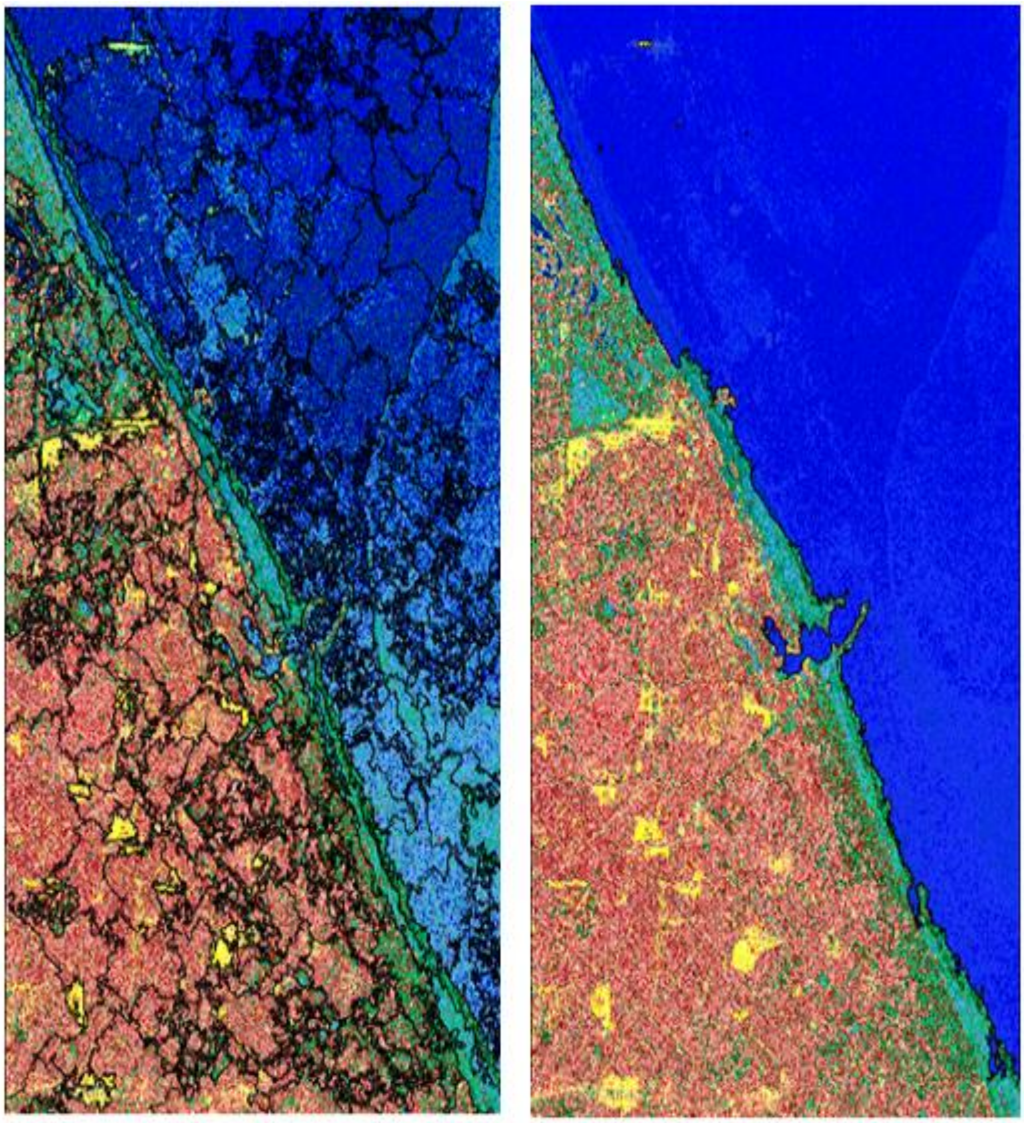

(a) (b)

Figure 5-8: (a) Wishart segmented image after the Multiresolution segmentation, (b) Final output, after applying Method 1 to the Wishart classified image

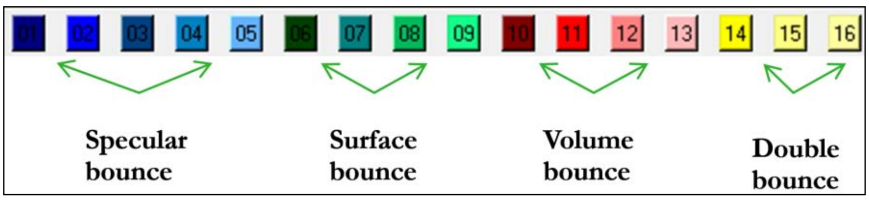

The classification analysis was performed in the classified Wishart segmented image to be able to classify the image by defining different kinds of thresholds and rules conditions in the different layers. The general process is described in Section 4.3.2. As result, a final output is shown in Figure 5-8 (b).

The extracted output Figure 5-9 was possible by exporting the results in shape file / raster file with all the image objects and in .tif format not to lose the georeference information achieved before and explained in Section 4.2.1.

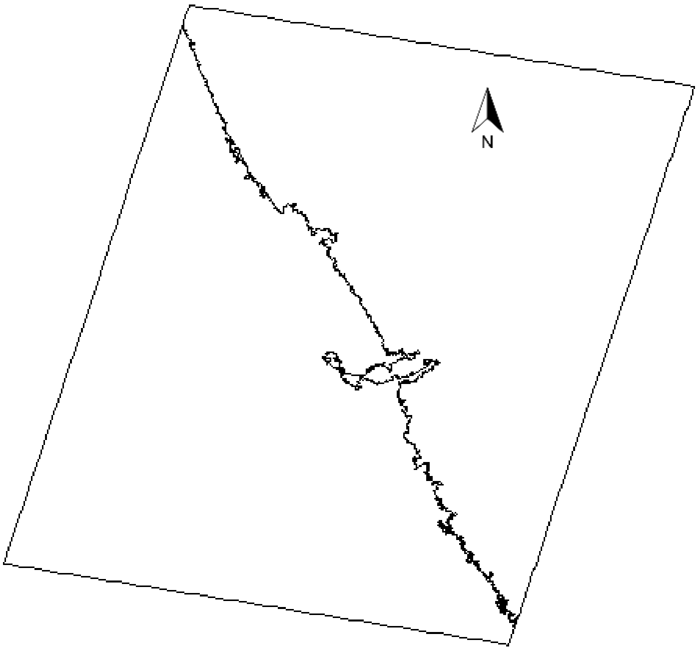

Figure 5-9: Shape file extraction output from Figure 5.8 (b)

The georeference Raster file is exported to ArcMap10 with the purpose to reorient the position of the mirror image. The image is reoriented as it is described in Section 4.3.3. The output shape file is shown in Figure 5-10 (a). After that, the shape file has an irregular shape and to make it more smoothly, Bend simplify filter was applied with the purpose to minimize the inconsistent border. Figure 5-10 (b) shows a smooth and more consistent line, compared to the first result.

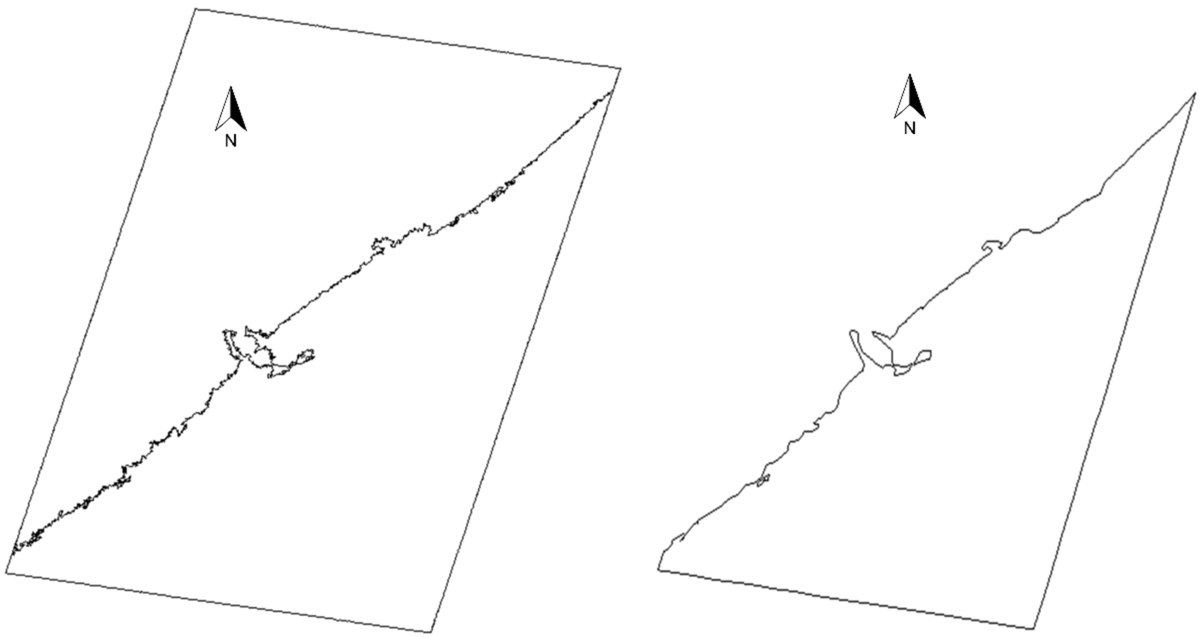

(a) (b)

Figure 5-10: (a) Reoriented shape file output of Figure 5-9 to the real position, (b) Simplified image from (a)

5.4. Results of Method 2

The second method first applies the multiresolution segmentation described in Section 4.3.1 and then classification using the Freeman and Durden decomposition image without any classification. Figure 5-11 (a) shows the result after the multiresolution segmentation on the Freeman and Durden decomposition image.

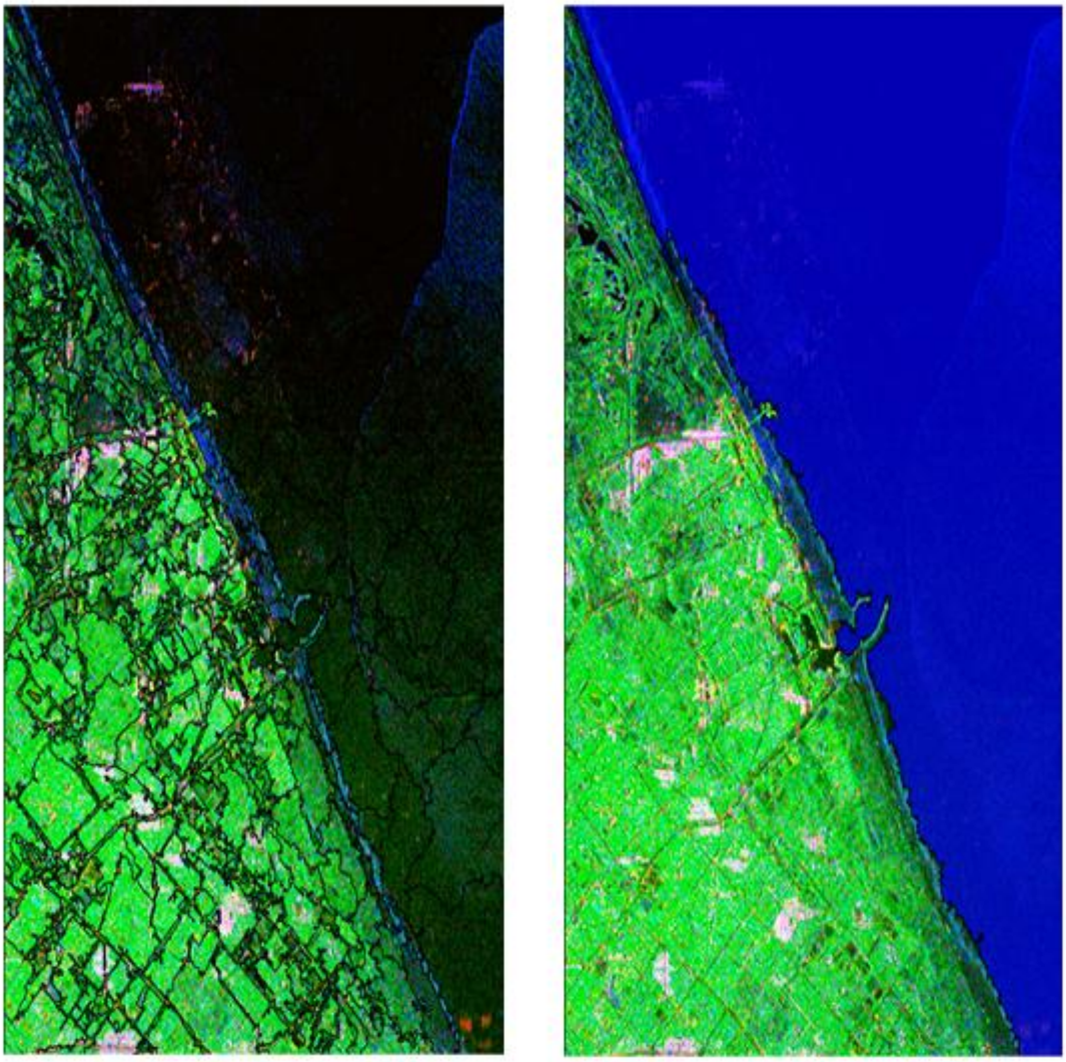

(a) (b)

Figure 5-11: (a) Freeman and Durden segmented image after the Multiresolution segmentation. (b) Final output, after applying Method 2 to the Freeman and Durden classified image. RGB colours, where Red represents Double bounce, Green represents volume bounce and Blue represents surface bounce.

The classification analysis was performed in the classified Freeman and Durden segmented image to be able to classify the image by defining different kinds of thresholds and rules conditions as specified in Section 4.3.5. Figure 5-11 (b) shows the final output after applying Method 2.

The extracted output Figure 5-12 was possible by exporting the results in shape file / raster file with all the image objects and in .tif format not to lose the georeference information achieved before and explained in Section 4.2.1.

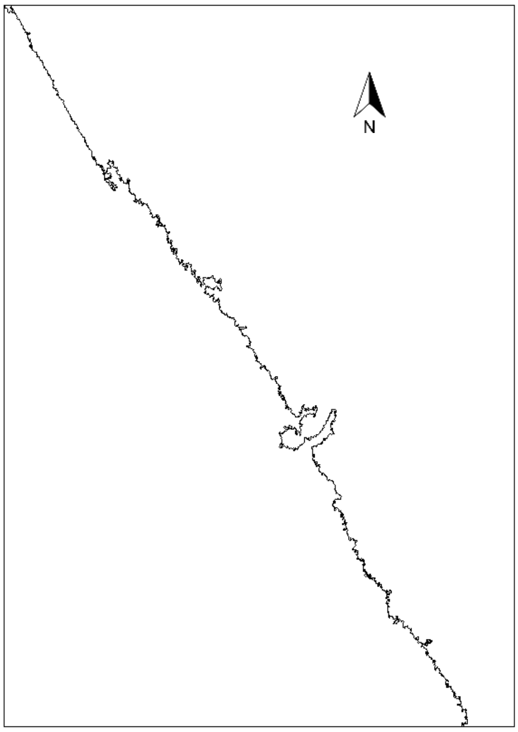

Figure 5-12: Shape file extraction output from Figure 5.11(b)

After the Shape file or Raster file is extracted, the result Figure 5-13 (a) is exported to ArcMap10 as same as the final processes described in Section 4.3.3.

The simplification algorithm used in this step was again Bend simplify. The simplification tolerance used in this case was 200 meters Figure 5-13 (b).

The final output is ready to be validated by using the data described in Section 3.3.3 and 3.3.4.

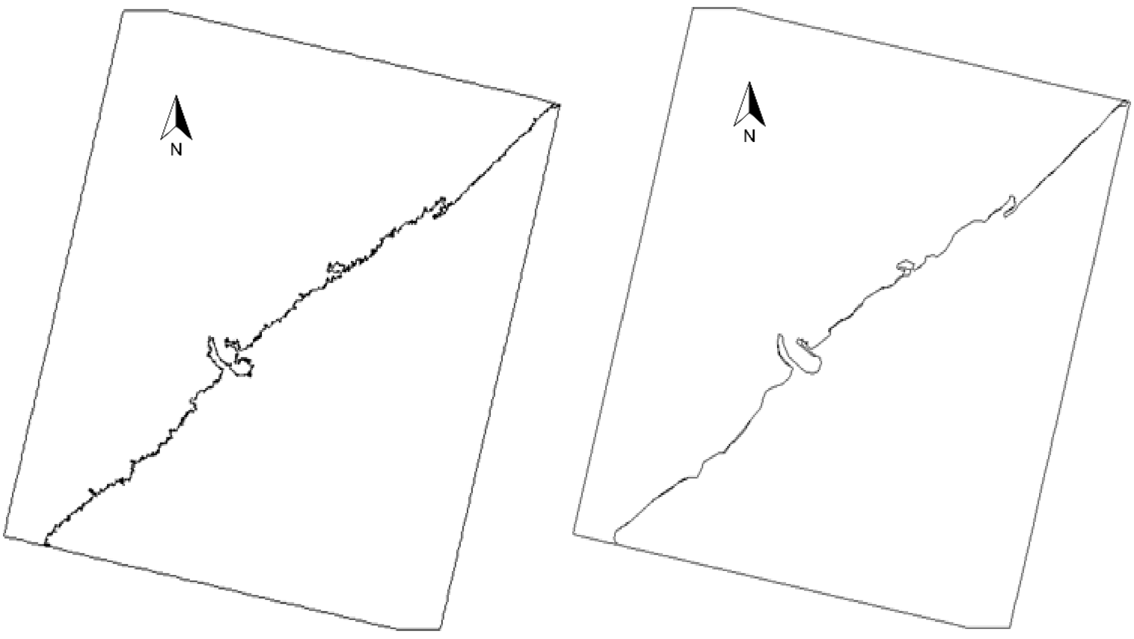

Figure 5-13: (a) Shape file output of Figure 5-12 reoriented to the correct position, (b) Simplified image output from (a)

5.5. Georeferencing

After applying affine transformation technique, it was necessary to assess the RMSE to evaluate the correct georeference of the images. Table 5-1 shows the RMSE in decimal degrees by image.

Table 5-1: RMSE evaluation, after affine transformation

Affine transformation	
Images	**RMSE**
Image1	0.00022
Image2	0.00021
Image3	0.00019
Image4	0.00022
Image5	0.00026
Image6	0.00027

5.6. Validation

Validation is a process which uses objective evidence to validate or confirm that the requirements or application has been met. The process of validation can be done under realistic use conditions or within a simulated use environment[50].

In that sense, two methods were applied for validation. The first applied a buffer method and the second validation method used image interpretation with Nautical Charts and Google Earth for comparison.

5.6.1. Buffer method

Buffer method was applied to compare the extracted shoreline to the Baseline from the Netherlands Hydrographic Service. From the reference, four buffers were created from the Baseline towards the land and one more from the Baseline towards the North Sea (see Figure 5-15). The criteria of this method are to analyse how well the lines detected coincide with the different buffers and in accordance with the current tide at the moment that the image was captured.

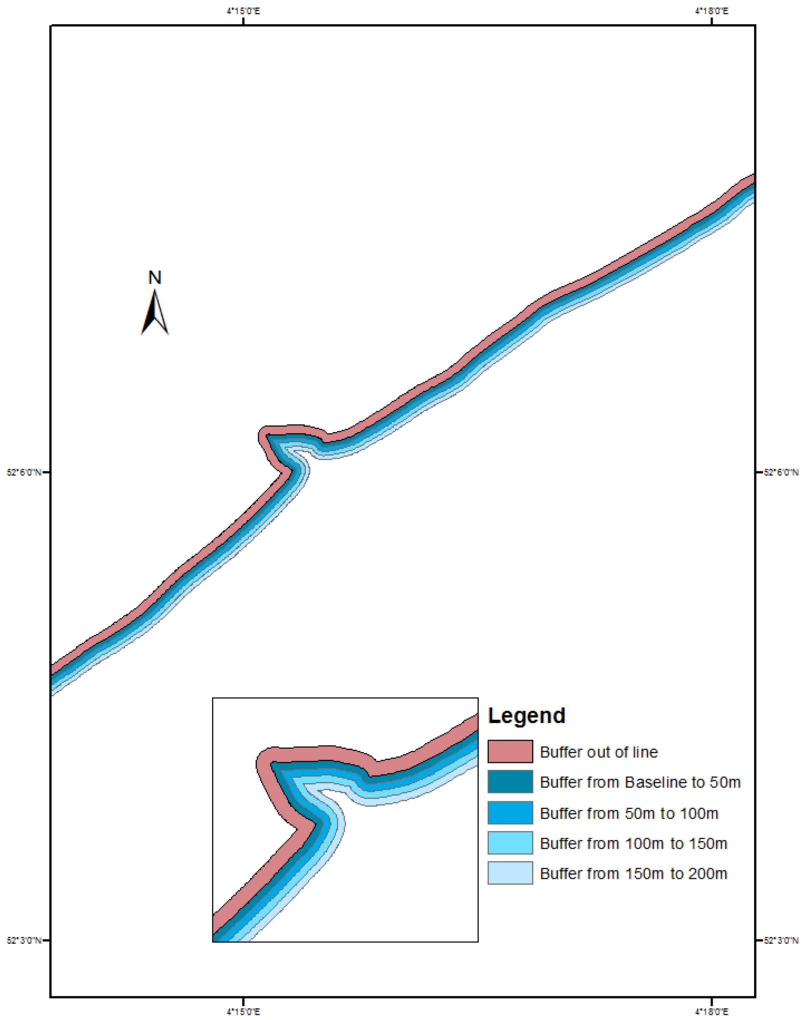

Figure 5-14: Final buffer technique generation

Therefore, the first buffer was made from the Baseline to 50 m facing the land. Continuously, another buffer was created from 50m to 100m. Then, the other two buffers were created following the same criteria. The last buffer was created from Baseline to 100m facing the North Sea to determine how much the line detected exceeds the Baseline (see Figure 5-15).

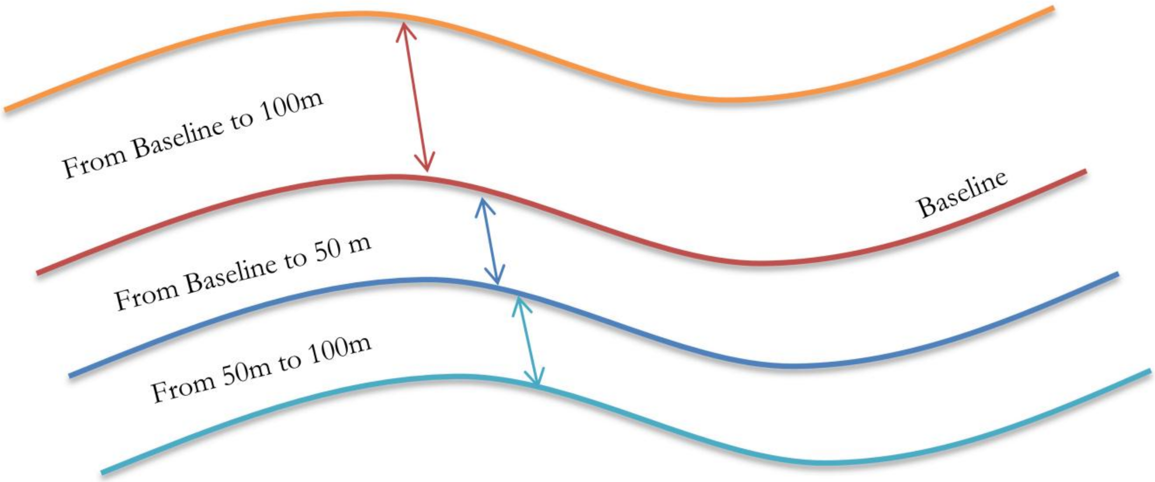

Figure 5-15: Buffer technique estimation taking as reference the Baseline from the Netherlands Hydrographic Service

As demonstration, the image dt_481_delft / 3 (Table 5-2) has a low tide level of -78 cm in vertical according the Time Table of that day and the shoreline to be detected should be approximately 50 m from the Baseline to land and around the first two buffers, Figure 5-16 shows the final output, ready to be validated by applying clipping method from ArcMap10. The output line was selected as input feature and the different buffers (individually) were included as clip features to extracts the overlay features between both inputs.

Table 5-2: Image 3 information

Image information	
Image	dt_481_delft / 3
Mode	Quad Polarization
Date	09 / 05 / 2010
Method	2
Capture time	06 hrs. 08 min 30 sec
Tide Level	-77 cm (Time table)

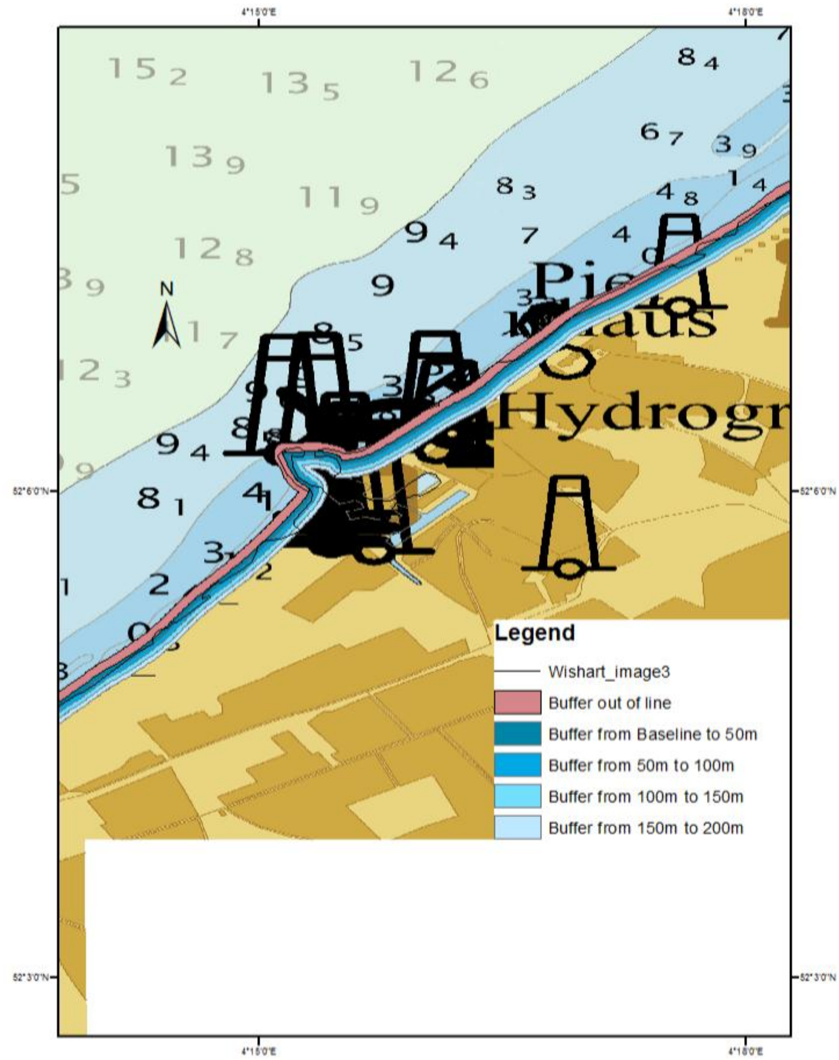

Figure 5-16: Final output for validation and analysis

Figure 5.17 shows the percentage of (a) Method 1 and (b) Method 2 on the detected line in the different buffers, where (a) 35%, (b) 29% of the detected line is inside the 0-50m buffer, (a) 21%, (b) 30% inside the 50-100m buffer, (a) 3%, (b) 9 % inside the 100-150m buffer, and (a) 2%, (b) 3% inside the 150-200m buffer. The remaining (a) 39%, (b) 29% of the detected line is to the seaside of Baseline.

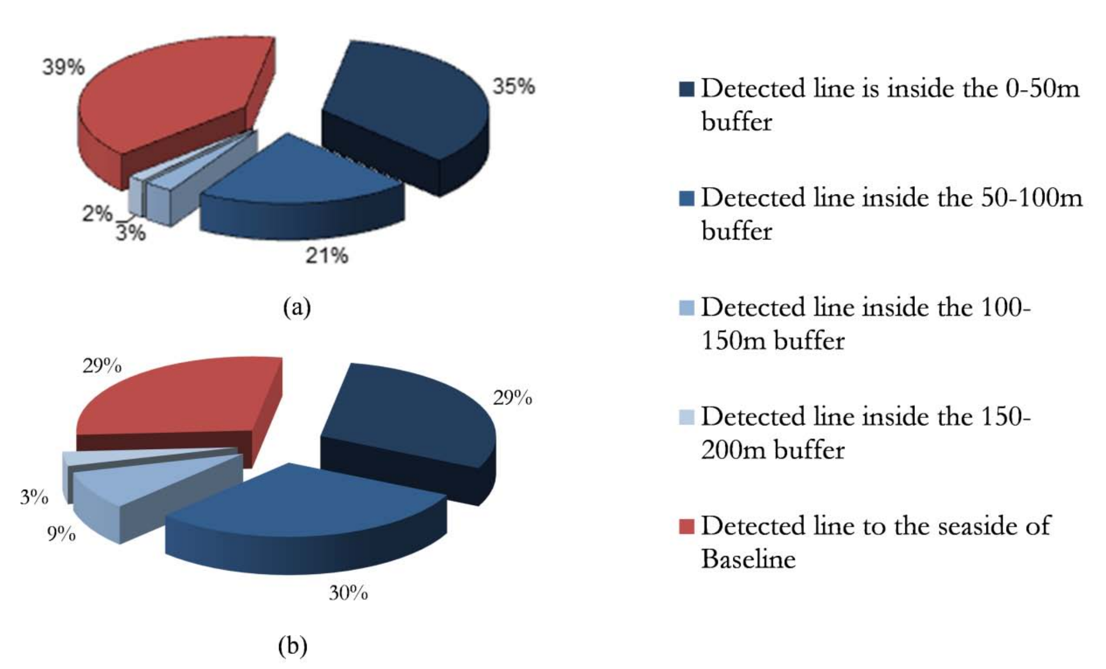

Figure 5-17: Shoreline Analysis from (a) Method 1 and (b) Method 2 after the validation process

In consequence, (a) 46%, (b) 59% of the detected line coincides with the adequate buffer, (a) 5%, (b) 12% passes the expected area and (a) 39%,(b) 29% of the detected line exceeds the Baseline.

5.6.2. Image interpretation

For the image interpretation technique the principal goal is to interpret the data acquired in order to understand the region being imaged. For interpretation, two methods, qualitative and quantitative analysis can be applied. In qualitative method, the analyst's expertise allows the extraction of information through photos, maps in which visual clues around structure and contrast are used. With knowledge of the study area, the analyst can often make a very good assessments of the types of land cover being imaged [51].
In this research, data acquired as Nautical Charts from the Netherlands Hydrographic Service Figure 5-18, Google Earth images Figure 5-19 and Field work photos are used for this validation analysis.

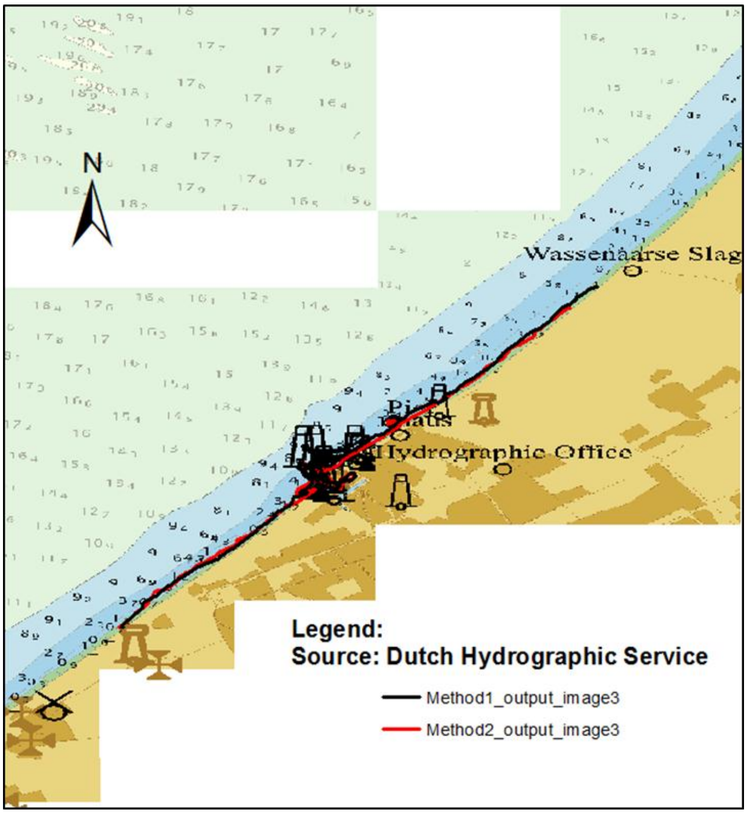

Figure 5-18: Image interpretation by using nautical charts from the Netherlands Hydrographic Service

Figure 5-19: Image interpretation by using Google Earth images

Finding the specific elements for the image interpretation depends in the exact characteristic useful for a specific objective and the manner in which those elements are considered depend on the field of application [3].

Most applications follow these basic characteristics: Shape, size, pattern, tone (or hue), texture, shadows, site, association and resolution [52].

For this research and because of the data that it was provided, only shape, size, pattern, site and association were selected as useful elements for image interpretation analysis.

Shape represents the general nature, form, configuration or outline of individual objects. Size of objects on images is related to the image scale. Pattern relates with the spatial arrangement of objects, the repetition of some common forms or relationship is characteristic of many natural and constructed objects. Site refers to the geographic position and is moderately important element in the identification of objects, in this case, shoreline. Finally, association refers to the relation between features in a specific area.

The image interpretation strategy was divided in two kinds of evaluation. The first one, using the Nautical charts from the Netherlands Hydrographic Service as reference data. The output line was inserted on the nautical chart and evaluated in three different scales; which are: 1:250 000, 1:100 000 and 1:50 000. The idea of this evaluation is to determine if the output lines coincide with the map and how useful this can be for the different kind of purposes, an example scale chart 1:250 000 can be used just for general information when the precision of the shoreline is not very important.

The other evaluation was done by using Google Earth images, having as support photographs from the fieldwork. The criteria of this method were to evaluate the output lines in two different areas, north and south with a fixed scale. The basic feature object characteristics, such as shape, size, pattern, site and association were used for the interpretation.

For the first evaluation, international regulations were used as reference information. According with [29] the choice of scale depends on the navigational requirements of international shipping. For example for coastal navigation, the adequate scales vary between 1:75 000 and 1:350 000. Where detail information from ports, harbour or accurate information from shoreline is not very relevant.

In that sense, the first figures to be analysed are Figure 5-20 and 5-21, both images using 1:250 000 and 1:100 000 are considered as medium scale. The images demonstrated a good visual match between the nautical coastline and the output line achieved in this research. Both methods are not having too much difference between each other by using this scale factor. Nevertheless, in Figure 5-21 there are some small differences between output lines but the distance at this scale is not significant.

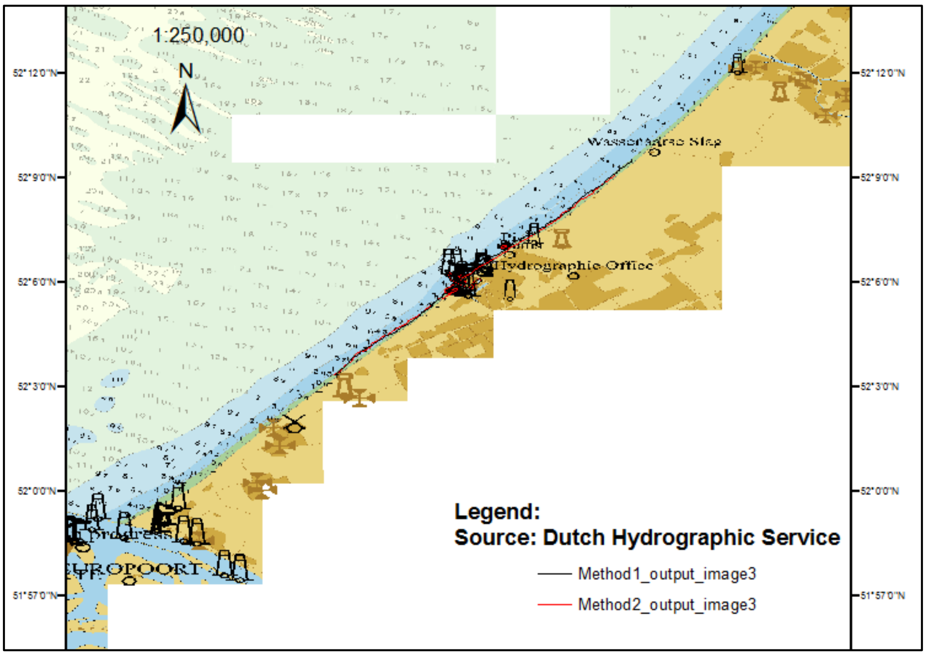

Figure 5-20: Nautical chart, scale 1:250 000

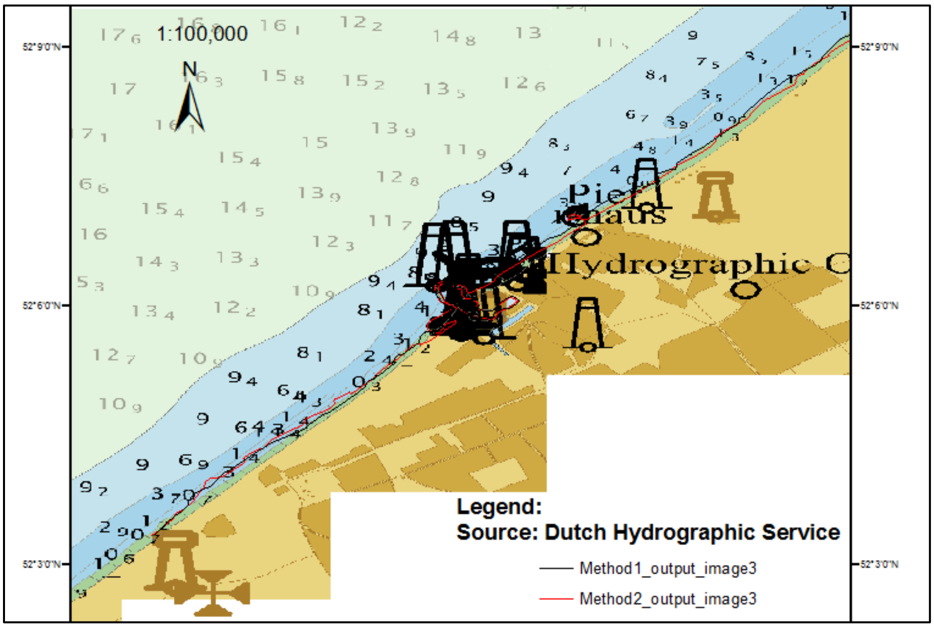

Figure 5-21: Nautical chart, scale 1:100 000

The last figure to be analysed by using the nautical chart is Figure 5.22, this kind of scale required good and precise information. According with [29] for congested coastal waters or harbours the scale varies from 1:30 000 to 1:75 000 and even larger, where, detailed, precise and accurate information is required with this kind of scales.

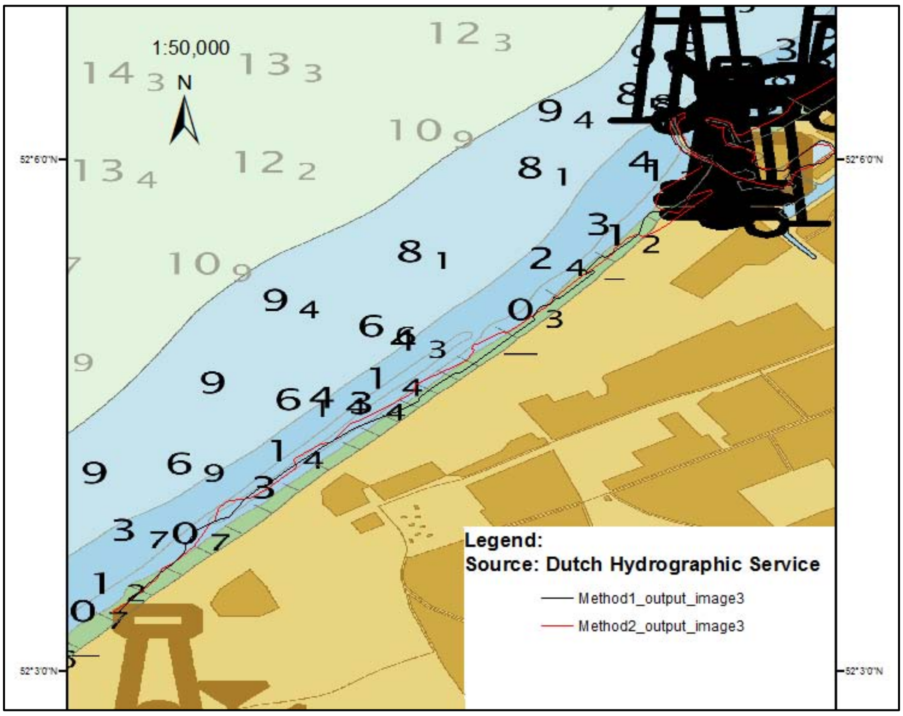

Figure 5-22: Nautical chart, scale 1:50 000

Figure 5.22 has a scale 1:50 000 considered as large scale. It shows an irregular line, where the harbour is well detected but not well described. Both methods have a similar pattern but the position of the line is not accurate at all. In this case, the output line is not recommended for reference shoreline, because there is not a good accurate match between the shoreline from the nautical chart and the detected output line.

For the second evaluation Google Earth image was used to interpret the real world with the output lines. Two different areas, north Figure 5.23 and south Figure 5.24 with a fixed scale were evaluated by using the basic feature object characteristics, such as shape, size, pattern, site and association (Table 5-3).

Figure 5-23: Google Earth image, north area. Black line method 1 and Red line method 2 from Image 3

Figure 5-24: Google Earth image, south area. Black line method 1 and Red line method 2 from Image 3

Table 5-3: Visual interpretation analysis from Google Earth image and Output lines

Visual Interpretation					
Area of interest	**Interpretation elements**				
	Shape	**Size**	**Association**	**Pattern**	**Site**
Shoreline North area Method 1	Linear Irregular	8.2 km	Parallel from land and sea	Continuously line, parallel the coast	Close to the real coastline
Shoreline North area Method 2	Linear Regular	8 km	Parallel from land and sea	Continuously line, parallel the coast	Almost with the real coastline
Shoreline South area Method 1	Linear Irregular	6 km	Parallel from land and sea but irregular in the last area	Continuously line, parallel the coast	Good located but not in the last area
Shoreline South area Method 2	Linear Regular	6 km	Parallel from land and sea but irregular in the last area	Continuously line, parallel the coast	Good located but not in the last area
Harbour Method 1	Irregular	1 km	Surrounding the area of interest	Following building shape	Well detected but not good detailed
Harbour Method 2	Irregular	1 km	Surrounding the area of interest and water areas	Not well	On location but with some irregularities
Pier Method 1	Not shape	-	-	-	-
Pier Method 2	Linear Regular	300 m	Surrounding the area of interest	Following building shape	Well detected but not good detailed

Image interpretation was done successfully, the interpretation elements help to describe and evaluate the output lines with the Google Earth image. With the previous knowledge of the study area, the interpretation technique was easier than just evaluating the image in a visual procedure. The output lines in the North area coincide better with the real coastline shape; the association, pattern and site are having good results in comparison with the output lines in the South area. More analysis with more field information can enable to understand the behaviour of the coast in this area.

5.7. Final results

The final results from the buffer method described in Section 5.6.1 were evaluated in two ways; First, by computing the overall results between the out of Baseline for all the 6 images per each method and the output lines inside the most adequate buffer, taking account the tide level. As an example, from Figure 5-25, the output lines coming from the images 3 and 6, with tide level of -77 and -50 cm respectively, are evaluated and expected to be inside the “Buffer from Baseline to 50m” and “Buffer from 50m to 100m”.

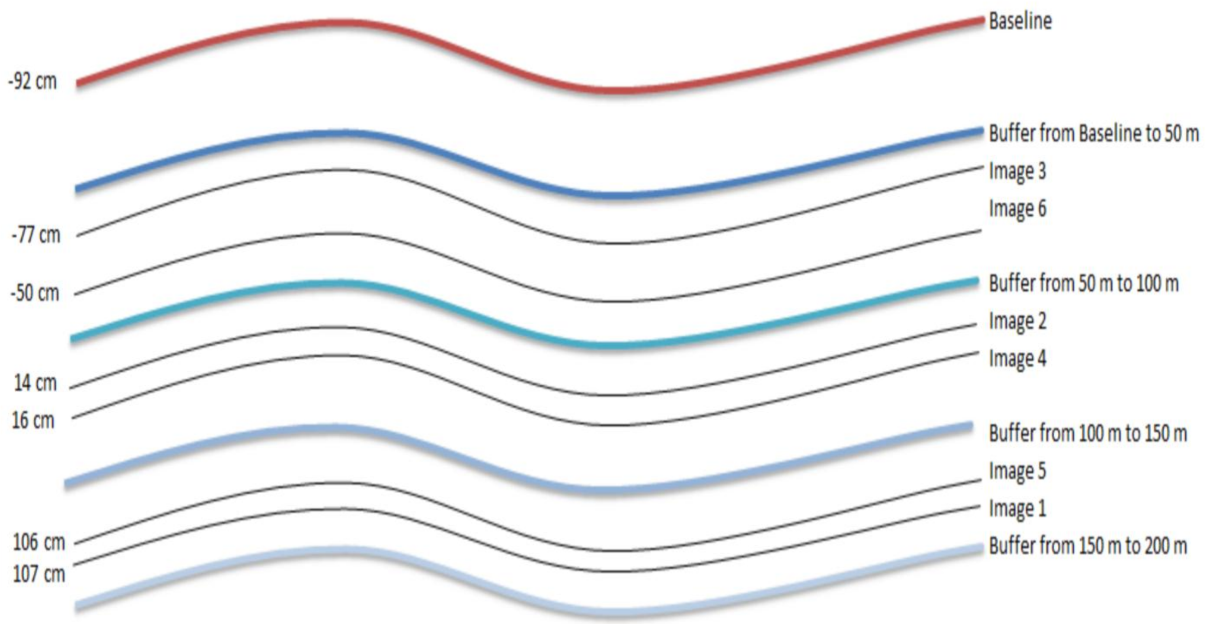

Figure 5-25: Buffer method and output lines with tide levels.

The lines which cross the Baseline are considered as "out of Baseline" and evaluated as bad output.
Table 5-4 represents the final analysis of output lines inside the adequate buffer. By applying this method, the accuracy of the output lines will be detected. Following these criteria, all the images were evaluated and the final overall results are shown in Table 5-5.

Table 5-4: Output shoreline to be detected, inside the most appropriate buffer

	Buffer from Baseline to 50m	**Buffer from 50m to 100m**	**Buffer from 100m to 150m**	**Buffer from 150m to 200m**
Image 1 Tide level: 107 cm			×	×
Image 2 Tide level: 14 cm		×	×	
Image 3 Tide level: -77 cm	×	×		
Image 4 Tide level: 16 cm		×	×	
Image 5 Tide level: 106 cm			×	×
Image 6 Tide level: -50 cm	×	×		

Table 5-5: Overall results from the first analysis

Final assessment	Method 1	Method 2
Overall out of Baseline	33%	36%
Most adequate detection	47%	45%

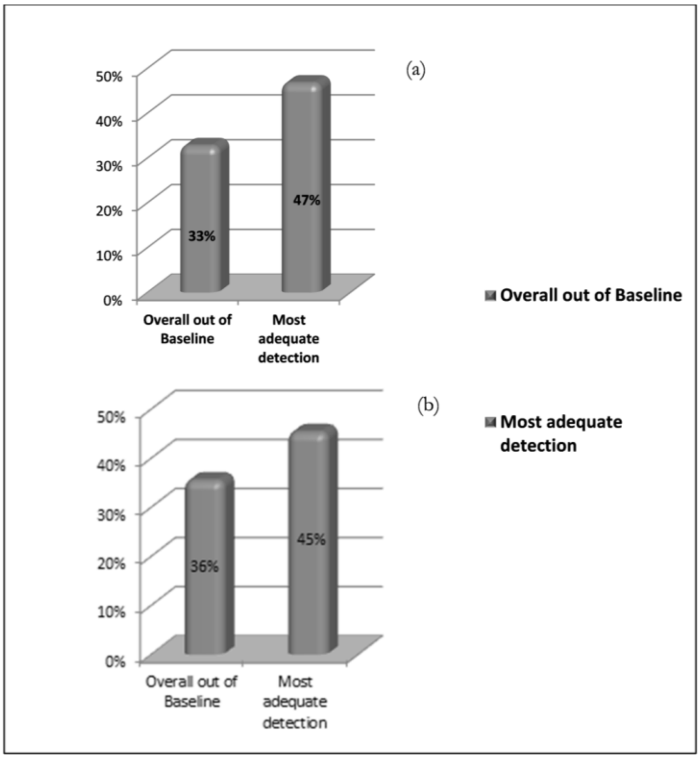

Figure 5-26: Statistic output from Table 5.2 between most adequate output lines vs. Out of Baseline from (a) Method 1 and (b) Method 2, where the overall out of Baseline in red shows (a) 33%, (b) 36% and the most adequate detection in blue shows (a) 47%, (b) 45%.

The second evaluation is following the same criteria of the first assessment by evaluating the "out of Baseline" but the difference in this case is the evaluation of the output lines which are inside the boundary between land and Baseline. The final overall results are shown in Table 5-6.

Table 5-6: Overall results from the second analysis

Final assessment	Method 1	Method 2
Overall out of Baseline	33%	36%
Between land and Baseline	67%	64%

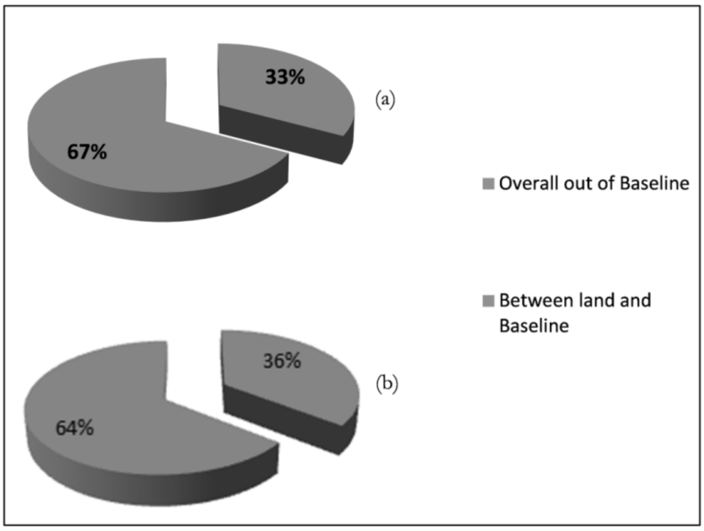

Figure 5-27: Graphic output from Table 5.3 output lines inside the boundary between land and Baseline vs. out of Baseline from (a) Method 1 and Method (b), where the overall out of Baseline in red shows (a) 33%, (b) 36% and the boundary between land and Baseline in blue shows (a) 67%, (b) 64%.

According the overall results, Method 1 has better results than Method 2. There difference between methods is not really significant. Both methods show moderate percentages at the moment to analyze the detected shoreline between land and the Baseline.

6. DISCUSSION

This chapter presents a discussion of the complete research, reviewing the usefulness of polarimetric data for shoreline detection, the methodology applied to achieve the outlined objectives, final analysis, special DLR campaign, their experimental product and some further methods to be implemented.

6.1. Polarimetric data for shoreline detection

Polarimetric data has the main characteristic to provide the complete polarization information. That has many advantages, such as the surface can be examined using single polarization, dual polarization and in quad polarization. Many authors were describing the usefulness of single or dual polarization for shoreline detection. This research explored the new capabilities of TerraSAR-X in quad polarization in a specific application, shoreline detection. The results show how good the polarimetric data can be decomposed, classified, segmented and finally exported, to extract the expected shoreline in shape file. The use of quad polarization with high spatial resolution satisfies the expectations.

Polarimetric applications in quad polarization mode is still a new topic, on which few scientific papers have been written and even during the recent 4th DLR science meeting, there were not yet sufficient investigation results of this mode. During the implementation of this study, quad polarization resulted a complicate and sometimes time consuming process, but its implementation in a new application, like shoreline detection, was having good results even without applying many tools.

6.2. Usefulness of polarimetric decomposition decision

The Freeman-Durden model-fitting approach has the advantage that it is based on the physics of radar scattering, not on a purely mathematical construct. The three component scattering mechanism model proved to be useful in providing features for distinguishing between surface cover types and in helping to determine the current state of the surface cover.

This model was developed aiming at the discrimination of flooded and non-flooded forest and to estimate the effects of forest inundation and disturbance on the fully polarimetric radar signature.

Because of that, this research applied that method as very useful tool to discriminate water from land, to maximize the use of the polarimetric data, by decomposing the image in three different layers to delineate the shoreline in the study area. The study area presents many wet areas with some vegetation surrounding the beach. There is no presence of large urban areas. Therefore, the method can be applied to a different area, as for example, Delft city. Delft city has the particularity to have many canals inside the city, with complicate man-made structures with complicated shapes. For that kind of environments, Freeman and Durden decomposition will not produces good results. For that reason, Yamaguchi [45], proposed a fourth component decomposition equivalent to a helix scattering power.

Another decomposition theorem was proposed by Van Zyl [40], in this method, volume and double backscattering can be distinguished, in comparison with Freeman and Durden decomposition. Figure 6-1 shows the difference between Freeman and Durden, Yamaguchi and Van Zyl decomposition based on build up areas, and the difference on volume and double bounce detection. Notice that (b) can be able to detect more build-up areas than (a), because of the fourth component proposed by Yamaguchi, and (c) can identify and separate the double bounce from the volume bounce.

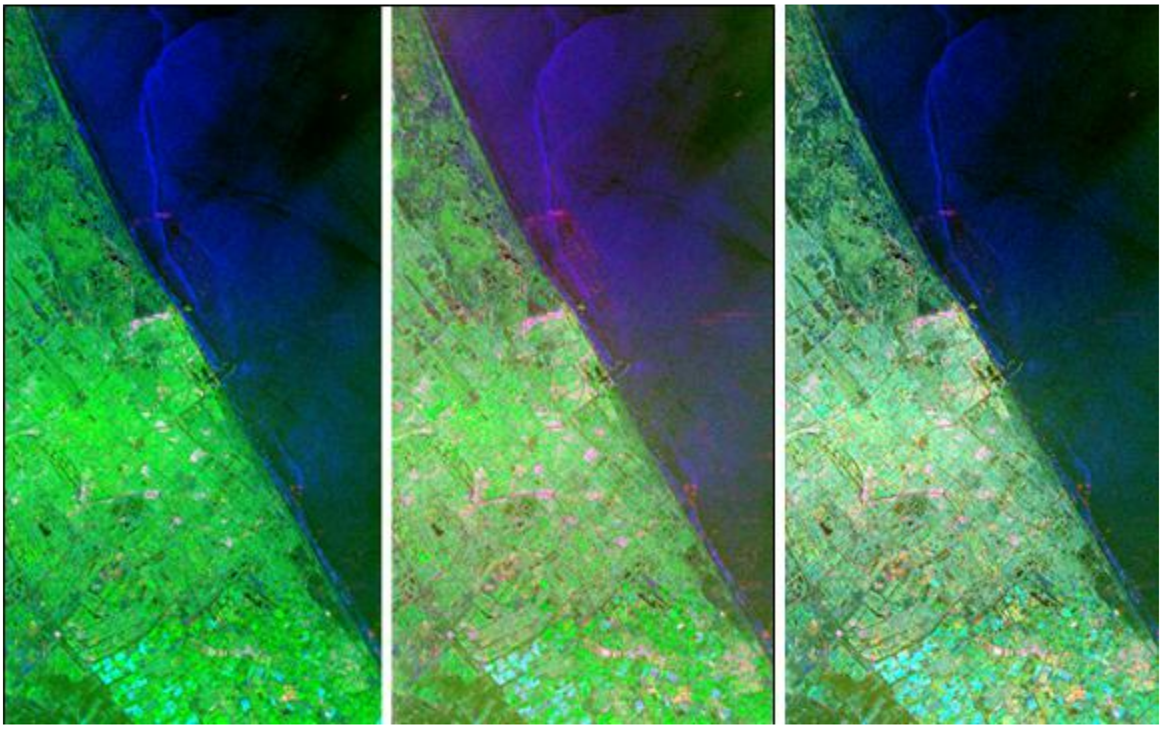

(a) (b) (c)

Figure 6-1: Difference between (a) Freeman and Durden decomposition, (b) Yamaguchi decomposition and (c) Van Zyl decomposition. Noticed that (b) has more detection in build-up areas in comparison with (a) and (c) can identify and separate better the double bounce from the volume. Where Red represents Double bounce, Green represents volume bounce and Blue represents surface bounce

6.3. Speckle reduction

The impossibility to use a multilooking procedure because the images could not be changed from the original resolution for the lack of a georeferencing application (Section 4.2.1), made it compulsory to use a filter to reduce the amount of speckle without decreasing the resolution and other characteristics. Lee refined filter used an algorithm able to preserve the polarimetric properties and statistical correlation between channels, not introducing cross talk and not degrading the image quality. The images preserved the characteristics of the feature object, but lost some information. The presence of speckle was not totally solved and because the windows size used in this research was relatively small, it was really difficult to make an accurate classification and segmentation. By increasing the windows size from $5 \times 5\, for\, 11 \times 11$ the speckle can be reduced much better, but as the objective of this research was the detection of shoreline, it was more convenient to preserve the edge of the feature objects without degrading and smoothing them to facilitate the detection of the line between features.

The advancement of SAR images with high spatial resolution demands better and more efficient speckle filtering algorithms, Lee [53] improved the sigma filter for speckle filtering developed in 1983 by reducing the old deficiencies presented in the past. The use of this filter for polarimetric data is a good alternative to deal with the big amount of speckle coming from the polarimetric data and from the high spatial resolution. In this study, it was not possible to apply this filter because it was not available in the PolSARpro software for TerraSAR-X. This problem should be solved in a near future, since the PolSARpro helpdesk management and they replied that it under development.

6.4. Georeferencing

The lack of a georeferencing application for TerraSAR-X quad polarization images after the Freeman and Durden decomposition application produced many complications, such as the impossibility to apply

multilooking to the images. The application of affine transformation results the most adequate option but it degrades the original shape and angle orientation of the image.
One good possibility to avoid this inconvenience was the modification of the header that is the metadata of the image, by using as reference an already georeferenced image, provided by DLR.
These inconveniences and disadvantages can be solved when quad polarization images will no longer be considered experimental products and when more researches provide the necessary tools.

6.5. Classification and segmentation

Wishart supervised classification was selected because of the good performance shown in some scientific papers and books, like Lee [35], Guangyi [54], Lopes [55], Lee [12], and because of the good results when classifying the Freeman and Durden decomposition image. As ground control point measurements were not available, training areas were selected from the image, based on the scattering characteristic of the Freeman and Durden RGB decomposition. The training areas were selected carefully and precise but the presence of speckle in the image made it more difficult and the classification results were not as good as expected. Because of that, the multiresolution segmentation with region growing technique was having difficulties to merge groups of pixels with the same value. The classification post-segmentation on the beach area was more difficult. The differences between sand and water were detected after the classification, but not good enough for a good shoreline extraction. After fieldwork, the segmentation and classification improved because of the knowledge of the area.
It is possible that atmospheric influences disturb the procedures. High humidity, strong winds and heavy fog can be detected by the microwave sensor.

6.6. Validation

Several methods exist for validating shorelines from RS images. Yu [23] concludes that their method demonstrated a good visual match between the detected shoreline and the manually contoured coastline. The results of Dellepiane [56] were quantitatively evaluated through the comparison with optical aerial images. Baghdadi [24] examined their results by examining the difference in the radar signal between land and sea (photo-interpretation). Manson [57] assessed that over 90% of the shoreline detected appears visually correct after the automatic delineation. It can be noticed that the most of the work related with this topic was validated and evaluated by using image interpretation techniques. For that reason, data from the Netherlands Hydrographic Service (NLHS) and Google Earth images were used as reference data for visual interpretation analysis.
This kind of assessment can only be qualitative evaluation of the outputs, even the interpretation by users can be different according with their experience and background. Therefore, the buffer method was implemented (Section 5.6.1). The idea is to evaluate whether extracted shorelines are properly located after the application of both methodologies. From this evaluation it seemed that neither of the methods, nor Method 1 nor Method 2 was producing accurate results, but it does not mean that it was a bad application or procedure during the implementation of these methodologies. The methods as it is mentioned in Section 6.5 were selected with previous literature review and by testing them with sample data. External inconvenience mentioned before, affected the good application and results from those methods.
For visual interpretation, the detected shoreline was showing good location in comparison with the medium scale nautical chart and with the help of Google Earth program. For the large scale nautical chart, the comparison with the output line was not appropriate, because it was not coinciding with the real location of the coastline.
PolSARpro keeps updating the software. In January 2011, a new version with some new application, including some fixed bugs for TerraSAR-X was realised, but that was too late to be used here.

The validation process in terms of qualitative evaluation was difficult to assess, since the detected shoreline is a line product and to compare that line without a good reference data, made this evaluation a difficult task. In Section 6.8, some further work is described to improve this situation.

6.7. Dual Receive Antenna

The data in this campaign was acquired in Stripmap mode in a dedicated 33 days lasting campaign, during April and May 2010.

During the experimental operation, twin and quad polarization modes were able to capture. The configuration of the DRA in Stripmap mode provides the full (quad) polarization data.

Quad polarization, like in dual polarization mode, horizontal and vertical polarization is transmitted in a pulse to pulse alternating mode. For the receive polarization, both antenna segments receive the different polarizations, as result, a Stripmap product is achieved, covering a swath width of a dual polarized image (15 km).

The main objectives of these products are:

- Quad polarization X-band high resolution SAR data for mapping and monitoring purposes
- Development of improved image processing and information retrieval techniques
- Development and definition of corresponding applications, geo information products and services

It was demonstrated in the 4th DLR science meeting, 14-16 February 2011, that quad polarization applications are still in their beginnings, not too much information is available about the use of this technique and some conclusions are based on preliminary results.

The purpose of this campaign was the evaluation of a new class of experimental products, to foster the improvement and development of new technologies and applications. The campaign was related in particular to SAR polarimetry, polarimetric interferometry and along track interferometry.

The main purpose of the investigation was the evaluation of the experimental TerraSAR-X products, the development of improved image processing and information retrieval techniques and the development and definition of new applications, geo-information products and services.

According with the 4th DLR science meeting in Munich, on 14, 15 and 16 on February 2011, there is not going to be any other special quad pol campaign in the next few years, due to the high cost of this kind of campaign represents. In that sense, quad polarization images from the last campaign are still going to be considered as experimental products. That has two big connotations. The first one is a positive point, the images will be provided for free for research purposes after the submission of approval proposal. The second point is negative, because it means that the well-known software companies are not going to develop any application if they are not considered for commerce. Open source software is considered a very important tool for this kind of products. Nevertheless, the insufficient applications and the technical support can be a disadvantage.

6.8. Further work

The next lines are going to be dedicated to those researchers who would like to continue with this project or to the people who were interested in this study to get some idea of what can be next. The idea is to improve the results. Experimental data is always risky, but working with risks and addressing them is making the study and knowledge more attractive.

The effort to get the most accurate shoreline using classification and segmentation methods met with several difficulties, and because of the tide levels and the local topography of The Netherlands coast; new possibilities to find better applications for this study will be discuss.

The Netherlands Hydrographic Service (NLHS) recommends comparing the shoreline with advance applications, but first, it is necessary to include some extra procedures, such as the correction of the water

level by using probably more accurate information than the tidal predictions that the NLHS publishes, due to the very gradual slopes of the Holland beaches. More accurate water level information is available at Rijkswaterstaat, which is also responsible for surveying the coastal zone as same as NLHS.
A digital terrain model is necessary to evaluate and analyse the different kinds of slopes in all the coast of the study area. According with Table 1-1 quad polarization can produce Digital Elevation Models (DEM), but this is still under experiment and depends also in the availability of the application for TerraSAR-X.
By using those elements, they will be very useful to detect the difference between land and sea, according the different tide scenarios (Figure 6-2)

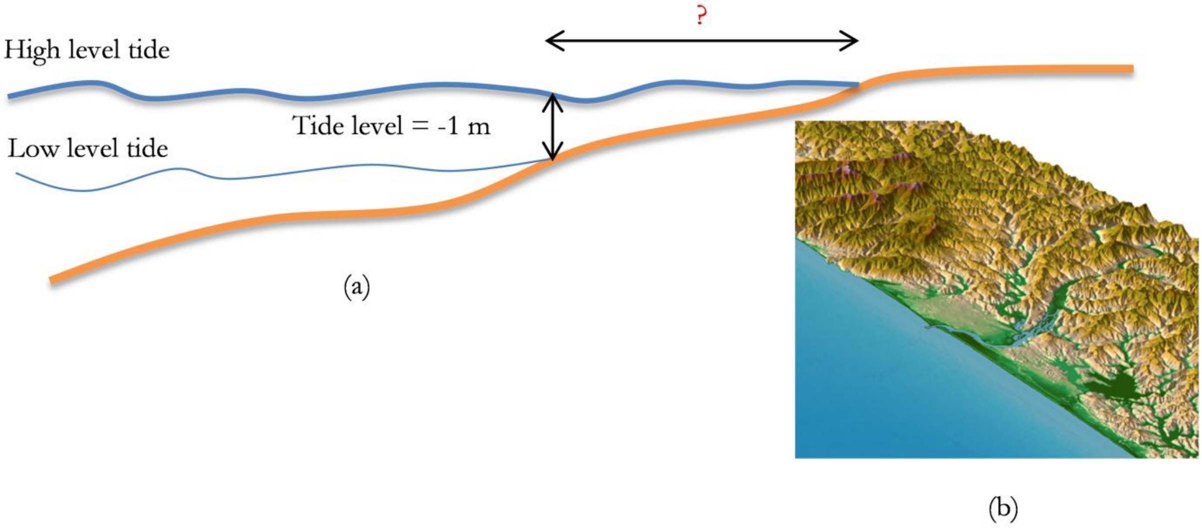

Figure 6-2: (a) Example tidal level scenario with -1m low sea level and (b) DTM generation from the analysis of the beach slope. Interrogation mark must be solved after the analysis of the DEM.

Validation can also be done by fieldwork in all the area of interest (around 10 km) and capturing ground control points in different tide levels. This kind of method is used to determine the coastline, but the purpose of this research is to minimize the cost of field survey and also to maximize the use of remote sensing techniques. Some other ideas are to identify the tide levels, like Hydrologic models by introducing the tide level and running the model for the specific scenario. The problem of these models is that they also need the generation of DTM to identify the different slopes on the study area. LIDAR can be also a useful tool to extract the shoreline but this kind of method is quite expensive in comparison with the last methods. LIDAR can be used to make a DEM, which can then be used in shoreline detection. Currently a new high resolution DEM is being recorded for The Netherlands (AHN2) based on LIDAR.

7. CONCLUSIONS AND RECOMMENDATIONS

The aim objective of this research was to evaluate if the high spatial resolution as fine as 3 m in Stripmap mode from the experimental TerraSAR-X campaign in quad polarization mode is suitable to map the shoreline of the South Holland province.

TerraSAR-X is a good alternative because of the high spatial resolution and new features, like quad polarization.

The main conclusion is that the experimental quad polarization image with high spatial resolution as fine as 3 m is suitable for the detection of the shoreline in the South Holland province. Accuracy could not be fully evaluated yet, and because of software limitations, and incomplete validation data, since the influence of the tide on the horizontal movement of the shoreline could not be properly included. The final results showed in Section 5.2 are not according with what it was expected.

During the implementation and literature review, few decomposition theorems were revised. For this research and for the study area, Freeman and Durden decomposition was selected because of the main characteristic to detect the physical characteristics of the feature object and because it was developed for detecting flood areas around forest (volume backscattering). Because there is not a specific theorem for shoreline detection, Freeman and Durden decomposition was determined as the most adequate. The decomposition results from the shoreline by applying Freeman and Durden decomposition theorem are good, in comparison with the real world (Google Earth image and fieldwork).

Speckle reduction was a mandatory step. Some filters for polarimetric data were revised and tested. After some comparisons, Lee Refined filter was selected because, it avoids cross talk and it does not affect the image resolution. Nevertheless, Lee in 2009, proposed a new and improved version of the Lee sigma filter [53]. PolSARpro includes this filter in their polarimetric tools applications but inclusive in this newest version, this filter does not work for TerraSAR-X in quad polarization mode.

The georeferencing application in this study was not the most convenient way to georeference the image. The image header was edited and then the image was georeference by doing affine transformation. The deformation in angles and shape was not very large, but those kinds of changes can determine meters of accuracy between the output shoreline detected and the real coastline.

In January 2011, PolSARpro released their last version 4.2, making georeferencing now available for TerraSAR-X products. Because of the short time, it was not possible to test this here.

For classification, Wishart supervised classification demonstrates to have a good performance without needing any ground control point data. The advantage to categorize the classes by different colours (Figure 4-7) makes this application more interesting.

The selection of the training areas can improve if the image does not contain big amounts of speckle like in this case. For example, by applying multilooking 4:1 and speckle filter reduction, can be Lee sigma filter, the classification and segmentation with region growing technique can be much more improved.

The Dual Receive Antenna campaign is having good results from the scientific point of view, some disadvantages, like the availability of the data (just in special campaigns) or the complex configuration described in the Section 2.7.2 may not be an impediment to work with it.

It is expected that according new studies, applications and methods using quad polarization images; software developers and researchers are going to be able to complete and make successful all the ideas and objectives of this study.

7.1. External procedures

- Before starts operating the experimental data, it was necessary to make an application to the German Aerospace Centre (DLR) (http://sss.terrasar-x.dlr.de/) by sending a research proposal. This proposal must consider the objective, methodology, study area, which and how many images are necessary for this research. Noticed that between the submission and approval it may take some weeks.
- The methodology of this research had some small changes, because of the software availability and their applications, the selection of the program must be related with the methodology and in specific when the data is under experimental mode.
- As the data is under experimental mode, technical support was limited and many problems, like "bugs" arose during the implementation.
- For the validation reference data, is important to have contact with the national entities. The Netherlands is one of the few countries where their data and information is provided free of charge for study and research purposes.
- The sea water information (tide levels) was acquired from the NLHS (http://www.defensie.nl/english/navy/hydrographic_service/) and from the Rijkswaterstaat (http://www.rijkswaterstaat.nl/water/)
- Because each quad polarization image includes the four polarizations (HH, HV, VH, VV) the analysis and evaluation took many minutes. In that sense, a good hardware was required and some patience as well.
- Frequent communication with the software managers was necessary during the implementation.
- A limited amount of fieldwork was necessary to have a better interpretation of the study area.

7.2. Recommendations

Taking into account the implementation and results in this research project, the following recommendations are made for further improvement:

- The opportunity to work with experimental data makes any research project more interested. Because of quad polarization remains in its nascent stages, DRA call is nowadays in an unlimited time. After proposal submission, the approval can take few weeks; it is recommendable to starts as soon as possible to do not lose that time.
- Before the selection of the polarimetric decomposition theorem, is very important to first evaluate the purpose and the study area. After that decision, it is possible to select an appropriate decomposition theorem, as it is shown in Section 6.2.
- Few polarimetric filters for speckle reduction are available, Lee sigma filter may present a good alternative to deal with the increased speckle, produced by the polarimetric scatters and because of the high spatial resolution. Other kinds of filters, like morphological filters can be explored, but it needs further investigation for polarimetric data.
- Finally, this research can be improved by the use of DTM. The possibility to create DEM with polarimetry data can be a good topic to be developed. Accurate tide information can be obtained from the Rijkswaterstaat.
- Good communication with the National entities and with the software managers can improve and can be very helpful during the implementation of any project.

LIST OF REFERENCES

[1] Deltacommissie. (2008, Working together with water. 138. Available: http://www.deltacommissie.com/doc/deltareport_full.pdf

[2] Greidanus H. and Otten M. P. G., "Coastal imagery from the polarimetric airborne SAR PHARUS," in *Geoscience and Remote Sensing Symposium, 2002. IGARSS '02. 2002 IEEE International*, 2002, pp. 1717-1719 vol.3.

[3] Lillesand T. M., Kiefer R. W., and Chipman J. W., *Remote sensing and image interpretation*, Sixth edition ed. New York: Wiley & Sons, 2008.

[4] van der Sanden J. J., "Anticipated applications potential of RADARSAT-2 data," *Canadian Journal of Remote Sensing,* vol. 30, pp. 369-379, Jun 2004.

[5] RADARSAT-2. (2009, *RADARSAT-2 Information*. Available: http://www.radarsat2.info/about/faq/faq_beam.asp

[6] DRA and SOAR. (2010, *RADARSAT-2/TerraSAR-X- Initiative*. Available: http://radarsat.space.gc.ca/pdf/2010_soar-dlr_en.pdf

[7] German Aerospace Center. (2009, TerraSAR-X / The German Radar Eye in Space. Available: http://www.dlr.de/en/Portaldata/1/Resources/forschung_und_entwicklung/missionen/terrasar_x/TSX_brosch.pdf

[8] Moon W. M., Staples G., Duk-jin K., Sang-Eun P., and Kyung-Ae P., "RADARSAT-2 and Coastal Applications: Surface Wind, Waterline, and Intertidal Flat Roughness," *Proceedings of the IEEE,* vol. 98, pp. 800-815, 2010.

[9] Lintz J. and Simonett D. S., *Remote sensing of environment*. Reading etc.: Addison-Wesley, 1976.

[10] Henderson F. M. e. and Lewis A. J. e., *Principles and applications of imaging radar*, Third edition ed. New York etc.: Wiley & Sons, 1998.

[11] Bijker W., "Radar remote sensing" Lecture class.

[12] Jong-Sen Lee and Pottier E., *Polarimetric radar imaging : from basics to applications*. Boca Raton: CRC Press, 2009.

[13] Ulaby F. T. e. and Elachi C. e., *Radar polarimetry for geoscience applications*. Norwood: Artech House, 1990.

[14] Oliver C. and Quegan S., *Understanding synthetic aperture radar images*. Boston etc.: Artech House, 1998.

[15] Hussin Y. A., "Polarimetric data," Lecture class.

[16] van Zyl J. J., Zebker H. A., and Elachi C., "Imaging radar polarization signatures: Theory and observation," *Radio Sci.,* vol. 22, pp. 529-543, 1987.

[17] Natural Resources Canada. (2008, *Tutorial: Radar Polarimetry Basics of SAR Polarimetry The scattering matrix*. Available: http://www.ccrs.nrcan.gc.ca/resource/tutor/polarim/chapter1/06_e.php

[18] Quegan S., "A unified algorithm for phase and cross-talk calibration of polarimetric data-theory and observations," *Geoscience and Remote Sensing, IEEE Transactions on,* vol. 32, pp. 89-99, 1994.

[19] DLR, "TerraSAR-X Ground Segment Experimental Product Description," ed: German Aerospace Center (DLR) 2006, p. 11.

[20] Mittermayer J. and Runge H., "Conceptual studies for exploiting the TerraSAR-X dual receive antenna," in *Geoscience and Remote Sensing Symposium, 2003. IGARSS '03. Proceedings. 2003 IEEE International*, 2003, pp. 2140-2142.

[21] DLR, "TerraSAR-X Ground Segment Basic Product Specification Document," ed: German Aerospace Center (DLR) 2006, p. 108.

[22] Maureen, Yeremy M., and Beaudoin, "Global Shoreline Mapping from an Airborne Polarimetric SAR," Defence R&D Canada2001.

[23] Yu Y. and Acton S. T., "Automated delineation of coastline from polarimetric SAR imagery," *International Journal of Remote Sensing,* vol. 25, pp. 3423-3438, Sep 2004.

[24] Baghdadi N., Pedreros R., Lenotre N., Dewez T., and Paganini M., "Impact of polarization and incidence of the ASAR sensor on coastline mapping: example of Gabon," *International Journal of Remote Sensing,* vol. 28, pp. 3841-3849, 2007.

[25] Sheoran A., Haack B., and Sawaya S., "LAND COVER/USE CLASSIFICATION USING OPTICAL AND QUAD POLARIZATION RADAR IMAGERY," George Mason University, Baltimore, Maryland2009.

[26] Carter R., *Coastal environments : an introduction to the physical, ecological and cultural systems of coastlines*. London etc.: Academic Press, 1988.

[27] Bird E., *Coasts : an introduction to coastal geomorphology*, Third edition ed. Oxford: Basil Blackwell, 1984.

[28] Nelson S. A. (2010, Coastal Zones. Available: http://www.tulane.edu/~sanelson/geol204/coastalzones.htm

[29] International Hydrographic Organization, "REGULATIONS OF THE IHO FOR INTERNATIONAL (INT) CHARTS AND CHART SPECIFICATIONS OF THE IHO," ed, 2010.

[30] Dutch Hydrographic Service. (2010, *Maritime Limits*. Available: http://www.defensie.nl/english/navy/hydrographic_service/geodesy_and_tides/

[31] Oceans and Law of the Sea, "United Nations Convention on the Law of the Sea (UNCLOS)," ed, 1982.

[32] Ministerie van Verkeer en Waterstaat. (2010, *Monitoring and measurement systems*. Available: http://www.rijkswaterstaat.nl/water/scheepvaartberichten_waterdata/monitoring_meetsystemen/

[33] European Space Agency. (2011, *About PolSARpro*. Available: http://earth.esa.int/polsarpro/about.html

[34] Natural Resources Canada. (2008, *Tutorial: Radar Polarimetry Coastal zone applications Shoreline detection*. Available: http://www.ccrs.nrcan.gc.ca/resource/tutor/polarim/chapter1/06_e.php

[35] Jong-Sen L., Grunes M. R., and de Grandi G., "Polarimetric SAR speckle filtering and its implication for classification," *Geoscience and Remote Sensing, IEEE Transactions on,* vol. 37, pp. 2363-2373, 1999.

[36] Novak L. M. and Burl M. C., "Optimal speckle reduction in polarimetric SAR imagery," *Aerospace and Electronic Systems, IEEE Transactions on,* vol. 26, pp. 293-305, 1990.

[37] Jong-Sen L., Grunes M. R., and Mango S. A., "Speckle reduction in multipolarization, multifrequency SAR imagery," *Geoscience and Remote Sensing, IEEE Transactions on,* vol. 29, pp. 535-544, 1991.

[38] Goze S. and Lopes A., "A MMSE SPECKLE FILTER FOR FULL RESOLUTION SAR POLARIMETRIC DATA," *Journal of Electromagnetic Waves and Applications,* vol. 7, pp. 717-737, 1993.

[39] Huynen J. R., "Phenomological theory of radar targets," 1970.

[40] van Zyl J. J., "Unsupervised classification of scattering behavior using radar polarimetry data," *Geoscience and Remote Sensing, IEEE Transactions on,* vol. 27, pp. 36-45, 1989.

[41] Holm W. A. and Barnes R. M., "On radar polarization mixed target state decomposition techniques," in *Radar Conference, 1988., Proceedings of the 1988 IEEE National*, 1988, pp. 249-254.

[42] Krogager E., "Aspects of polarimetric radar imaging " phd, Copenhagen, 1993.

[43] Cloude S. R. and Pottier E., "A review of target decomposition theorems in radar polarimetry," *Geoscience and Remote Sensing, IEEE Transactions on,* vol. 34, pp. 498-518, 1996.

[44] Freeman A. and Durden S. L., "A three-component scattering model for polarimetric SAR data," *Geoscience and Remote Sensing, IEEE Transactions on,* vol. 36, pp. 963-973, 1998.

[45] Yamaguchi Y., Moriyama T., Ishido M., and Yamada H., "Four-component scattering model for polarimetric SAR image decomposition," *Geoscience and Remote Sensing, IEEE Transactions on,* vol. 43, pp. 1699-1706, 2005.

[46] Jong-Sen L., Grunes M. R., Schuler D. L., Pottier E., and Ferro-Famil L., "Scattering-model-based speckle filtering of polarimetric SAR data," *Geoscience and Remote Sensing, IEEE Transactions on,* vol. 44, pp. 176-187, 2006.

[47] ITC Faculty of Geo-Information Science and Earth Observation. (2009, *Geometric aspects of mapping*. Available: http://kartoweb.itc.nl/geometrics/index.html

[48] European Space Agency. (2011, POLARIMETRIC SAR DATA CLASSIFICATION. Available: http://envisat.esa.int/polsarpro/Manuals/5_Polarimetric_SAR_Data_Classification.pdf

[49] Definiens, *eCognition Developer 8*. Munchen: Definiens AG, 2009.

[50] *Quality management systems - Fundamentals and vocabulary,* ISO, 2005.

[51] Richards J. A., *Remote sensing with imaging radar*. Heidelberg: Springer, 2009.

[52] Olson C. E., "Elements of photographic interpretation common to several sensors," *Photogrammetric Engineering,* vol. 26, pp. 651-656, 1960.

[53] Jong-Sen L., Jen-Hung W., Ainsworth T. L., Kun-Shan C., and Chen A. J., "Improved Sigma Filter for Speckle Filtering of SAR Imagery," *Geoscience and Remote Sensing, IEEE Transactions on,* vol. 47, pp. 202-213, 2009.

[54] Guangyi Z., Yi C., Yilun C., Junjun Y., Jian Y., and Yang S., "Pol-SAR images classification using texture features and the complex Wishart distribution," in *Radar Conference, 2010 IEEE*, 2010, pp. 491-494.

[55] Lopes A. and Sery F., "Optimal speckle reduction for the product model in multilook polarimetric SAR imagery and the Wishart distribution," *Geoscience and Remote Sensing, IEEE Transactions on,* vol. 35, pp. 632-647, 1997.

[56] Dellepiane S., De Laurentiis R., and Giordano F., "Coastline extraction from SAR images and a method for the evaluation of the coastline precision," *Pattern Recognition Letters,* vol. 25, pp. 1461-1470, 2004.

[57] Mason D. C. and Davenport I. J., "Accurate and efficient determination of the shoreline in ERS-1 SAR images," *Geoscience and Remote Sensing, IEEE Transactions on,* vol. 34, pp. 1243-1253, 1996.

APPENDIX I: FIXED BUGS FROM POLSARPRO 4.1.5 DURING IMPLEMENTATION

Bug found 1
Quad polarization data extraction

Path:	\PolSARpro_v4.1.5\Soft\data_convert\
File name:	PSP_Extract_Data.tcl
Line:	2971
Description:	global FileInput1 FileInput2 IEEEFormat (original)
Fixed:	global FileInput1 FileInput2 FileInput3 FileInput4 IEEEFormat (modified)

Bug found 2
Subset extraction

Path:	\PolSARpro_v4.1.5\GUI\data_import\
File name:	SubArea_GraphicEditor.tcl
Code block lines:	1210
Description:	An error message is shown once click on the button "extract"
Problem:	The variable 'TERRASAR_X' is unknown due to the fact that there is not TERRASAR_X
Fixed:	Modified TERRASAR_X for TERRASARX

Bug found 3
Wishart supervised classification for TerraSAR-X quad polarization mode

Path:	\PolSARpro_v4.1.5\GUI\data_process_sngl\
File name:	TrainingAreas_GraphicEditor.tcl
Code block lines:	Between 1331 and 1355
Description:	An error message is shown once click on the button "Save" (Save the Training Area List)
Problem:	The variable 'MaskFonction' is unknown due to the fact that no value has been assigned to this variable.
Work around:	Setting the variable 'MaskFonction' to "0" (Zero)
Fixed:	Add two new Lines of code after line 1334 as the following: Line 1335:#don't know biz, force to 0 Line 1335: set MaskFonction "0"

APPENDIX II: DIFFERENT TIDE LEVELS PHOTOGRAPHS FROM STUDY AREA

Photographs:
Photographs taken in Scheveningen beach (Den Haag) during high tide on 29 January 2011 at 10 30 h. The water level rises from the "Casino" (big oval building) to the shore.

Photographs:
Photographs taken in Scheveningen beach (Den Haag) during low tide on 29 January 2011 at 1830 h. The water level decrease up to the "Casino" (big oval building).

APPENDIX III: NAUTICAL CHARTS INCLUDING METHODS 1 AND 2 OUTPUTS

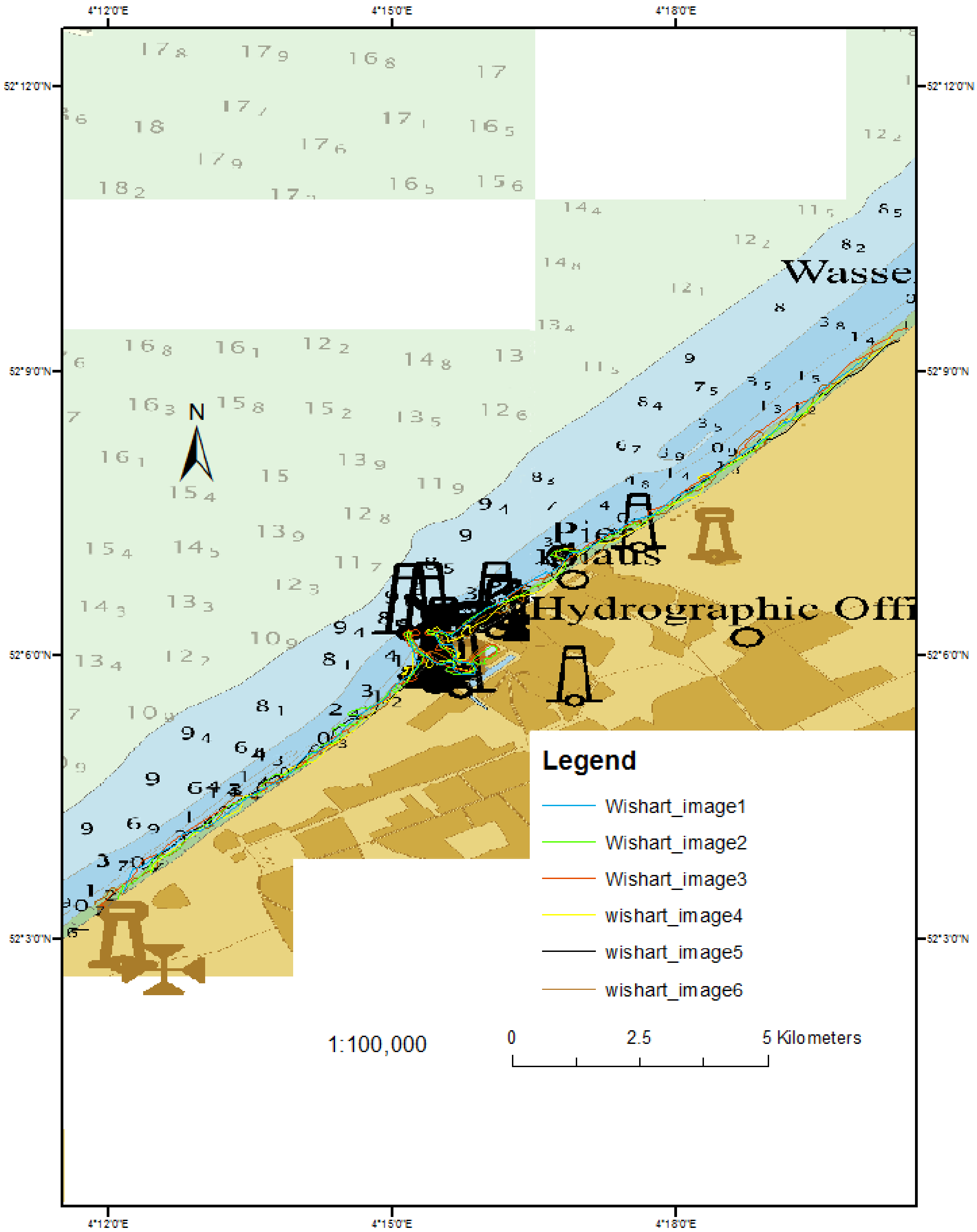

Nautical chart scale 1:100 00. Method 1 outputs from the six (6) quad polarization images.

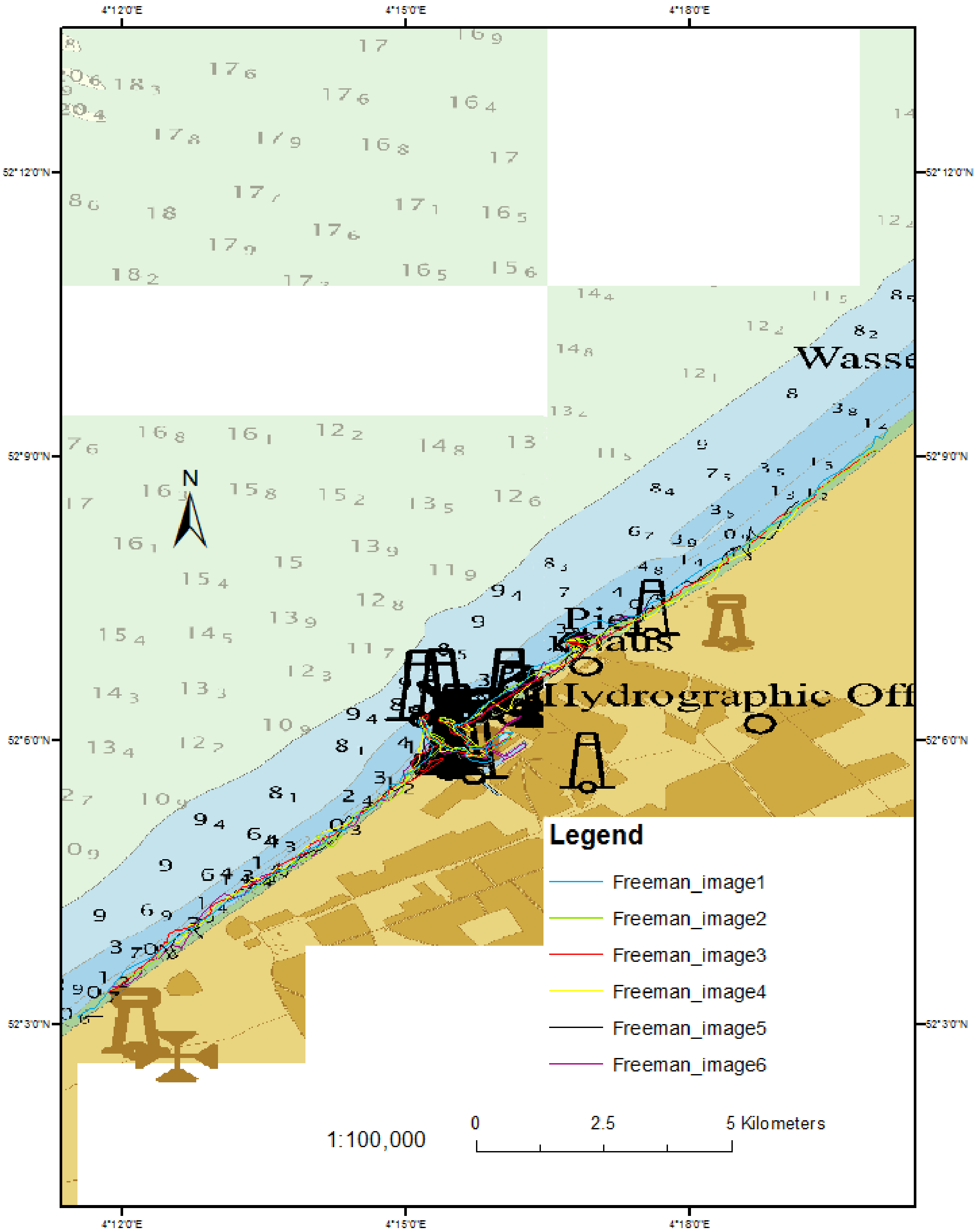

Nautical chart scale 1:100 00. Method 2 outputs from the six (6) quad polarization images.

APPENDIX IV: SHORELINE ANALYSIS FROM METHODS 1 AND 2

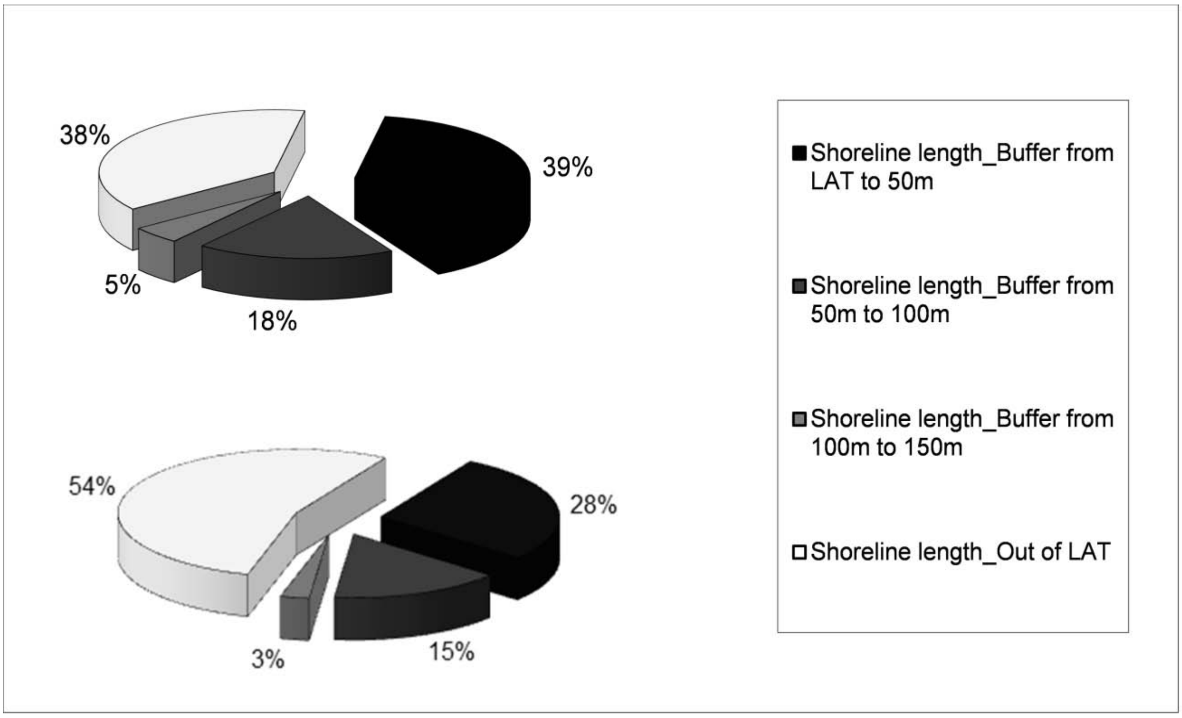

Image 1. Shoreline analysis from (a) Method 1 and, (b) Method 2 after validation process.

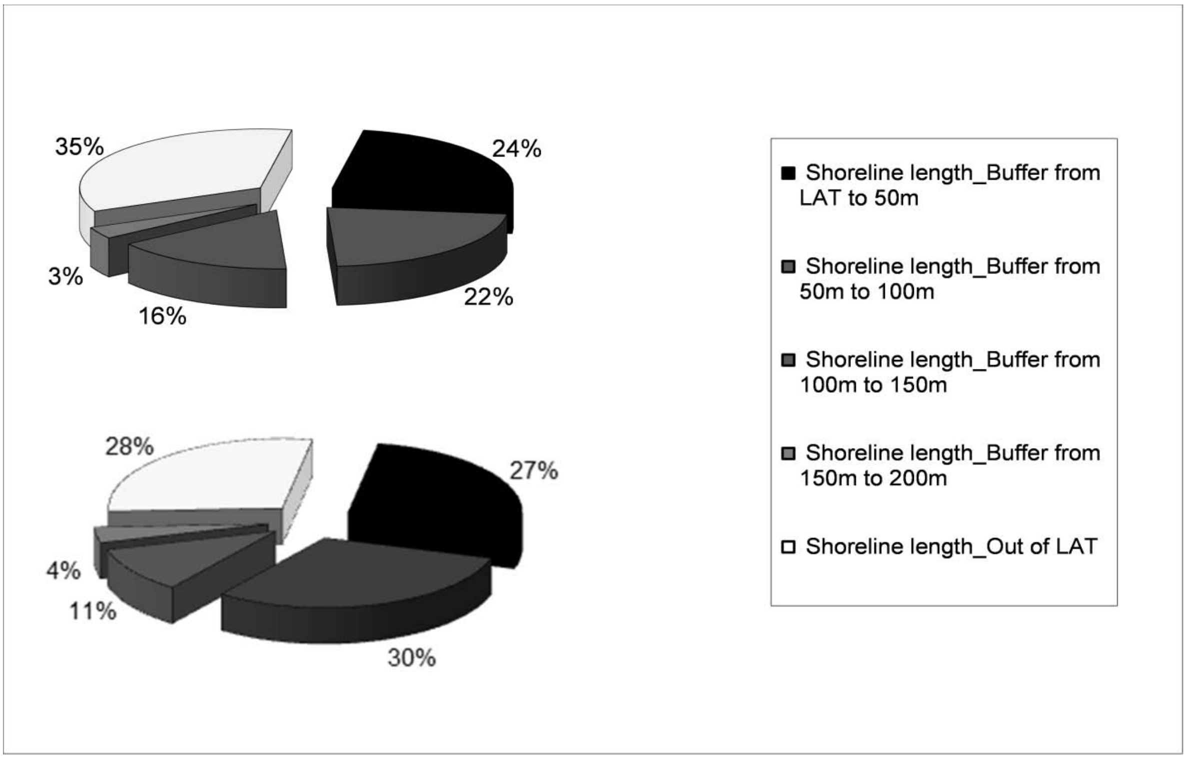

Image 2. Shoreline analysis from (a) Method 1 and, (b) Method 2 after validation process.

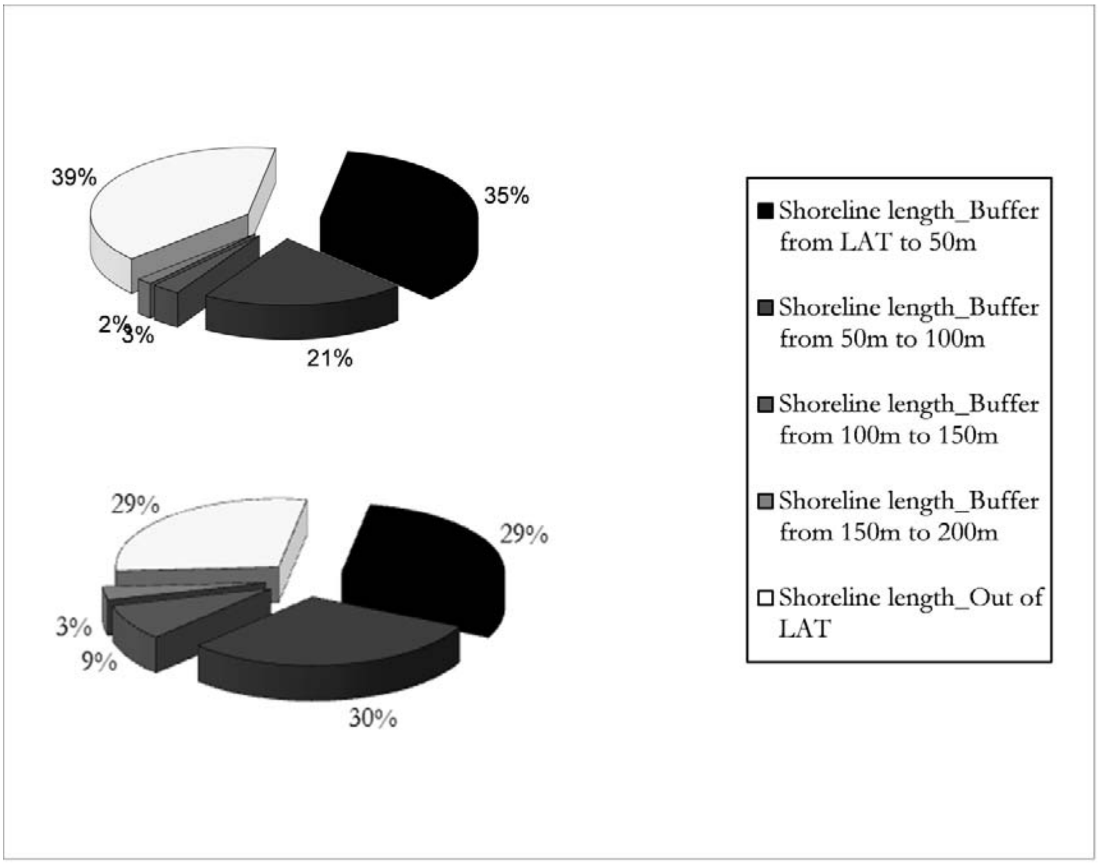

Image 3. Shoreline analysis from (a) Method 1 and, (b) Method 2 after validation process.

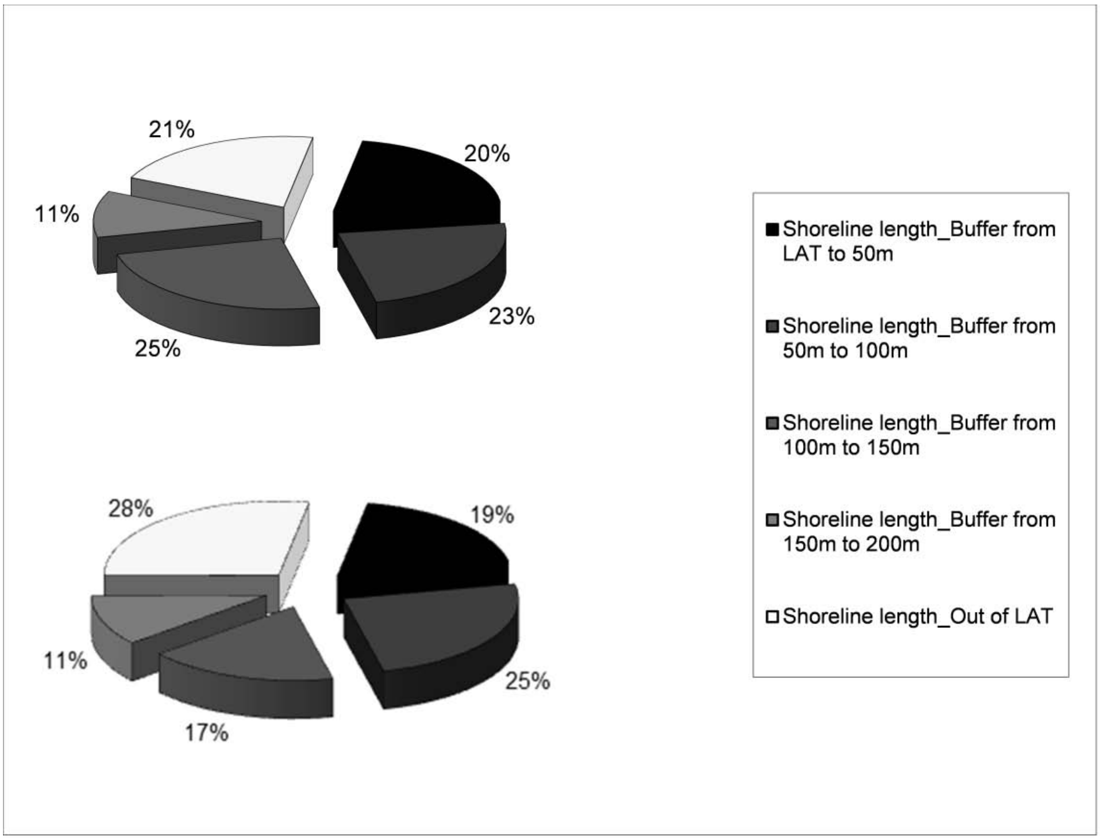

Image 4. Shoreline analysis from (a) Method 1 and, (b) Method 2 after validation process.

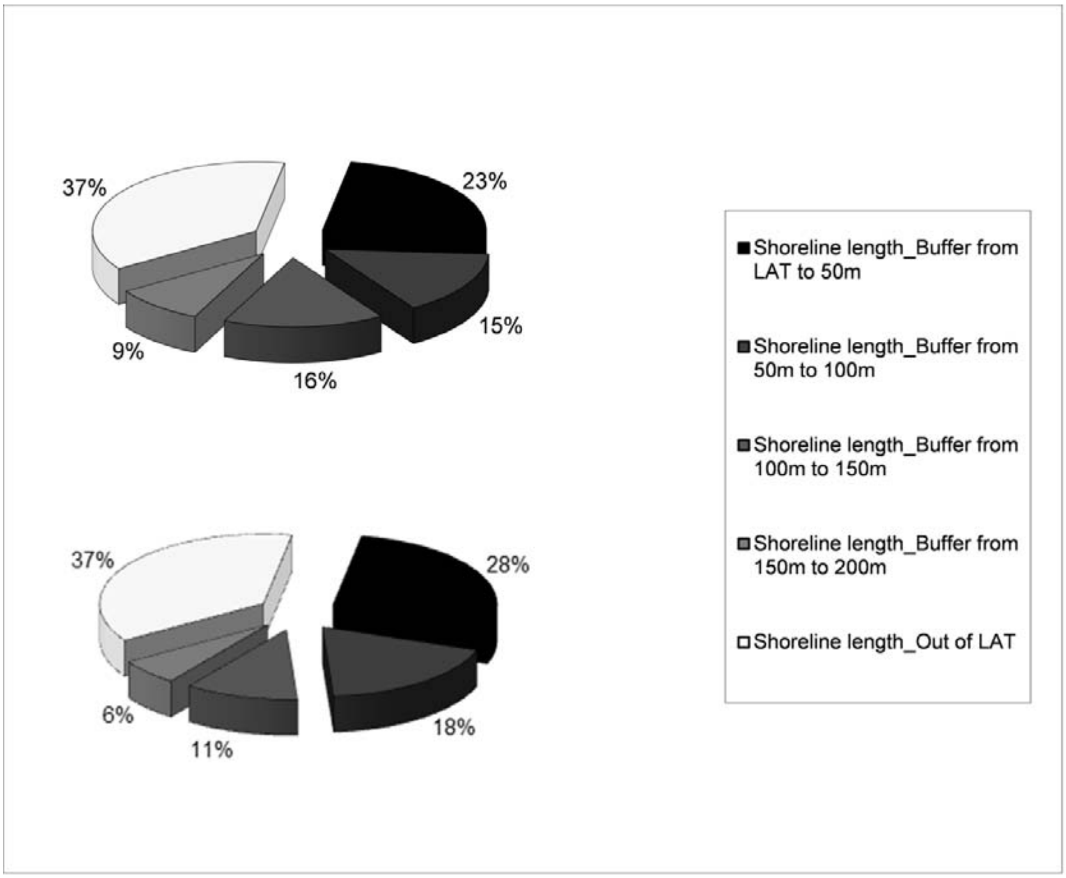

Image 5. Shoreline analysis from (a) Method 1 and, (b) Method 2 after validation process.

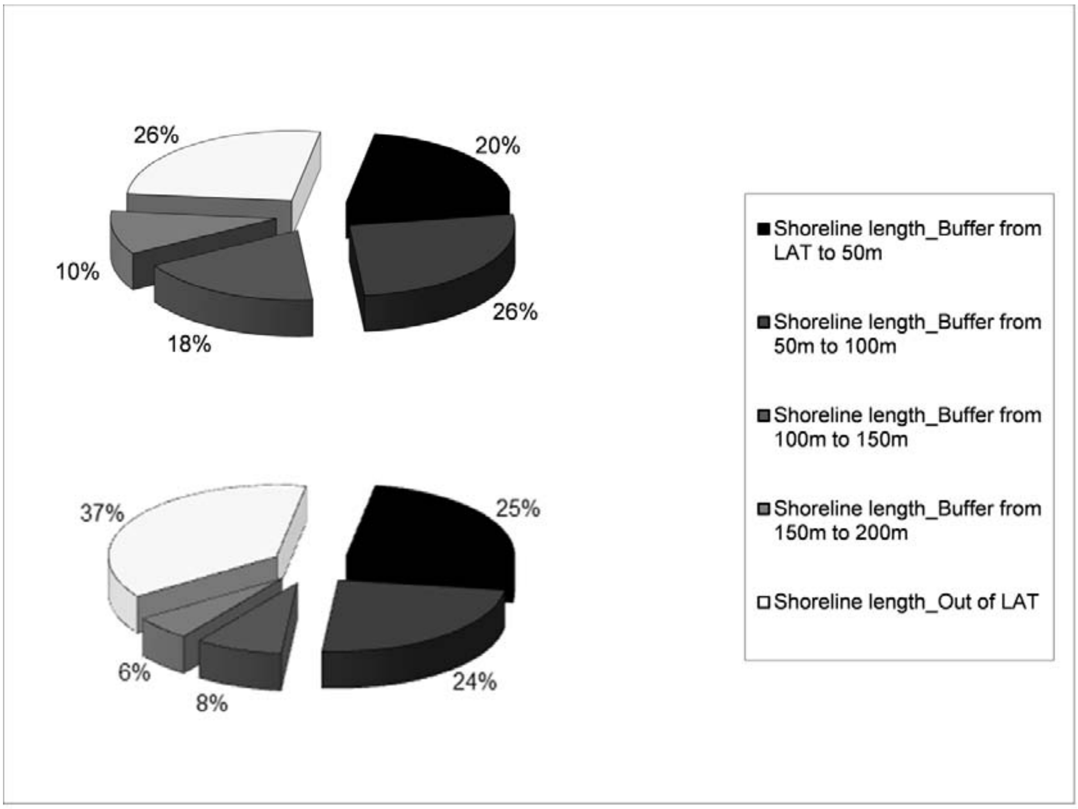

Image 6. Shoreline analysis from (a) Method 1 and, (b) Method 2 after validation process.

APPENDIX V: METADATA OF TERRASAR-X IMAGES

Image ID	Image April 17	Image April 28	Image May 09	Image April 26	Image April 15	Image May 7
Orbit direction	Descending	Descending	Descending	Ascending	Ascending	Ascending
Acquisition time	17/04/10 06:08:36.91	28/04/10 06:08:29.31	09/05/10 06:08:30.16	26/04/10 17:26:51.59	15/04/10 17:26:50.96	07/05/10 17:26:51.22
Relative orbit number	167	167	167	167	167	167
Sensor mode	Stripmap mode	Stripmap mode	Stripmap mode	Stripmap mode	Stripmap mode	Stripmap mode
Projection	Slant Range	Slant Range	Slant Range	Slant Range	Slant Range	Slant Range
Polarization mode	Quad polarization	Quad polarization	Quad polarization	Quad polarization	Quad polarization	Quad polarization
Latitude Northing	51.9522837	51.9534103	51.9529050	51.9695464 9	51.9691274	51.6588059
Longitude Easting	4.2630675	4.2599021	4.2589841	4.2899691	4.2897210	4.25492897
Incidence angle	24.6183319	24.633821	24.62406	38.792329	38.789000	38.137068
Azimuth resolution	6.5999999	6.5999999	6.5999999	6.5999999	6.5999999	6.5999999
Number of layers	4	4	4	4	4	4
Antenna Configuration	DRA	DRA	DRA	DRA	DRA	DRA
Data Type	Complex	Complex	Complex	Complex	Complex	Complex